MECHANICAL ENGINEERING SOLUTIONS

Design, Simulation, Testing and Manufacturing

Vol. 1

Editor
Tigran Parikyan

ИНЖЕНЕРНЫЕ РЕШЕНИЯ В МАШИНОСТРОЕНИИ

Проектирование, моделирование, испытание и изготовление

Том 1

Редактор

Тигран Ф. Парикян

Yerevan, Armenia

Ереван, Армения

American University
of Armenia Press

MES 2018

SEP 17-19
Yerevan, Armenia

Proceedings of the

1st INTERNATIONAL CONFERENCE
MECHANICAL ENGINEERING SOLUTIONS
Design, Simulation, Testing & Manufacturing

Organizers:

National Polytechnic University *of* Armenia

AUA
American University *of* Armenia

Dedicated to:

- 2800th Anniversary *of* the city *of* Yerevan
- 85th Anniversary *of* National Polytechnic University *of* Armenia

IFToMM

Under the patronage of the International Federation for the Promotion of Mechanism and Machine Science

Ministry of Education and Science of Armenia
Science Committee

ՌՈՍԳՈՍՍՏՐԱԽ ԱՐՄԵՆԻԱ

UNIDO

Mechanical Engineering Solutions MES-2018 – T. Parikyan (ed.)

ISBN 978-9939-1-0895-7

Proceedings of the 1st International Conference
MECHANICAL ENGINEERING SOLUTIONS
Design, Simulation, Testing and Manufacturing
September 17-19, 2018, Yerevan, ARMENIA

MES2018

MECHANICAL ENGINEERING SOLUTIONS

Design, Simulation, Testing and Manufacturing Vol. 1

Editor

Tigran Parikyan

Advanced Simulation Technologies
AVL List GmbH, Graz, Austria

Joint Publication of
National Polytechnic University of Armenia and American University of Armenia
Yerevan, Armenia

ISBN 978-9939-1-0895-7

ISBN 978-9939-1-0894-0

TABLE OF CONTENTS

Vol. 1

SECTION A:
Design / Vibrations / Powertrains / Vehicles

SECTION B:
Mechanisms / Robots / Biomechanics

Vol. 2

SECTION A:
Design / Vibrations / Powertrains / Vehicles

SECTION B:
Mechanisms / Robots / Biomechanics

SECTION C:
Manufacturing / Machining / Cutting Tools

PREFACE

These are the Proceedings of the 1st International Conference "MECHANICAL ENGINEERING SOLUTIONS: Design, Simulation, Testing and Manufacturing" (MES-2018), which took place on September 17-19, 2018, in Yerevan, Armenia.

The conference was organized by the National Polytechnic University of Armenia (NPUA) in partnership with the American University of Armenia (AUA), under the patronage of the International Federation for the Promotion of Mechanism and Machine Science (IFToMM), and was hosted by the AUA.

The financial support of the following sponsors is greatly acknowledged:

- Science Committee of the Ministry of Education and Science of Armenia
- Rosgosstrakh-Armenia Insurance CJSC
- Armenia Field Office of the United Nations Industrial Development Organization (UNIDO)

The purpose of the MES-2018 conference is to initiate a forum to regularly bring together researchers and academic staff from technical universities and practitioners from industrial companies in the field of mechanical engineering. With its multi-topic program and international scale, it has to establish a networking and educational platform, and to facilitate contacts and cooperation between universities, research and development centers and industrial companies from different countries.

While mainly focusing on technical issues of designing, calculating, producing and using various machines and mechanical systems (such as precision, load capacity, performance, etc.), advanced educational methods and models, as well as market aspects like customer benefits, economic efficiency, latest trends, etc. are also considered. Most of the contributions indicate existing or potential practical applications of known or newly developed designs, technologies and equipment, as well as theories, methods, algorithms and software.

These Proceedings contain 29 papers (two of them – keynote lectures) presented at the conference by scientists and engineers from 10 different countries.

According to the topics, the papers are organized in three sections:

SECTION A: Design / Vibrations / Powertrains / Vehicles

SECTION B: Mechanisms / Robots / Biomechanics

SECTION C: Manufacturing / Machining / Cutting Tools

The official languages of the conference are English and Russian. At the end of each paper there is a short abstract in the second official language.

Below are the names and affiliations of the conference co-chairs, International Advisory Board, Local Program and Organizing Committees.

Bakhadirov Gayrat, Earthquake Engineering and Mechanics Institute of Uzbek Academy of Sciences (Uzbekistan)
Belyi Mikhail, Dassault Systemes Simulia Corp. (USA)
Blythe Neil, GE Transportation (USA)
Ceccarelli Marco, University of Cassino and South Lazio, President of IFToMM (Italy)
Chirikjian Gregory, Johns Hopkins University (USA)
Darbinyan Hrayr, Shanghai Kunjek Hand Tools & Hardware Co. Ltd. (China)
Eichberger Arno, Graz University of Technology (Austria)
Friswell Michael, Swansea University (UK)
Frolov Sergey, Semenov Institute of Chemical Physics, Russian Academy of Sciences (Russia)
Gevorgyan Gevorg, Continental Mechanical Components Germany GmbH (Germany)
Glazunov Victor, Mechanical Engineering Institute of the Russian Academy of Sciences (Russia)
Hayrapetyan Gevorg, John Deere GmbH & Co. KG (Germany)
Janic Miron, SET Sustainable Energy Technologies GmbH (Austria)
Katevas Nikos, Technological Educational Institute of Sterea Ellada (Greece)
Katrašnik Tomaž, University of Ljubljana (Slovenia)
Keoshkeryan Ruben, Fraunhofer-Gesellschaft (Germany)
Khmelev Vladimir, Biysk Technological Insitute (Russia)
Kravchenko Pavel, Volgodonsk Institute of Engineering and Technology, Branch of NIAS "MEPhI" (Russia)
Makarov Vladimir, Perm National Research Polytechnic University (Russia)
Mikhailov Alexander, Donetsk Technical University (Ukraine)
Minasian Minas, State Marine Technical University of St. Petersburg (Russia)
Nosenko Vladimir, Volga State University of Technology (Russia)
de Oliveira Leopoldo, University of São Paulo (Brazil)
Papadimitriou Ilias, Georg Fischer AG (Switzerland)
Parikyan Tigran, AVL List GmbH (Austria)
Piraner Ilya, Cummins, Inc. (USA)
Preis Vladimir, Tula Technical University (Russia)
Skripnik Alexei, OOO AVL (Russia)
Stepanov Yuri, Oryol State University (Russia)
Tavkhelidze David, Georgian Technical University (Georgia)
Turmanidze Raul, Georgian Technical University (Georgia)

Local Program Committee

Sargsyan Yuri (NPUA)
Balasanyan Boris (NPUA)
Hajian Aram (AUA)
Arzumanyan Karen (NPUA)
Ghazaryan Sarik (NPUA)
Parikyan Feliks (NPUA)
Harutyunyan Mikael (NPUA)
Musayelyan Gagik (NPUA)
Stakyan Mihran (NPUA)
Verlinski Sergey (NPUA)
Zeytunyan Sargis (AUA)

Local Organizing Committee

Hajian Aram (AUA)
Ghazaryan Sarik (NPUA)
Balasanyan Boris (NPUA)
Danilova Rubina (AUA) – Conference Secretary
Hovhannisyan Tatevik (NPUA)

Zeytunyan Sargis (AUA)
Keryan Aram (AUA)

I wish to thank the team members who helped with the organization of the conference and with the publication of these proceedings. My special thanks to the reviewers of the abstracts and papers, who helped us to improve the quality of the submissions. I would also like to thank the authors of the published and presented papers and other participants of the conference. Without the contribution of all the mentioned persons, the conference would not have been successful.

Editor
Tigran Parikyan
Advanced Simulation Technologies
AVL List GmbH, Graz, Austria

SECTION A

Design / Vibrations / Powertrains / Vehicles

Proceedings of the 1st International Conference MES-2018 / ИРМ-2018
MECHANICAL ENGINEERING SOLUTIONS
Design, Simulation, Testing and Manufacturing
September 17-19, 2018, Yerevan, ARMENIA

MES2018-K1

EARLY CONCEPT PHASE SIMULATION: HOW TO BECOME FASTER IN POWERTRAIN DYNAMICS CALCULATION PROJECT WHILE KEEPING HIGH QUALITY OF RESULTS

Tigran PARIKYAN[1]

[1]AVL List GmbH, Graz, AUSTRIA, e-mail: tigran.parikyan@avl.com

EXTENDED ABSTRACT (KEYNOTE LECTURE)

Software tools for multi-body dynamics (MBD) simulation of internal combustion engines and powertrains become more and more sophisticated, covering more complex physical phenomena. On the other hand, the models used in the simulation have a tendency of increasing the number of DOF in the system of equations to be solved, as a result of finer FE-meshes of flexible bodies used. This results in a higher quality of results, describing the dynamic behavior of the systems closer to reality.

It seems therefore, that in all powertrain dynamic calculations one has to use only these high-end tools delivering finer results – and no others, especially because the increasing performance of computers makes such type of simulation feasible. However, in the real engine development process as seen from the industry point of view, the quality of the results is only one of the criteria to be met. The other one is the development time, which has to be kept possibly short and has a further tendency to be reduced.

A methodology combining high quality and performance implies splitting the whole calculation workflow into two phases: 1) early "concept" (or layout) phase and 2) final "design" (or detailed analysis) phase. Typically, very fast tools are used in the concept phase (solution mostly in frequency domain), which allow for a fast (though not precise) evaluation or check of critical parts of the system (e.g. main bearing or web); here one can additionally simulate multiple variants, thus enabling a coarse optimization of the system. Only after that, high-end tools are applied to
a) verify the assumptions made and optimization performed in the concept phase; b) make a fine-tuning of some parameters to achieve even better results.

The simplification of the modeling in the concept phase serves not only for fast and robust simulation, but also for better understanding of dynamic phenomena separated from each other (e.g. torsional vibrations from the bending ones), so that the system can be analyzed "in layers". Such an approach makes it possible to concentrate on essential issues within a separate sub-task. Besides that, an efficient optimization is only feasible if the number of parameters to optimize is small, which is achieved by decomposing the optimization tasks into sequential sub-tasks.

Integration of "concept" and "design" software tools as two levels within a single powertrain dynamic analysis software suite is especially beneficial, as it makes use of the shared data for the crankshaft and the other parts of powertrain (e.g. basic geometry and material, CAD model, volumetric FE mesh, 3D structured model, 1D equivalent torsional model), as well as of common GUI and post-processing tools. Due to that, a smooth transition between the levels of modeling depth becomes easily and quickly possible.

The strategy mentioned above, is demonstrated using the program modules of *AVL EXCITE™* solution suite having two levels – *Designer* and *Power Unit* [1, 2], with a focus on early concept phase [3]:

- Unbalance: for assessing of free forces and moments, as well as of driveline reaction torque, and for selection of proper counterweights and eventually balancer shafts;

- Torsion: for selecting of a proper flywheel and torsional vibration damper; to perform 1D torsional modes analysis (undamped and damped [4]) and torsional forced response (solution in frequency domain) [5], to reveal and avoid the possible resonances [6], to transform the properties of frequency-dependent dampers to be used in time-domain simulation [7];
- MBLoad: to calculate the main bearing load and web section forces and moments, as well as 3D forced response of any node of the crankshaft (solution in frequency domain) [7];
- Bearing: Hydrodynamic slider bearing calculation – rigid shell, 2D approach [9];
- Strength: Stress and durability of crankshafts – Gough-Pollard method to find most critical web fillets [10, 11];
- Mount Layout Tool: 3D dynamics of rigid engine on rubber or hydraulic mounts, for low-frequency NVH evaluation [11];
- Shaft Modeler: pre-processor to create structured models for crankshafts, camshafts, rotors, etc. – assembling, modal analysis [13], gyroscopic modal analysis [4] and automatic generation of equivalent torsional vibration model [14];
- AutoSHAFT: pre-processor for Shaft Modeler, converting CAD models into structured models for crankshafts using integrated FE-mesher and FE-solver [15], generation of stress mesh for a stress analysis after dynamic simulation in time domain [3].

The use of the mentioned modules is demonstrated on some standard examples. A smooth transition from the early "concept" phase (level *Designer*) to the detailed analysis "design" phase (level *Power Unit*) is illustrated, and the similarities and differences of results are discussed.

REFERENCES

1. EXCITE™ Designer, *Software package for crank train and driveline analysis in early concept phase*, AVL List GmbH (Release v2018).
2. EXCITE™ Power Unit, *Software package for flexible multi-body dynamics*, AVL List GmbH (Release v2018).
3. Resch, T., Knaus, O., Mlinar, S., and Pogatsch, G., "Application of Multi-Body Dynamics for the Crankshaft Layout in the Concept Phase," *MTZ Paper* **11** (2004).
4. Parikyan, T., "Complex Modes Analysis for Powertrain and Driveline Applications," pp. 2761-2774, *International Conference on Noise and Vibration Engineering ISMA*, Leuven, Belgium (2016).
5. Parikyan, T., "Multi-Cycle Torsional Vibration Simulation with AVL EXCITE Designer," *ASME Paper* ICEF2011-60091 (2011).
6. M. Janic, et al., "Development of Industrial Continuously Variable Electromechanical Drivetrain Systems Based on Virtual Model Approach," *Proc. 1st Int. Conf. Mechanical Engineering Solutions: Design, Simulation, Testing and Manufacturing (MES-2018)*, Paper No. MES2018-05 (accepted for publication), Yerevan, Armenia (Sept. 2018).
7. T. Parikyan, et al., "Equivalent Modeling of Torsional Vibration Dampers in Frequency and in Time Domain For a Smooth Transition Between Concept and Design Phases," *Torsional Vibration Symposium*, Paper No. 3A–2, Salzburg, 2017.
8. Parikyan, T., and Resch, T., "Statically indeterminate main bearing load calculation in frequency domain for usage in early concept phase," *ASME Paper* ICEF2012-92164 (2012).
9. H.-J. Butenschön, "Das hydrodynamische, zylindrische Gleitlager endlicher Breite unter instationärer Belastung", Diss. Dr.-Ing., Karlsruhe, 1976.
10. Calculation of Crankshafts for Diesel Engines, *Classification Notes No. 41.3*, DNV, January 2002.
11. Sandberg, E. (DNV AS, Norway), "Some classification aspects on crankshafts," *CIMAC Congress* 2004, Kyoto, Paper No. 13.
12. T. Parikyan, N. Naranca, and J. Neher, "Powertrain Resilient Mounting Design Analysis," *Accepted for presentation at ASME ICEF2018.*
13. Parikyan, T., Resch, T., and Priebsch, H.H., "Structured model of crankshaft in the simulation of engine dynamics with AVL EXCITE," *ASME Paper* 2001-ICE-435, ICE-Vol. 37-3, p105-114 (2001).
14. Parikyan, T., "Unified Approach to Generate Crankshaft Dynamic Models for 3D and Torsional Vibration Analyses," *ASME Paper* ICES2003-591 (2003).
15. Todorovic G. and Parikyan T., "Automated Generation of Crankshaft Dynamic Model to Reduce Engine Development Time," *SAE Paper* 2003-01-0926 (2003).

Proceedings of the 1st International Conference MES-2018 / ИРМ-2018
MECHANICAL ENGINEERING SOLUTIONS
Design, Simulation, Testing and Manufacturing
September 17-19, 2018, Yerevan, ARMENIA

MES2018-05

DEVELOPMENT OF INDUSTRIAL CONTINUOUSLY VARIABLE ELECTROMECHANICAL DRIVETRAIN SYSTEMS BASED ON VIRTUAL MODEL APPROACH

Miron JANIC[1], Michael MIKLAUTSCHITSCH[2], Tigran PARIKYAN[3], Saša BUKOVNIK[4]

[1,2] SET Sustainable Energy Technologies GmbH, Klagenfurt, Austria
miron.janic@gmail.com, Michael.Miklautschitsch@set-solutions.net

[3,4] AVL List GmbH, Graz, Austria
tigran.parikyan@avl.com, sasa.bukovnik@avl.com

ABSTRACT

Due to the market demand for economically more efficient equipment, controlled-speed drives for different machines are getting more and more attention. Usually, when speed control is used, frequency converters (full-scale converters), geared variable-speed couplings, or hydrodynamic variable speed gears are being considered. However, installing a high-power electrical drive can lead to high acquisition costs and considerable efficiency loss.

A mechatronic system called SETCON® is developed by SET and can reach 25 MW of transmitted power at a rated speed of up to 15000 rpm.

In the development of such a system, the company SET uses proven methodology known as Virtual Model Approach (VMA) relying on high-end software tools, including MBD software AVL EXCITE™ as its basis.

Development of 4.1 MW power system presented here has been tested in real conditions and the test-bed measurements were compared to those of the virtual model, giving an excellent match.

INTRODUCTION

Reduction of energy consumption in any machine not only reduces costs, but also contributes to the reduction of gas emissions having green-house effect.

There is a huge potential for saving energy, emission reduction, as well as for implementation of renewable energy sources, especially in industrial machinery.

In order to develop an optimal solution for industrial applications which fully utilizes the potential for energy saving, an innovative, fast and relatively inexpensive development approach is necessary.

Virtual Model Approach (VMA) could be defined as a development process with "first-time-right" principle [1, 2]. It considers all external loads acting on and boundary conditions present within a complex mechatronic system, and evaluates its dynamic response, enabling the engineer to come to an optimum solution even before the first real part is produced.

Similar to a standard developing process, VMA consists of several development phases. For industrial machinery there are typically two development phases:

- **Early concept phase** – where the main requirements in form of dimensions and functional characteristics of the machinery are defined.
- **Final design phase** – where all functional requirements and subsystem dimensioning are checked and verified for real working conditions.

The major advantage of VMA compared to the "classic development" approach is that:

- The development time becomes extremely short;
- The number of destroyed prototypes is reduced to a minimum (in the best case – none!).

During many years of experience in accelerated product development at SET, it became evident that it is simply not acceptable to use old-fashioned methods of producing and destroying a large number of

prototypes to achieve the defined characteristics of the future product. By using the VMA, with dynamic simulation in almost realistic conditions, many phenomena and undesired reactions of the entire system can be discovered in an early virtual phase and the design can be changed to avoid these reactions. Of course, testing is still the ultimate and most important stage of validation of the desired functions, but it is now only the final step.

Certainly, virtual product development is something that every company aspires to have. Modern tools for numerical simulation and control are becoming increasingly sophisticated and can predict some phenomena of the system or its part. On the other hand, simulation tools predicting all the phenomena of the **complete system,** still have to be developed. Moreover, the use of a variety of software tools to unite the entire simulation workflow into a single functioning system is not a particularly common practice for various reasons.

Generally, each electromechanical system is a set of several subsystems. We can roughly classify them into mechanical, electrical and control subsystems. The functional requirements of a product (in this case electromechanical differential gearbox) implies the implementation of **all three** subsystems (**Figure 1**).

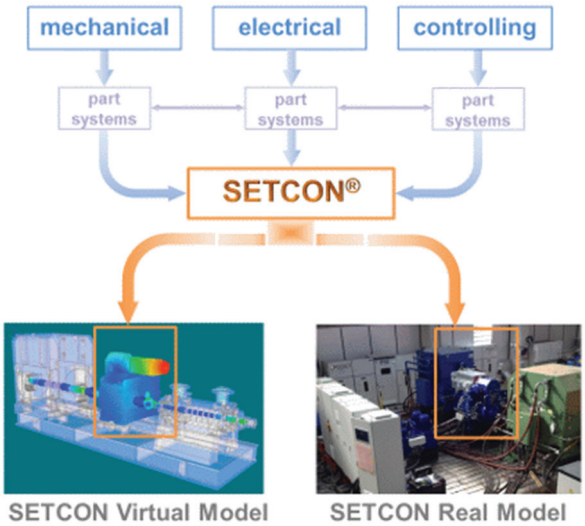

Figure 1. Virtual Model Approach (VMA)

VMA methodology effectively interconnects the dynamic simulation of all three subsystems and as a result represents the physical behavior of the entire system even at a very early stage of product development.

For applying the VMA methodology SET uses several simulation tools, where AVL EXCITE™ [3, 4] is the main tool which takes most of dynamic influences on the system into account.

In what follows, the development of SETCON® using VMA methodology will be explained in detail.

SETCON® SYSTEM

As oil and gas prices continue to fluctuate, causing a demand for production to vary at refineries, and the EU Eco-design regulations become stricter, more and more operators are turning to controlled speed drives for their machines.

Even if the practice of dynamic adjustment of the power to actual needs becomes a kind of standard for some applications, in most of the areas of the industry it has still to be introduced.

In those rare cases where a speed control is used today, the installed machines usually use:

- Frequency converters (full-scale converters);
- Geared variable-speed couplings;
- Hydrodynamic variable speed gears.

However, when a higher electrical drive power is required, the purchase costs and the efficiency losses with the mentioned solutions often become too high.

A good alternative could be electro-mechanical variable speed gearboxes containing servo-motors, which combine the benefits of conventional drive technologies with higher efficiency and reliability.

SETCON® [5] is an example of such an electro-mechanical variable speed gearbox designed to control speed in pumps, compressors, fans, and blowers. With up to 95% overall efficiency (incl. Main Drive), it is more efficient compared to the other systems on the market (**Figure 2**) [5].

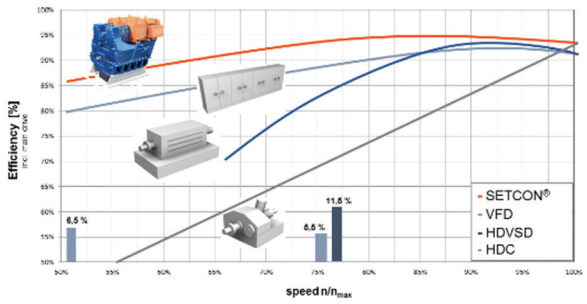

Figure 2. Total Efficiency (comparison)

The power of SETCON® can be up to 25 MW, and the speed up to 15000 rpm. It has a wide range of industrial applications with necessity for a variable speed control.

The working principle of SETCON®

The SETCON® consists of a differential gear (planetary gear) including the spur gear unit (1), a three-phase motor with a low-voltage converter as the differential drive (2+3), an electric motor as medium-voltage main drive (4), a driven machine (5) e.g. a pump or other variable-speed output shaft (6). The medium-voltage main drive – the motor (4) is connected directly to the power supply and drives the differential's ring gear at constant speed. Connected to the output shaft (6), the planet carrier transmits the variable speed through the optional spur gear unit to the

pump. The differential's sun gear is connected to the differential drive. The speed of the differential drive is controlled firstly to ensure that the speed of the output shaft (6) varies while the speed of the main drive (4) is constant, and secondly to control the torque in the driven machine's entire drive train (**Figure 3**).

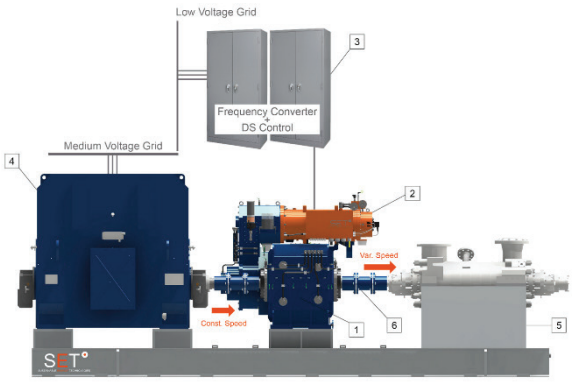

Figure 3. The working principle of SETCON®

A number of SETCON® systems in different power classes have been successfully developed. In this paper, detailed development will be shown for the 4.1 MW system using VMA, as well as some VMA applications used for higher power classes of the SETCON® system.

VIRTUAL MODEL APPROACH (VMA)

The basic purpose of VMA is that at the early stage of the development of an electromechanical system, one gets as realistic a picture as possible of all the phenomena that are present in the real operation of this machine. Understandably, there are a lot of unknowns and many obstacles in defining the entries and boundary conditions of a new system as precisely as possible. Therefore, by selecting the best design solutions alongside with using some previously established and validated parameters of the system, one comes to an optimum design in the required conditions even at a very early stage of the development process.

The VMA generally consists of several development steps which can be divided into:

- ***Building subsystems***
- ***Simulations of VMA***
- ***Extended analyses***
- ***Complete system in VMA***
- ***Validations***

Building subsystems

The first step in developing of every system is building its model.

As already mentioned (**Figure 1**), the electro-mechanical system consists of 3 subsystems:

- Mechanical
- Electrical
- Control

For a proper and detailed understanding of the whole electromechanical system, each subsystem must be first modeled separately. These can be then investigated further in detail by splitting into several different part-systems following a similar approach.

The part-systems are analyzed to understand the phenomena and then optimized so that the final improvement of the complete subsystem is achieved.

Each of these three main subsystems consist of several input components or part-systems such as an oil system, a partial control or electric system.

The **Control subsystem** represents a comprehensive connection of the entire product. Although, together with the **Electric subsystem**, it has a big influence on the dynamic response of the complete system, its numerical simulation is relatively well predictable and controllable.

The main tool used to define the Control and Electrical subsystems is MATLAB/Simulink (**Figure 4**) and its connections to the AVL EXCITE™.

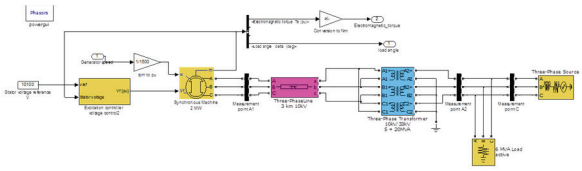

Figure 4. Electrical & Control subsystems

The **Mechanical subsystem** is a complex one, and its behavior is very difficult to predict. Therefore, it must be modelled very accurately in VMA.

For a proper dynamic modeling of the electro-mechanical drivetrain, the following influences are considered:

- Linear stiffness of all included mechanical parts – bodies;
- Nonlinear behavior of connections – joints (gears, bearings, bushings);
- Electro-mechanical behavior of motors;
- Electric behavior of the high voltage grid.

The complexity of the VMA increases steadily during the development process, due to more detailed input data as well as to the requirements to the control system.

Those refinement efforts lead to a high-fidelity model in **Final design phase** which is necessary for a comprehensive insight into the system dynamic behavior.

VMA: EARLY CONCEPT PHASE

To design the system in a time-efficient way while keeping the high-quality standards, it has proved to be a good engineering practice to split up the whole design and analysis process into several phases.

Decomposing the whole design process into subsequent tasks and applying the appropriate analysis tools enables for better grasp of the properties and behavior of the whole system and its parts, each time concentrating on improving its specific parameters.

This kind of decomposition assumes definite simplification of modeling of a system and its components at subsequent stages, implying different levels of depth in system description and evaluation.

Torsional vibration analysis

As transmission of torque and rotational motion are the main objectives of the driveline system under consideration, it makes sense to start with the analysis of its discretized torsional system – a reduced 1D equivalent of 3D flexible multibody system (**Figure 5**) [6].

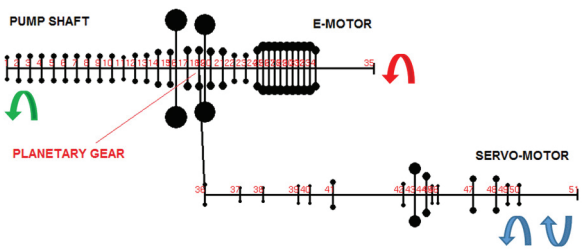

Figure 5. Equivalent torsional system

Performing modal analysis of the equivalent torsional system results in a spectrum of torsional natural frequencies (**Figure 6**).

mode [-]	frequency [Hz]	mode [-]	frequency [Hz]	mode [-]	frequency [Hz]
1	0.7	11	319.5	21	794.1
2	1.0	12	396.9	22	823.6
3	25.3	13	443.9	23	904.6
4	54.4	14	479.9	24	921.2
5	60.0	15	485.8	25	933.5
6	64.4	16	598.2	26	955.1
7	103.1	17	650.5	27	978.0
8	163.4	18	666.0		
9	228.8	19	722.8		
10	313.3	20	738.4		

Figure 6. Damped frequencies (up to 1 kHz)

Each of these natural frequencies is characterized by its mode shape (**Figure 7**). It can be seen that while at lower natural frequencies the mode shapes show the excitation of motion of the whole system, the higher natural frequencies tend to excite separate shafts or their connections (the so-called local mode shapes).

We also see that the long shafts (motor shaft and the pump shaft) deform at rather low frequencies already.

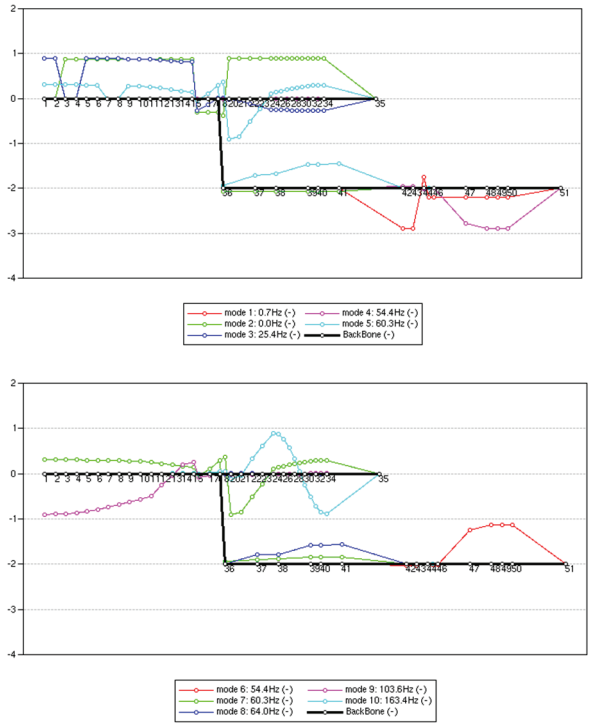

Figure 7. Torsional mode shapes

In case a damped modal analysis is performed [7], each mode is additionally characterized by its damping. This is quantified by the mode damping factor (**Figure 8**) and can be visualized for each specific mode in form of harmonic oscillations with decay (**Figure 9**).

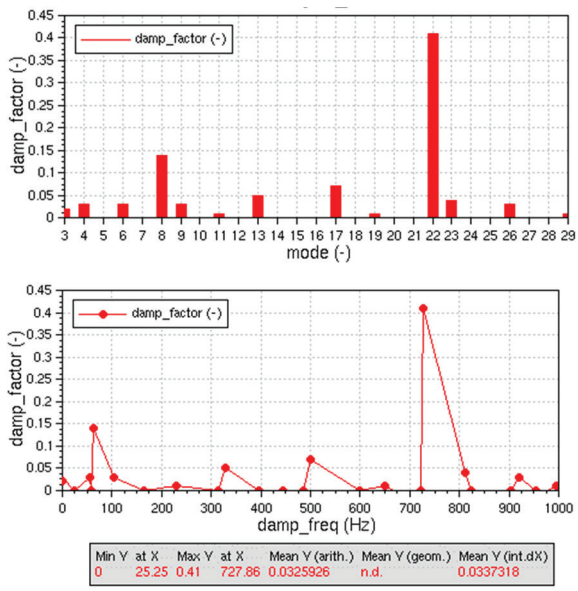

Figure 8. Damping factors of torsional modes

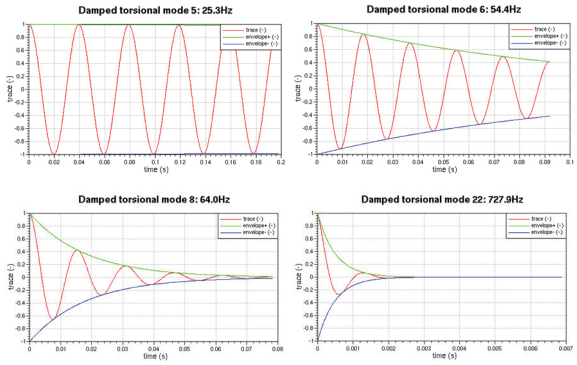

Figure 9. Decayed harmonic oscillations of different modes

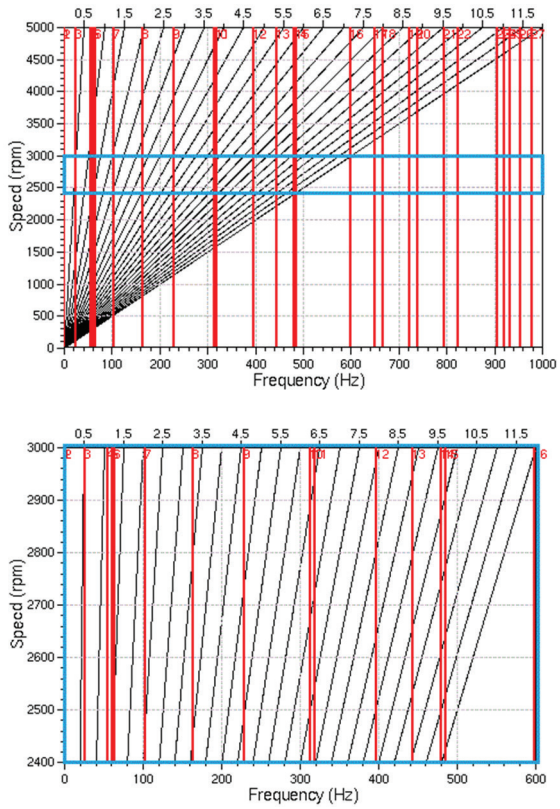

Figure 10. Critical speed diagram (up to 1 kHz):
a) full speed range - from 0 to 5000 rpm;
b) operation speed range - from 2400 to 3000 rpm

These natural or damped frequencies can also be shown on the critical speed diagram, either in full or in specific operation range of speeds at pump shaft (**Figure 10**). Here, the intersection of the natural frequencies with order lines marks potential resonance speeds of the system.

However, to find out whether such potential resonance become real ones, a forced response analysis of the torsional system is needed [8].

TVA of the system - forced response - speed sweep

To see the real response of the system, we perform a torsional vibration analysis, simulating forced response of the system to a special vibratory torque applied to the end of the pump shaft. This torque represents a kind of "white noise" signal, as it has the same magnitude in each of the harmonic components (**Figure 11**), thus providing an equal excitation in each harmonic order.

The results of the torsional vibration analysis can be seen below. These can refer either to the system as a whole (**Figure 12**), thus providing some integral indices for the system evaluation (the first plot clearly shows the resonances of the whole system), or to the parts of the system, showing a different influence of excitation on different mass points (**Figure 13**) or elastic elements (**Figure 14**).

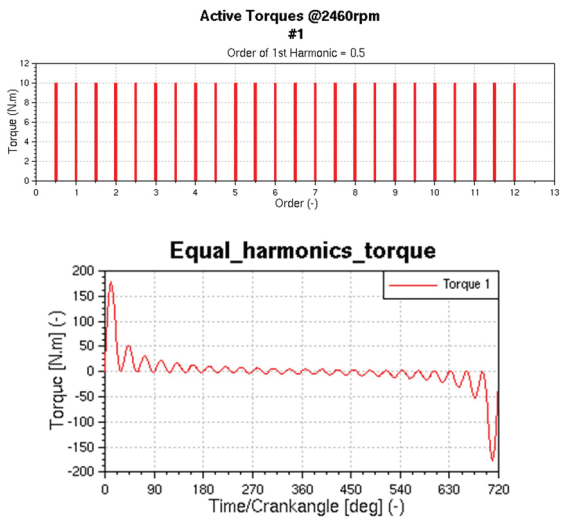

Figure 11. "Equal-harmonics" test torque:
a) in magnitudes of harmonics; b) vs. rotation angle

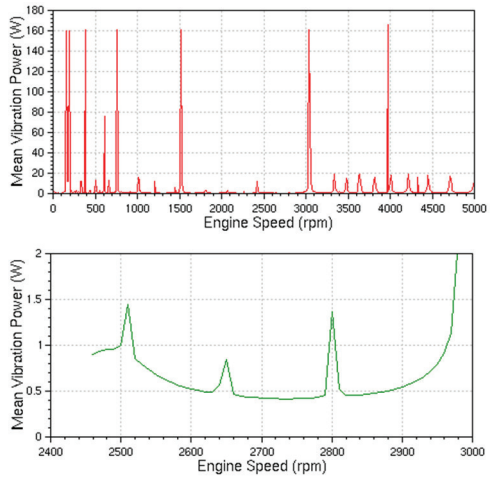

Figure 12. Mean vibration power of the torsional system (sum over all elastic elements): top – full speed range; bottom – operation speed range.

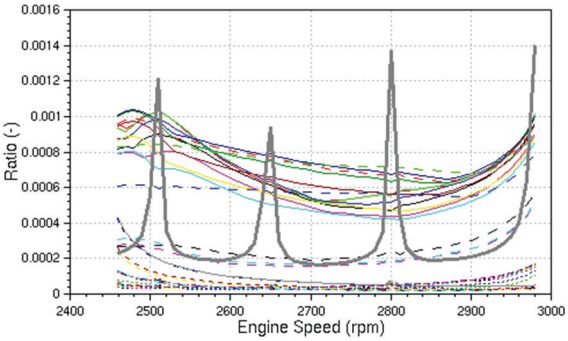

Figure 13. Speed irregularity of all mass points of the torsional system (in operation speed range)

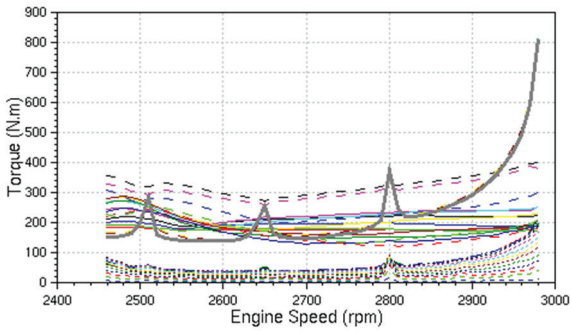

Figure 14. Maximum total torque of all elastic elements of the torsional system (in operation speed range)

Gyroscopic modal analysis of the pump shaft

The previous section described torsional analysis (including the pump shaft), but for a long/flexible shaft bending vibrations also become very important.

The pump shaft is the only part of the system which can be changed, because this is a part of the installation at the customer side (the rest of the system is produced by SET).

Taking this into account, the pump shaft has to be analyzed first alone, and later also within the system. The pump shaft possesses high mass and inertia, and is rather flexible because of its length (as was already seen by the torsional modes). This makes a gyroscopic modal analysis [7, 9] of the pump shaft an important task to analyze its dynamic properties.

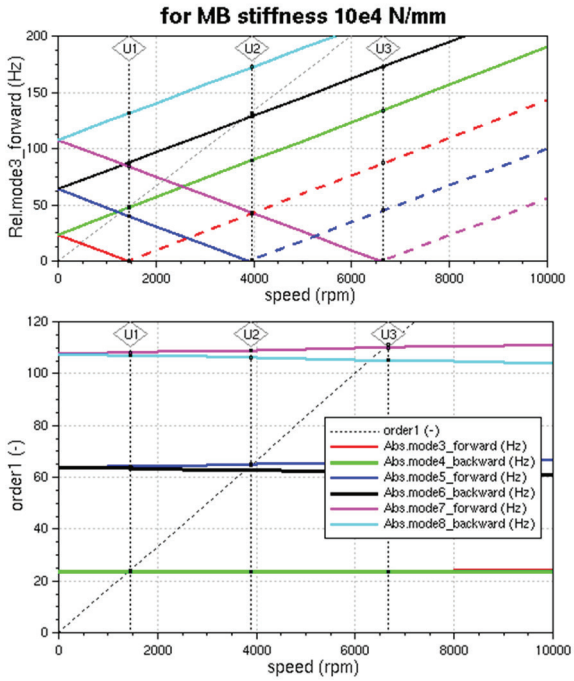

Figure 15. Mode and whirl tracking diagram: a) in rotating and b) in absolute coordinate system

The pump shaft is supported by two radial bearings. For a specified value of stiffness of the bearings, the gyroscopic modal analysis results in a mode and whirl tracking diagram, showing the dependence of natural frequencies on pump shaft rotation speed, with a specified value of main bearing stiffness (**Figure 15**), and resulting in different types of mode shapes (**Figure 16, a** and **b**).

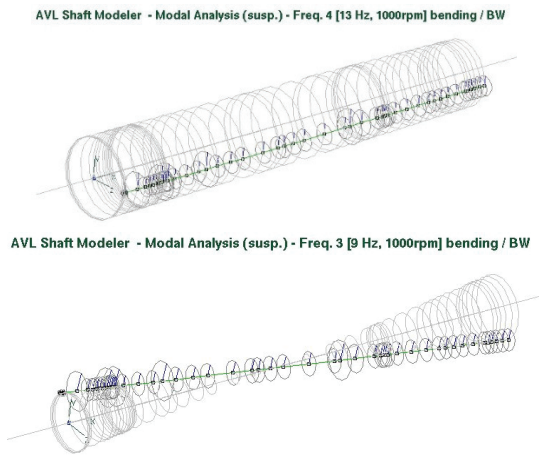

Figure 16 a. Different gyroscopic mode shapes (backward whirl)

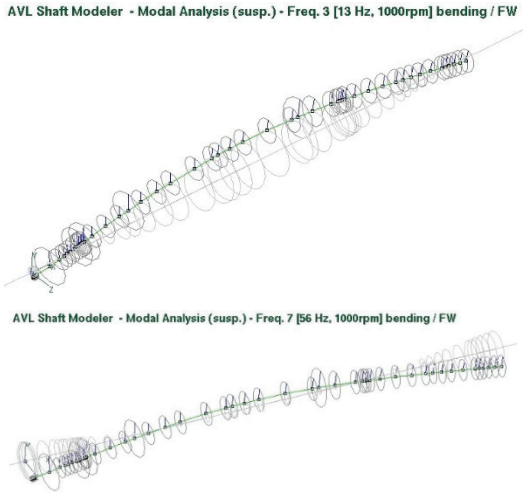

Figure 16 b. Different gyroscopic mode shapes (forward whirl)

As we see, the operation speed range does not contain the resonances which could lead to instability (**Figure 17**).

Unstable Resonances (REL)

Speed	Frequency
rpm	Hz
1418.0	0.0
3892.6	0.0
6596.0	0.0

Unstable Resonances (ABS)

Speed	Frequency
rpm	Hz
1418.0	23.6
3892.6	64.9
6596.0	109.9

Figure 17. Unstable resonances: critical speeds and corresponding frequencies in relative (REL) and absolute (ABS) coordinate systems

Influence of bearing stiffness

The results of the gyroscopic modal analysis strongly depend on the stiffness of radial bearings supporting the shaft (**Figure 18**).

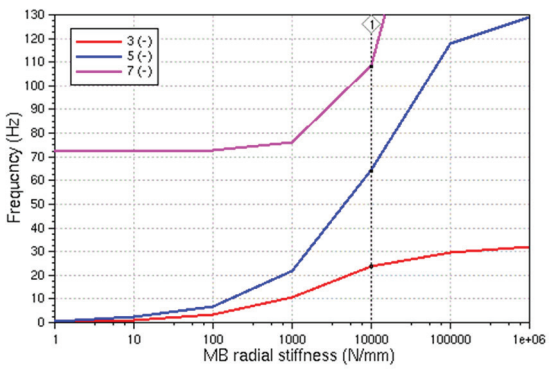

Figure 18. Dependence of frequencies at unstable resonances on radial bearing stiffness

Taking the known range of operating speeds (from 2460 to 2980 rpm for this particular equipment) into account, one can define the barred stiffness range for the radial bearings (**Figure 19**) which will keep the pump shaft away from resonances. This information can be used during the layout of the bearing by selecting an appropriate geometry, shell material and oil type. It can also be used for the motion control of the drivetrain, by passing the dangerous regions quickly without full load.

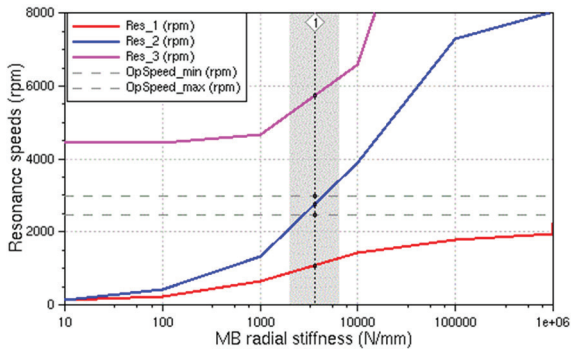

Figure 19. Dependence of speeds at unstable resonances on radial bearing stiffness

VMA: FINAL DESIGN PHASE

After finishing the early concept phase investigations and defining the main parameters, the final design phase dynamic simulations of VMA model are being performed to optimize the product. The requirements of VMA in this phase are:

- Functionality check;
- Reliability assessment of system parts;
- Requirements of standards and certification;
- Special requirements.

The investigation procedure to fulfill these requirements is explained below.

While in the early concept phase of VMA the dynamics of the mechanical system is considered in a reduced formulation (1D torsional modal analysis and forced response of the system, as well as 3D modal analysis of a separate shaft), in final design phase the modal analysis and force response of the system take the full FE modeling of the carrying structures (i.e. housings) into account – see a mode shape with modal energy visualized (**Figure 20**).

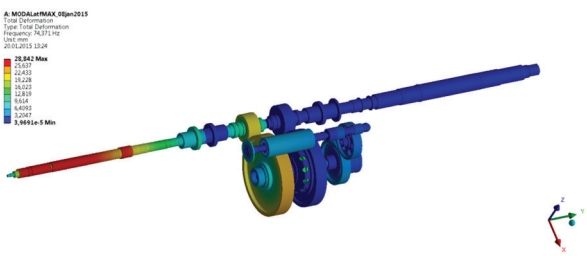

Figure 20. Modal analysis of the complete system with energy levels visualized

The ISO13709 standard [10] requires that the torsional eigenfrequencies of the complete system should lie at least 10% above/below any possible excitation frequency. Those standard requirements are applicable to some restricted number of applications only, because the modern industrial machinery usually operates at multiple speeds in a very wide speed range. Additionally, these systems have many coupled rotating shafts and gears, which makes it virtually impossible to avoid all the coincidences of the natural and excitation frequencies. For this reason, the ISO13709 standard defines further requirements for additional consideration and a deeper analysis regarding imposed dynamic conditions and transient stresses.

The modal analysis of the complete electro-mechanical system is just the first step in understanding of system dynamics. It is usually required for system certifications in many cases, too.

In any case, the final statement about the probability and the intensity of the possible resonances can be given based on the complete system simulation only (with all subsystems), including all nonlinearities, damping estimations, etc. Those final simulation steps in VMA include the transient analysis using MBD software AVL EXCITE™ [4, 11].

The VMA can be considered an imitation of testing before a real-life testing. For this purpose, one has to define the measurement points (positions of transducers) which map the model resonances (**Figure 21**).

These virtual measurement points record all the dynamical responses of the simulation model. An advantage of such virtual "transducers" is that they can be positioned everywhere in the model.

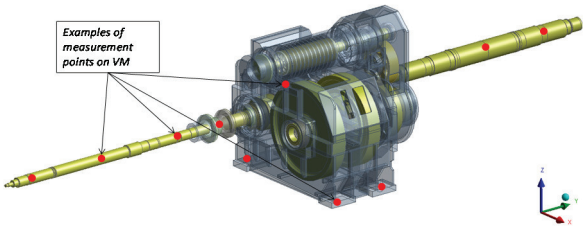

Figure 21. Measurement points in VM

The modeling strategy used at SET is to represent the components of the MBD simulation model that have the most influence on the complete system dynamic behavior, as flexible bodies. Thus, besides the flexibility of the shafts, clutches, carriers and ring gears, the full flexibility of all gearboxes and housings as carrying structures is necessary, as they can significantly contribute to the dynamic behavior of the system, while keeping them rigid could shift or hide resonances.

The results from MBD simulation are evaluated both in frequency and in time domains.

The virtual testing procedures in frame of VMA is similar to that of "standard" real-live one:

- Run-up;
- Speed-sweep.

The aim of the run-up procedure is to get the first estimate of the resonant behavior of the system in the complete speed range. To confidently identify the critical speeds, the run-up should be slow enough to allow the system to unfold the vibration amplitudes at resonant frequencies (**Figure 22** – red line shows the acceleration ramp).

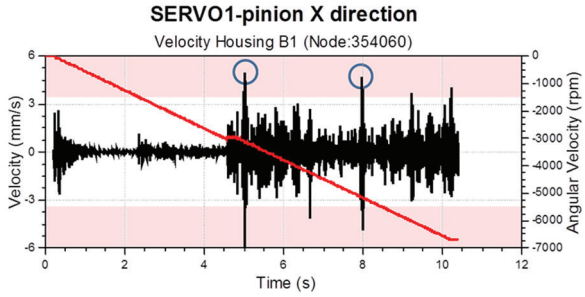

Figure 22. Run-up results in VMA

In addition to run-up, several very detailed steady-state dynamic analyses at different constant nominal speeds (the so-called speed-sweep) in the complete speed range are performed (**Figure 23**).

The constant nominal speed causes the system to be excited for a longer time, resulting in steady-state amplitudes for all output parameters.

These results are necessary for further VMA integration, which can be done by direct connection, i.e. a co-simulation using another software (e.g. MATLAB/Simulink) or by an indirect transfer of results (e.g. dynamic node displacements) to FE or Fatigue simulation tools [12,13,14].

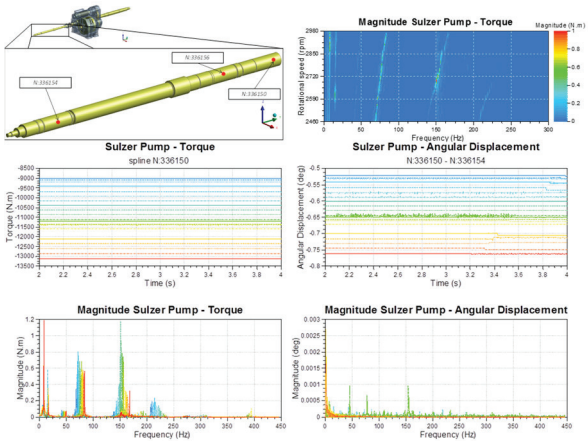

Figure 23. Speed-sweep results in VMA

VMA: EXTENDED ANALYSES

In addition to the detailed run-up and speed-sweep analyses, some more complex dynamic phenomena could and should be investigated in VMA like, for example, the potential for micro-pitting reduction, electric grid interruptions, slider bearings EHD behavior (**Figure 24**) and many others.

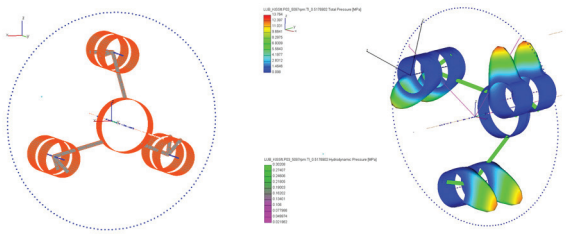

Figure 24. Slider bearings EHD investigation

VMA offers a possibility to investigate a complete system behavior in extreme situations even beyond the point of destruction, which gives a considerable advantage in further detailed development of highly dynamic mechatronic systems.

The VMA model is typically prepared using perfect geometry based on CAD and FEM inputs. What the VMA approach with advanced simulation tools like AVL EXCITE also enables, is the consideration of imperfections of the system resulting from production and assembly processes. These are:

- Unbalance of rotating parts;
- Misalignment of rotational / assembly axis;
- Run-out at bearings and gears;
- Surface roughness for slider bearings;
- Geometry imperfections of gear teeth.

Such imperfections can cause inefficient operation of the system, NVH issues, a failure of components and subsequently a failure of the complete system.

Performing a set of parameter variations for typical imperfections can point out what are the most critical ones and consequently direct the production and assembling process to avoid them. In addition, such parameter study will point out which imperfections will have no significant influence on the system behavior.

Knowing this, the manufacturer can, for example, focus on balancing of the components that have significant influence on the system behavior only and avoid balancing of the other components. The same is valid for surface finish, gear geometry, etc. This will result in a better product quality and lower production cost.

While developing SETCON®, the parameter study of unbalances of the shafts is performed by adding different unbalance levels on several locations of the shafts. The results of each unbalance case are compared to the ideal system, showing that the critical unbalance is the unbalance of the pump shaft. The level of force introduced by this unbalance can be 4x the force achieved by the ideal system. Knowing the bearing load carrying capacity the VMA model will provide the information about max. allowed unbalance level for the critical shaft.

VMA: COMPLETE SYSTEM

Finally, the complete electro-mechanical system is prepared following the VMA (**Figure 25**). With the experience and confidence of the methods and procedures used in developing and validating of the several highly dynamic industrial machinery, and by taking all the assumptions and the experience gained from previous investigations, into account – the same VMA could be implemented for any industrial machinery system.

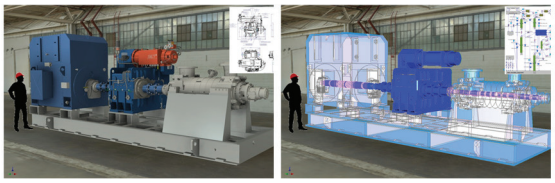

Figure 25. CAD model vs. VMA model

The influences of the electromagnetic and control sub-systems are applied in the same way to the model of 4.1 MW SETCON®.

For the reasons already explained, all carrying structures used for the complete system in VMA are kept as flexible bodies for standard resonance investigations. Depending on the investigation targets, the components included in the complete VMA could be chosen to be flexible or rigid.

One must be aware that any VMA is only an approximation of reality, but with a high potential to detect many dynamic phenomena even at the very early stage of product development.

VALIDATION

The final stage in any VMA procedure is a real model (RM) testing, implying a validation of the simulation results. The main objective of the validation process is to find the most influential and potentially dangerous resonances in the tested RM and compare their positions and intensity level with the VMA model. It is possible (and desirable) to use the real test results of the RM in order to predict and improve the dynamic behavior of the considered electro-mechanical system.

The SETCON® system 4.1 MW for feed pump application is tested in real conditions and test results are compared to verify previous VR-model simulation results. Several measurement points are investigated in detail.

Figure 26 shows measurement positions at RM that are compared both in time and in frequency domain with the same VM measurement points.

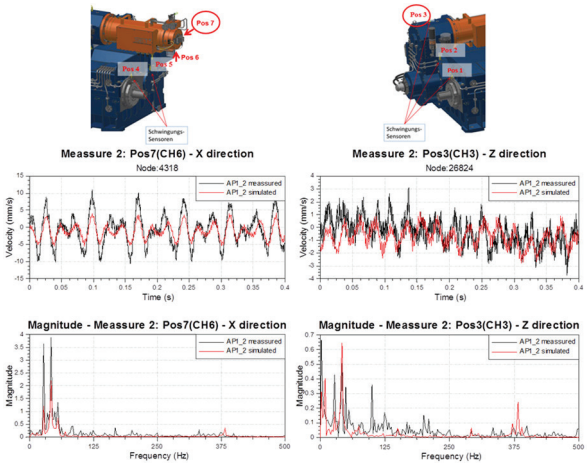

Figure 26. Verification of VMA

The validation procedures on different measurement points give very good correlations with VMA models.

This practically means that the real machinery (RM) will behave in accordance to almost the same dynamic patterns as predicted by VMA which effectively gives an opportunity to prevent many unnecessary destructions of the complete prototypes, saving enormous amounts of development time, as well as money.

CONCLUSIONS

The energy efficiency of industrial machinery is not just a means to improve the products in a highly competitive environment, but should also be considered a contribution to a better ecology.

It is possible, desirable and necessary to significantly improve the development process of the industrial machinery.

Currently, the certification processes and standards become more demanding, requiring a certain level of dynamic simulation to be used in the development process of industrial machinery.

The possibilities of Virtual Model Approach (VMA) presented in the paper, go even further in developing the new and improving the existing electro-mechanical systems.

The developed methodology of VMA and the applied tools enable a pre-optimization of the individual sub-systems, as well as dynamic investigations of a complete electro-mechanical industrial machinery on a virtual test bed (or in real operating conditions) – even before any hardware is available.

The effective direct integration of a mechanical, electrical and controlling system in VMA is a powerful methodology for efficient development of complex mechatronic systems.

REFERENCES

1. Janic, M. and Bukovnik, S., "Management Demand: 'First-Time-Right'; A new drive-train technology development based on a Virtual Model Approach," European Wind Energy Association Annual Event (EWEA 2014), Barcelona, Spain, Vol. 1, pp. 172-181.
2. Janic, M., "Development of High-Speed Railway Gearbox," AVL International Simulation Conference ISC-2017, Graz, Austria.
3. EXCITE™ Designer, *Software package for crank train and driveline analysis in early concept phase*, AVL List GmbH (Release v2018).
4. EXCITE™ Power Unit, *Software package for flexible multi-body dynamics*, AVL List GmbH (Release v2018).
5. Hehenberger, M., "Increased efficiency and reliability through an electro-mechanical differential system providing variable speed to pumps and compressors," *European Fluid Machinery Congress, Institution of Mechanical Engineers* (2016).
6. Parikyan, T., "Unified Approach to Generate Crankshaft Dynamic Models for 3D and Torsional Vibration Analyses," *ASME Paper* ICES2003-591 (2003).
7. T. Parikyan, "Complex modes analysis for powertrain and driveline applications," *Proceedings of International Conference on Noise and Vibration Engineering (ISMA),* Leuven, Belgium, pp. 2761-2774 (2016).
8. Parikyan, T., "Multi-Cycle Torsional Vibration Simulation with AVL EXCITE Designer," *ASME Paper* ICEF2011-60091 (2011).
9. *AVL Shaft Modeler with AutoSHAFT Users Guide*, AVL (Release 2018).
10. Standard ISO 13709:2009 - Centrifugal pumps for petroleum, petrochemical and natural gas industries.
11. Offner, G., "Modelling of condensed flexible bodies considering non-linear inertia effects resulting from gross motions," *Proc. IMechE, Part K: J. Multi-body Dynamics* (June 2011).
12. ANSYS Workbench, Release 17.0.
13. WinLife, Steinbeis-Transferzentrum.
14. MATLAB/Simulink, Registered trademarks of The MathWorks, Inc. (Version R2017b).

РАЗРАБОТКА ПРОМЫШЛЕННЫХ НЕПРЕРЫВНО РЕГУЛИРУЕМЫХ ЭЛЕКТРОМЕХАНИЧЕСКИХ ТРАНСМИССИЙ НА ОСНОВЕ МЕТОДА ВИРТУАЛЬНОГО МОДЕЛИРОВАНИЯ

М. Янич, М. Миклаучич
СЭТ Устойчивые энерготехнологии ГмбХ, Клагенфурт, Австрия
Т. Парикян, С. Буковник
АВЛ Лист ГмбХ, Грац, Австрия

АННОТАЦИЯ

Из-за рыночного спроса на экономически более эффективное оборудование, все больше внимания уделяется приводам с регулируемой скоростью для разных машин. Обычно, когда используется управление скоростью, рассматриваются преобразователи частоты (полномасштабные преобразователи), редукторные муфты с переменной скоростью или гидродинамические приводы с переменной скоростью. Однако установка мощного электропривода может привести к высоким затратам на приобретение и значительной потере эффективности.

Мехатронная система под названием SETCON® разработана СЭТ и может достигать 25 МВт передаваемой мощности с номинальной скоростью до 15000 об / мин.

В разработке такой системы компания СЭТ использует проверенную методологию, известную под названием «Метод виртуальный модели», опираясь на высококачественные программные средства, в том числе на программное обеспечение AVL EXCITE™.

Разработка энергосистемы мощностью 4,1 МВт, представленная здесь, была протестирована в реальных условиях, и стендовые измерения сравнивались с измерениями виртуальной модели, что показало отличное совпадение.

Proceedings of the 1st International Conference MES-2018 / ИРМ-2018
MECHANICAL ENGINEERING SOLUTIONS
Design, Simulation, Testing and Manufacturing
September 17-19, 2018, Yerevan, ARMENIA

MES2018-22

Case study on Detecting Rub Issue on Compressor

Nicolas PETON[1], Sergey DRYGIN[2], Tagumpay DE GUZMAN[3]

[1]Baker Hughes, a GE company, Nantes, France, e-mail: Nicolas.Peton@bhge.com

[2]Baker Hughes, a GE company, Moscow, Russia, e-mail: Sergey.Drygin@bhge.com

[3]Baker Hughes, a GE company, Taguig, Philippines, e-mail: Tagumpay.Deguzman@bhge.com

ABSTRACT

This case is a vibration issue on a Recycle Gas Compressor. The Machinery Diagnostics Engineer was requested on site to collect only steady state data using a multichannel data collector. When Unit was running at full load condition, vibration at Compressor suddenly increased and exceeded Alert setpoint. Operation at this condition is unsafe and can be result of serious unit damage.

This case study is designed to outline how the high vibration issue was successfully diagnosed based on very limited set of information - only steady state data collection, the root cause for the high vibration found and correction actions recommended and applied.

The source of high vibration was considered as rotor unbalance, appearing due to material build up at the rotor. It was the initial issue, leading to the Rubbing symptom in the compressor seals and the rotor thermal bow.

Compressor rotor inspection was recommended. Signs of significant rubs were found. Compressor rotor was replaced. Vibration level at Unit Startup was well below OEM setpoints.

INTRODUCTION

General Electric (GE) is an American multinational conglomerate corporation, one of the worldwide leaders of machine manufactures and industrial solutions provider. Baker Hughes, a GE company (BHGE) is the world's first and only full-stream provider of integrated oilfield products, services and digital solutions. Bently Nevada, a part of BHGE Oil & Gas Digital Solutions with Machinery Diagnostic Services portfolio, with more than 40 years of offering unbiased diagnostic assistance regardless of the manufacturer. Our team is comprised of more than 150 Machinery Diagnostic Engineers, globally distributed, with decades of experience and over 10,000 MDS projects executed.

The historical DCS trend plots for the recycle gas compressor were provided to MDS engineer. Selected process measurements were defined by the end-user with an obvious vibration spiking. The information provided was limited related to abnormal operation. In most cases, operators rely on intuition and experience to assess machine status.

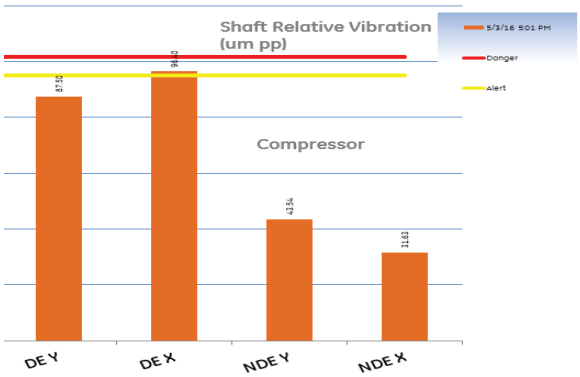

Figure 1 Overall vibration vs. OEM alarm/danger set-points.

Based on the DCS data, vibration amplitudes fluctuated, then rapidly raised up at full load. The dominant high vibration level – 98 um pp, higher than Alert (H), very close to Danger (HH) setpoint was synchronous component (106.25Hz or 1X order component for full speed), (Figure 1).

Shaft relative vibration data acquisition was performed using Bently Nevada multichannel data collector ADRE 408 system connected to the Bently Nevada 3500 machinery monitoring and protection system. The high vibration level was observed at compressor bearings. The phase data analysis of filtered 1X shaft rotation vibration component demonstrated unidirectional, in-phase shaft motion for Drive End and Non-Drive End Bearing planes (Figure 2).

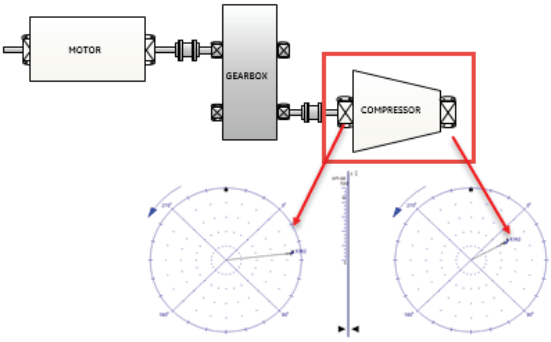

Figure 2. Train diagram with related Polar plot from compressor DE bearing.

Vibration assessment using only steady state data was performed. No transient mode was available to capture data during machine speed changes and its associated force or stiffness change; these are important parameters that would reveal new sets of information related to balance resonances, synchronous amplification factor (SAF), shaft centerline movement or even GAP reference.

The source of mentioned synchronous excitation was considered as increased centrifugal force – rotor unbalance, appeared due to material build up at the rotor. The reason of these deposits on the rotor is long time Unit operation without maintenance. Because the unbalance mass became part of the rotor, the 1X unbalance force acted through the Dynamic Stiffness of the system to cause vibration (Fundamentals of Rotating Machinery Diagnostics). The relationship of dynamic response of the rotor system can be written as:

Vibration = Force / Dynamic Stiffness (1)

It was the initial issue. As the unbalance-induced vibration was increased, the rotor deflection produced 1X cycling stress that led the rub symptom in the compressor seals and then rotor thermal bow. A thermal rotor bow can develop while the machine is running. If a hotspot develops on one side of a rotor and that part will expand, the uneven expansion will produce one-sided thermal growth and therefore develop a bow.

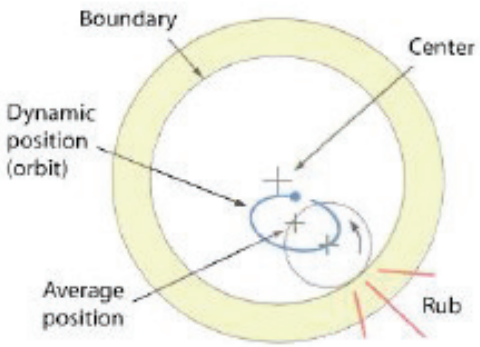

Figure 3. Rub will occur when position of rotor uses up available space.

Rotor Rub is defined as a physical contact between rotating elements and stationary machine parts (Machinery Malfunction Diagnosis and Correction). The heavy rub suspected in this case was almost a possibility. Machinery rubs are usually a secondary malfunction. Rub can be caused by excessive shaft vibration due to unbalance, fluid induced instabilities, extreme shaft centerline position due to misalignment or insufficient internal clearance. Rub due to insufficient clearance became common because of the desire to improve machine efficiency.

In this case, the excessive motion of rotating shaft/rotor relative to the clearance of interstage seals led to rub condition. 1X rolling or roving phase was not observed, although the possible wiping of material led to huge 1X vibration. The shape of orbits for both bearings demonstrated the sign of restricted movement at the bottom side.

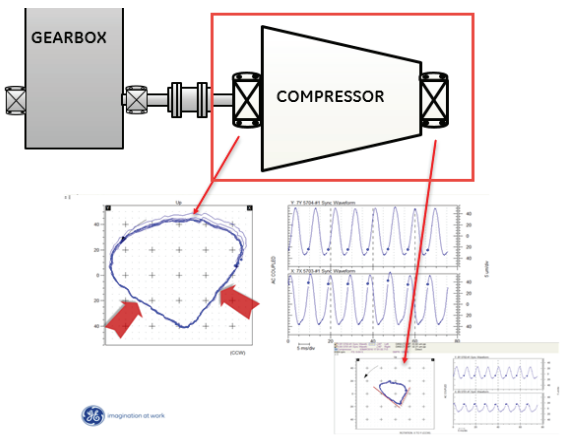

Figure 4. Compressor DE/NDE related Orbit plots exhibited restricted movement at bottom side.

The unit was shut down and compressor rotor inspection was recommended to Customer. Signs of significant rubs – wiped out metal – were found on the rotor (Figure 5). Compressor rotor was replaced. Vibration level at Unit Startup was well below OEM setpoints.

Figure 4 Actual rotor condition and rub location.

To avoid such situation in the future the acceptance regions alarming for 1X vector were recommended to the Customer to track changes and for early detection of material deposit on the rotor. An Acceptance Region alarm is comparable to an Out of Band alarm with four separate boundaries. Two of the boundaries are set by phase setpoints and the other two boundaries are set by amplitude setpoints. The measured parameter must leave the "allowed" sector between these boundaries to activate this alarm.

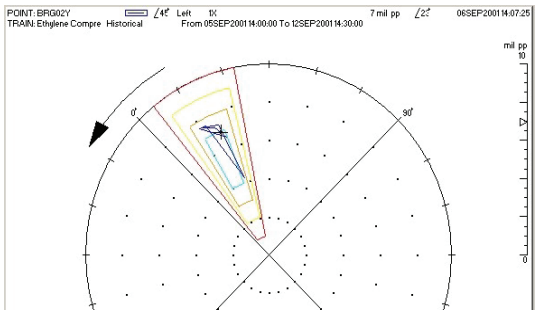

Figure 5 Sample acceptance region alarming.

CONCLUSION

The source of high vibration was due to increase in dynamic force (unbalance due to damage or material deposit/buildup). There was an apparent rubbing that led to material wipe out on rotor sleeve and damage to interstage seals.

Compressor constitutes an important part of the mechanical equipment in oil & gas industry and used for main and auxiliary process cycles. This recycle gas compressor is designed to provide a steady flow of process gas in the plant.

An online monitoring system is essential for critical compressors. This will provide safe and reliable production. GE/Bently Nevada's professional software packages System1 can also significantly contribute to enhance machinery management capabilities by providing even more useful machinery diagnostics and recommended corrective actions for machinery operators, managers, and maintenance personnel.

REFERENCES

1. D.E. Bently, *Fundamentals of Rotating Machinery Diagnostics, (Design and Manufacturing).* American Society of Mechanical Engineers (2003)
2. Robert C. Eisenmann, Sr., P.E. and Robert C. Eisenmann, Jr. *Vibration Analysis and Troubleshooting for the Process Industries.* Pearson Education, Inc (2005)
3. BHGE, DS Bently Nevada, *Machinery diagnostic technical training.*

ИССЛЕДОВАНИЕ СЛУЧАЯ ОБНАРУЖЕНИЯ ПРОБЛЕМЫ В СВЯЗИ С ИЗНОСОМ КОМПРЕССОРА

Николас ПЕТОН, Сергей ДРЫГИН, Тагумпай ДЕ ГУЗМАН

Бейкер Хьюз, Компания Дженерал Электрик
Нант, Франция / Москва, Россия /
Тагуиг, Филиппины

АННОТАЦИЯ

Данный случай представляет собой описание проблемы повышенной вибрации газового компрессора. Инженер по диагностике оборудования был вызван для сбора данных только стационарного режима работы компрессора, используя многоканальный сборщик данных. При работе на номинальной нагрузке вибрация компрессора внезапно увеличивалась и превысила уставку "Предупреждение". Эксплуатация в этом состоянии небезопасна и может быть результатом серьезного повреждения агрегата.

Этот случай описывает пример успешного диагностирования проблемы повышенного уровня вибрации, выявления причины и предоставления рекомендаций по устранению проблемы.

Причиной высокого уровня вибрации было определено увеличение центробежной силы – дисбаланса ротора, возникшего из-за отложений на роторе. Это была первоначальная проблема, которая привела к появлению симптомов задевания в уплотнениях компрессора и тепловому изгибу ротора.

Остановка компрессора и проведение ревизии проточной части компрессора были рекомендованы Заказчику. Признаки значительного износа – затиры были обнаружены на роторе. Ротор компрессора был заменен. Уровень вибрации при запуске устройства после ремонта был значительно ниже значений "Предупреждение" и "Авария".

Proceedings of the 1st International Conference MES-2018 / ИРМ-2018
MECHANICAL ENGINEERING SOLUTIONS
Design, Simulation, Testing and Manufacturing
September 17-19, 2018, Yerevan, ARMENIA

MES2018-28

Crankshaft and Bearing Analysis and Design Optimization Process

Ilya L. Piraner, Jiawei Liu, Amit Gabale

Cummins Inc., Columbus, IN, USA, e-mail: ilya.l.piraner@cummins.com

ABSTRACT

Design of the modern diesel engine crankshaft presents multiple challenges related to contradictory requirements of engine durability and packaging. In this approach, a high level concept study is used initially to determine overall engine size, speed and cylinder pressure. The next step is a more detailed crankshaft optimization within predefined geometrical space. Various requirements should be satisfied to achieve reliability and durability targets for crankshaft and bearing system. Since optimization requires studies of multiple designs, quickly executable and simplified models are used at this stage. In the described process a coupled quasi-static beam and rigid hydrodynamic bearing model is used to quickly obtain performance characteristics of the crankshaft and the bearings. This model requires a high level of parameterization. Once a parametric model of the crankshaft and bearing system is built, a DOE study is performed for multiple engine conditions and response surfaces are generated for all relevant performance characteristics. Response surfaces are used for quick system optimization for various conditions and given set of constraints. After the best design is selected, it undergoes a validation process using a combination of quasi-static bending and dynamic torsional models along with the detailed 3D FE models. The final stage of the design validation process is building a flexible multibody simulation model for a combination of the crankshaft and relevant portion of the driveline, to ensure the durability of the crankshaft under dynamic loading.

INTRODUCTION

Design of the modern diesel engine crankshaft is a complex process where multiple requirements related to engine durability, packaging and cost must be satisfied and balanced. Normally engine size is determined by the required power and geometrical constraints based on high level engine performance models. Once overall engine size, speed and cylinder pressure are defined, a more detailed crankshaft optimization within predefined geometrical space is performed. Various contradictory requirements should be satisfied to achieve reliability and durability targets for the crankshaft and bearing system. For example, increased crankshaft durability requires taking more space from the bearings by increasing crankshaft web thickness and fillet size. This in turn reduces the load carrying capacity and durability of the bearings. The best design is a trade-off between crankshaft and bearing durability characteristics, which is ideal for an optimization process. At Cummins a process has been developed where technical requirements are used as constraints and minimization of bearing friction is used as an optimization goal. Since optimization requires studies of multiple designs, quickly executable and sufficiently simplified models are used at this stage. These models require a high level of parameterization which is achieved through a combination of preliminary DOE studies using 3D CAD and FE models for the crankshaft and driven components. For example, crankshaft stiffness and stress concentration characteristics are calculated based on regression formulae built using simplified parametric models of a crankshaft throw. DOE studies of the entire crank/bearing system are used to build Response surfaces, which in turn are used for quick optimization of the system key parameters considering various engine conditions and the given set of constraints. After the best design is selected, it undergoes local feature optimization and an overall validation process using a combination of quasi-static and dynamic models. In the end a full three dimensional flexible multibody simulation model for a combination of crankshaft, block and relevant portion of the driveline is used to ensure durability of the crankshaft under dynamic loading. For this purpose commercial

software Excite from AVL has been selected and validated through strain measurements in the working engine.

DESIGN PROCESS OVERVIEW

The current trend in the Cummins' Analysis Lead Design initiative is to develop a multi-level approach to crankshaft and bearing analysis. The overall process of crankshaft development is shown in Figure 1.

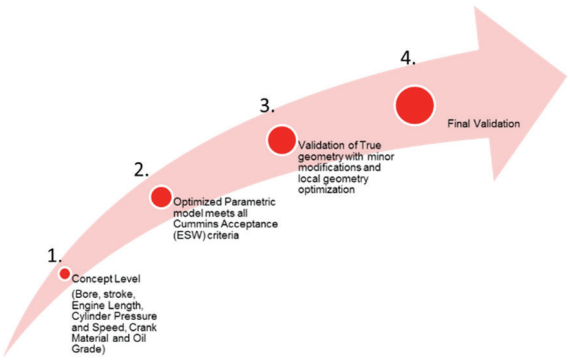

Figure 1. Crankshaft Development Stages

Though this process clearly designates four stages, the true crankshaft analysis is conducted at stages 2 through 4 with stage 4 used predominantly as design confirmation. A high level concept study is done to come up with overall engine parameters: overall engine dimensions, bore, stroke, cylinder pressure for the speed range, crankshaft and bearing material, etc. This stage defines the envelope for crankshaft dimensions; within this envelope the dimensions must be optimized to achieve the best performance in terms of reliability, efficiency and cost. This work happens at stage 2 (preliminary crankshaft and bearing analysis) of the design process where efficient simulation methods and models should be used. The main characteristics of these models are speed, robustness, simplicity as well as sufficient accuracy. These methods are used to explore the design space via parametric studies, DOE and optimization processes to come close to the final design which would satisfy all major requirements. Normally, the inputs for computational models on that level are developed based on historical data or easily calculated based on engine major dimensions; execution time for one simulation would be just a few minutes. The next level (stage 3) of modeling is much more complex; it requires CAD/FE data, involves detailed 3-dimentional analysis and may involve multi-body simulation. While adding complexity often helps in understanding the true physics of complex interactions, inevitably it adds cost and computational time. Therefore, such methods are used predominately as a final validation of the design at stage 4.

A number of considerations need to be addressed in the preliminary crankshaft and bearing design analysis. Among these considerations are crank stress, bearing performance, crankshaft balance, integrity of bolted joints, damper durability and the impact of the crank on block stress and deformation. Though each consideration may require a detailed and complicated analysis, simplified approaches have been developed over the years by the industry and successfully applied at Cummins. The primary focus of the preliminary analysis is to make sure that crankshaft fillet stresses meet design targets while satisfying bearing performance characteristics in terms of Minimum Oil Film Thickness (MOFT) and Peak Oil Film Pressure (POFP). The simplest crankshaft analysis scheme is the so-called statically determinate scheme (S-D) and is still the primary methodology established by International Association of Classification Societies (IACS) [1]. According to this approach bending and torsional loading are considered separately. For torsion a classic dynamic lumped mass scheme for the entire crankshaft with necessary elements of the drive line is adopted. For bending, each of the crankshaft throws is considered statically and independently, being supported at the middle of the main journals. Bearing loads are calculated as a summation of loads coming from the adjacent throws. IACS developed a set of formulas for calculating stress concentration coefficients for main and pin fillets separately for bending and torsion for a range of dimensionless parameters. While the approach to torsional analysis is well established and is deemed to be sufficient, consideration of the crankshaft throws independently for bending analysis is not sufficiently accurate. A model where all throws are considered simultaneously with account for main bearings support becomes statically Indeterminate (S-I). Figure 2 shows that for a V8 crankshaft, the difference in the maximum calculated bending stress between S-D and S-I models may reach 20%.

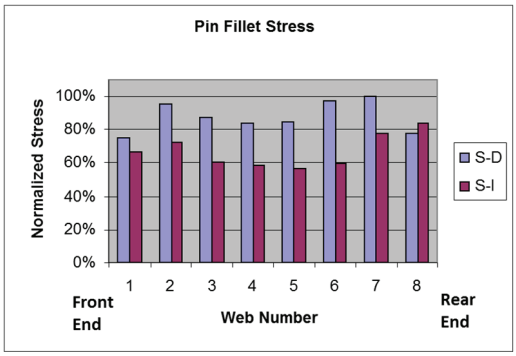

Figure 2. Comparison between Statically-Determinate (S-D) and Statically-Indeterminate (S-I) models

Therefore for this purpose of bending stress analysis Cummins uses a model which couples statically indeterminate quasi-static crankshaft scheme with a fast model for hydrodynamic bearings. An

advantage of such a scheme is that while being still sufficiently simple and robust it takes into account such effects as internal bending moments, bearing clearance, journal and bearing misalignments, and bearing support stiffness.

COMPUTATIONAL MODELS

Various techniques have been developed in 70's and 80's for quasi-static (Q-S) crankshaft analysis. Cummins implemented a coupled crankshaft/bearing scheme first suggested by Welch and Booker [2]. Figure 3 shows schematics of the crankshaft model which is solved using the matrix transfer method [3]. It allows for a simple expression relating state vectors Z_i^R and Z_{i+1}^L:

$$Z_{i+1}^L = T_i Z_i^R \qquad (1)$$

where the extended state vector Z has following components:

$Z^T=[u_y\ \phi_x\ m_x\ f_y\ u_x\ \phi_y\ m_y\ f_x\ 1]$,

u_y and u_x are displacements along corresponding axes,
ϕ_x and ϕ_y are angles,
m_x and m_y are moments and,
f_y and f_x are forces along the axes.

Index "L" indicates state vector on the left side of support and index "R" on the right side.

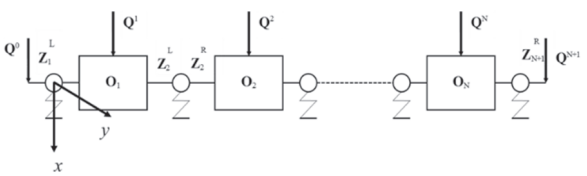

Figure3. Crankshaft Model

Transfer matrix T_i includes both internal parameters of object O_i (geometry and material characteristics) as well as the external loads applied to the object (Q^i) and is built based on beam representation of the throw. Similarly, a transfer matrix of the support P_j can be created which links the state vectors before and after support #j:

$$Z_j^R=P_jZ_j^L \qquad (2)$$

Schematics of main bearing support model is shown in Figure 4, where:

k_{xj} and k_{yj} are support stiffness in two directions,
ϕ_{xj}^0 and ϕ_{yj}^0 are angular misalignments of the support,
u_{xj}^0 and u_{yj}^0 are linear misalignments of the support,
u_{xj}^h and u_{yj}^h are hydrodynamic displacements of the journal center within bearing clearance.

Assuming hydrodynamic displacements are given and taking into account (1) and (2) a simple matrix multiplication yields equations relating state vectors at the ends of the crankshaft:

$$Z_{N+1}^R = P_{N+1}\ T_N\ P_N\ \ldots\ T_1\ P_1\ Z_1^L \qquad (3)$$

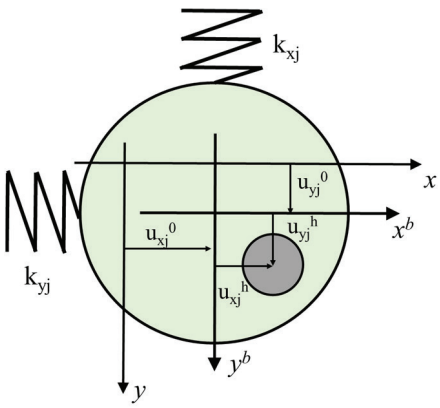

Figure 4. Bearing Support Model

Expression (3) can be rearranged to obtain the resultant system of four equations with respect to four unknowns: u_{y1}, ϕ_{x1}, u_{x1}, and ϕ_{y1}. This in turn allows the calculation of the remaining state vectors according to (1) and (2).

After the state vectors Z_j are found, reactions in the main bearings can be calculated as

$$R_{xj} = -k_{xj}(u_{xj} - u_{xj}^0 - u_{xj}^h)$$
$$R_{yj}= -k_{yj}(u_{yj} - u_{yj}^0 - u_{yj}^h) \qquad (4)$$

Therefore, neglecting the inertial force associated with journal motion within the bearing clearance, load to the bearing #j can be written as follows:

$$\mathbf{F}_j=-\mathbf{R}_j=\mathbf{F}_j(\mathbf{Q},\mathbf{U}^0,\mathbf{U}^h,\mathbf{a}) \qquad (5)$$

where: **Q** is a combined vector of external force,
$\mathbf{U}^0$ - a combined vector of misalignments,
$\mathbf{U}^h$ -combined vector of hydrodynamic displacements,
a - set of crankshaft design parameters (crankshaft dimensions such as journal lengths, diameters, etc. as well as material properties).

On the other hand, the mobility method [4] can be used for individual hydrodynamic displacement $\mathbf{u}_j^h$ and velocity $\mathbf{v}_j^h=d\mathbf{u}_j^h/dt$, which can be written as follows:

$$\mathbf{v}_j^h = g\ \mathbf{M}(\mathbf{u}_j^h,L_j/D_j)\ |\mathbf{F}_j| + \boldsymbol{\omega} \times \mathbf{u}_j^h\ , \qquad (6)$$

where:
M – Mobility vector

L_i and D_i – bearing length and diameters, and
ω – half of the journal velocity.

Therefore, for the main bearings, a system of 2x(N+1) differential equations needs to be solved. Approximations given in [5] with some modifications to account for grooves in the main bearings were found to give remarkably good results in a wide range of parameters. An iterative process is used to converge on the bearing orbit and oil temperature.

As was mentioned earlier, transfer matrix T in the expression (1) is built based on a beam representation of the crank throw. While such a model mimics real throw topology if built based on geometry it tends to significantly underestimate crankshaft stiffness. It was shown [6], that the accuracy of a crankshaft analysis can be significantly improved if just a few parameters of the frame model are adjusted based on the FE solution for each half of the throw. The main idea is that for bending, the most compliant element of the throw is the web. Under a torsional load, deformation is split evenly between web and the pin journal. Then considering pure bending in two planes, torsion for each of two planes, and torsion for each of two halves of the throw, the following expressions can be written:

$$I_w = R/(\varphi_1 E - f/I_p - c/I_m)$$

$$I_w^p = ER/G/(\varphi_2 E - f/I_p' - c/I_m) \qquad (7)$$

$$I_p^p = f/G/(\ (2U_1/R-\varphi_3) - c/I_m^p)$$

$$I_w' = GR/2/E/(G\varphi_3 - G\ U_1/R + c/I_m^p)$$

where:
I_w - web cross-sectional (in plane) moment of inertia
I_w^p - polar moment of inertia of the web beam element
I_p^p - polar moment of inertia of the pin
I_w' - cross-sectional moment of inertia of the web in the perpendicular plane
I_p -cross-sectional moment of inertia of the pin for bending in the plane of the throw,
I_m - cross-sectional moment of inertia of the main,
E - Young's modulus,
$\varphi_1,\varphi_2,\varphi_3$ – angular compliance of the half throw for bending in two planes and torsion,
U_1 – linear compliance coefficient under torsion load ($U_1 = u_x/T$ as shown in Figure 5),
R- crank radius
f - half-length of pin
c- half-length of main journal

Once forces and moments in the crankshaft are defined, stress in the fillets can be calculated using stress concentration coefficients or stress-to-moment ratios. These are calculated for each main and pin fillet as a ratio of maximum stress in the fillet over the bending moment. Since the load path is different for the firing and the inertia loads, two ratios are calculated for each fillet and used separately depending on the sign of the bending moment in the web.

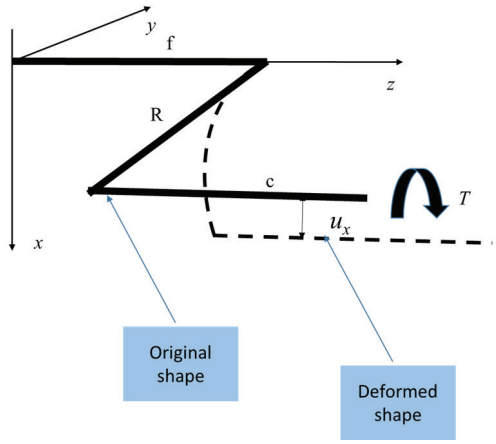

Figure 5. Definition of Torsional Compliance

While in-house programs are very efficient and allow full control over the simulation process and opportunities for improvements, commercial tools become attractive because they offer a well-developed graphical user interface, new modeling opportunities and integration with optimization processes. Gamma Technologies (GT) has adopted similar techniques for crankshaft and bearing analysis and therefore Cummins was able to smoothly transition from the use of in-house codes to their commercial equivalents [7]. Figure 6 shows an example of crankshaft representation within GT GUI.

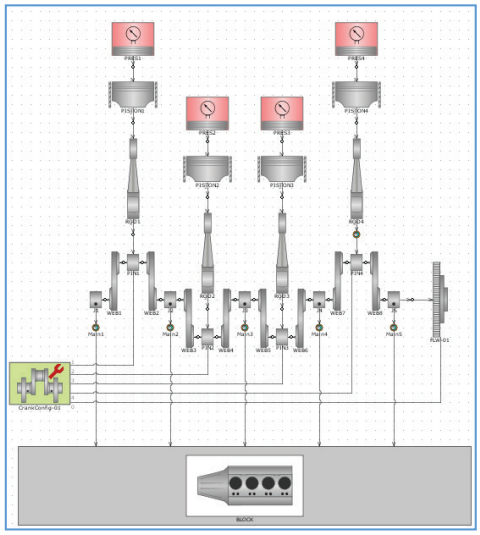

Figure 6. Four Cylinder Crankshaft Model Representation in GT-SUITE

A significant advantage of GT is that it allows to simply turn any of the model numerical values into parameters which will be sent into special table well suited for parametric or DOE studies as shown in

Figure 7. The key here is to analytically map all necessary characteristics to crankshaft critical parameters. The simplest example of that is web thickness which can be defined as (Cylinder Spacing – Main Journal Length – Pin Journal Length)/2 for a given cylinder spacing. Many other characteristics require significant DOE studies to come up with the analytical definition necessary for parameterization. For example definition of stress-to-moment ratios and crankshaft throw stiffness required building simplified CAD and FE models. To make the parameters independent of the actual crank size, all parameters were taken as a ratio to crank pin diameter. Via study of several existing crankshafts it was possible to determine the likely ranges of these ratios. These were taken into consideration when setting the parameter ranges in the DOE. Mapping the DOE output variables was done back to dimensionless parameters, not a specific part size, and then scaled according to specific pin diameter.

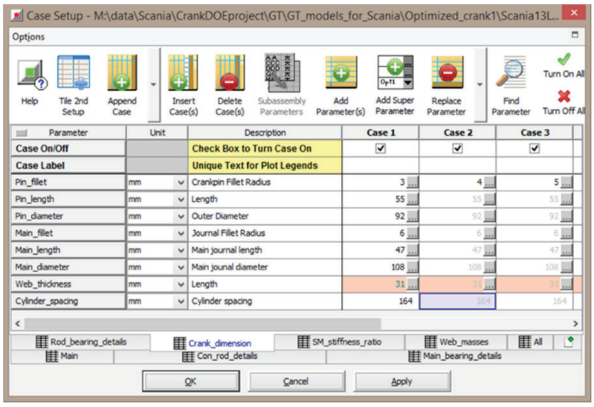

Figure 7. Key Crankshaft Geometric Parameters

Once the crankshaft model is fully defined using critical parameters along with true ranges for a particular application, a DOE study can be performed. With the order afforded by the use of central composite design of experiments, it became feasible to map key design output variables (fillet stresses, rod and main bearing film properties, crank balance, etc.) against key input variables (crankshaft and bearing geometry, engine speed, cylinder pressure, etc.). MINITAB tools are used to build surface response functions based on the DOE and optimize the design using multiple constraints. The employed strategy is to minimize power loss associated with bearing friction, while satisfying limits on fillet bending stress and bearing performance characteristics such as oil film pressure and thickness. A typical outcome of MINITAB optimization in shown in Figure 8, where Power Loss indicates bearing power loss, Main_EFR and Pin_EFR represent effective fully reversed stress in the fillets and MOFT(L) and MOFT(U) represent minimum oil film thickness correspondingly on the lower and the upper shell. Red lines and red numbers in the design space indicate optimum values. In this example the limiting factors were stress in the pin fillet and oil film thickness in the upper shell as indicated by desirability numbers.

The beauty of optimization using surface response functions is the short amount of time it takes to come up with the optimal characteristics. Because of this, it becomes easy to explore the space by changing constraints and balancing out various requirements. For example, different crankshaft material can be used, so the limit on stress can be changed and the impact on the design can be evaluated. Similarly, there is normally a choice of bearing materials, so the limits on bearing oil film pressure and thickness can be adjusted and the new optimal design can be found within seconds showing impact on crankshaft dimensions and friction. Since only bending stress is considered at this stage, the stress limit is adjusted based on historical data for torsional stress which comes from torsional analysis.

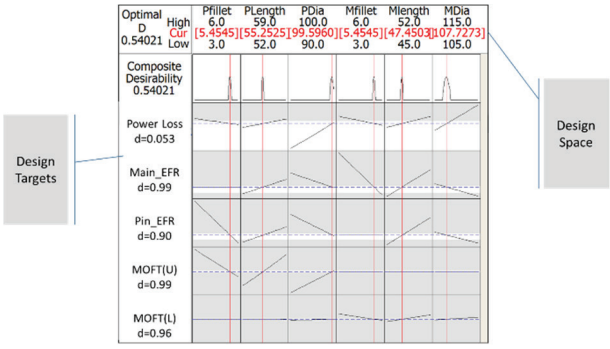

Figure 8. Typical Optimization Outcome

Once an optimal design is determined the process moves to stage 3 – Combined Stress (COMS) Analysis as shown in Figure 9. Here the simplified crankshaft throw FE model is replaced with a fully featured CAD model to provide more precise stiffness and inertia characteristics, and the analysis is repeated for realistic geometry. In parallel with bending analysis in GT a torsional model is built and torsional dynamic analysis is performed for the same conditions. Bending loads at the middle cross-sections of the main journals from GT and dynamic torque from torsional analysis are combined and sent into the COMS program. The other input is stress files corresponding to unit load cases which include pin loads, inertia loads and the moments applied at the main journals. The unit loads analysis is done on a single throw model, selecting nodes at different locations since crankshaft fatigue limit normally varies by location. For example, crankshaft fillets are normally induction hardened or rolled which improves fillet fatigue limit significantly; journals are normally induction hardened while portions of the webs are either machined or left as is. Therefore analysis for these locations is done separately and as a result local geometry of the webs and oil hole diameter and location can be adjusted to satisfy stress criteria. Boundary conditions for the unit load cases are applied through a combination of soft and stiff discs and rings

as shown in Figure 9. This gives a more realistic load distribution over journal surface.

Since bending stress is simulated in a quasi-static mode an additional quick analysis is performed as a screening test to address crankshaft rear and front end vibration, which is frequently referred as flywheel whirl. This phenomena is well described in the literature [8-10], and requires true dynamic representation of the system including accounting for gyroscopic effect, which takes significant time to build and solve. Therefore, at stages 2 and 3 a simplified approach is used. It is based on the model suggested in [11] and is shown in Figure 10.

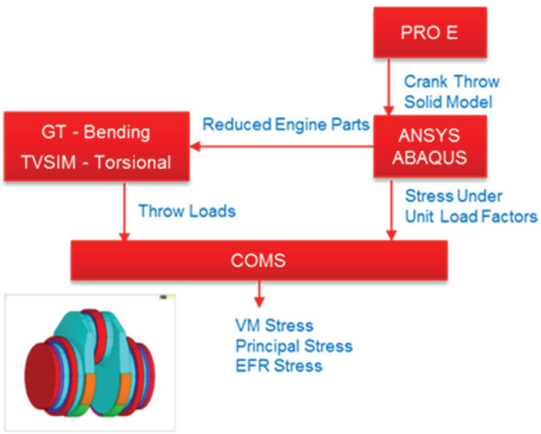

Figure 9. Combined Stress Analysis

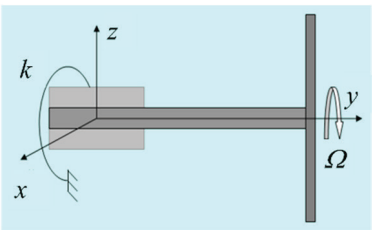

Figure 10. Simplified Scheme for Flywheel Whirl Analysis

It is shown that the gyroscopic effect splits the otherwise constant natural frequency of the shaft ω_n in two frequencies; a forward - ω_{nf} which is higher than ω_n, and reverse - ω_{nr} which is lower than ω_n. Equation (8) provides a way to calculate these frequencies [11]:

$$\omega_{nf/r} = \pm \frac{I_{yy}}{2I_{xx}}\Omega + \sqrt{((\frac{I_{yy}}{2I_{xx}}\Omega)^2 + k/I_{xx})} \quad (8)$$

Where:
sign "+" relates to ω_{nf} and sign "-" relates to ω_{nr};
Ω is shaft rotational speed,
I_{xx} and I_{yy} are correspondingly disk moments of inertia with respect to Y and X axis, and
k is shaft bending stiffness.

Since a quasi-static bending model is normally available at that stage it is easy to find rear end bending stiffness as a ratio of the applied moment to the crankshaft rear end angular displacement as shown in Figure 11.

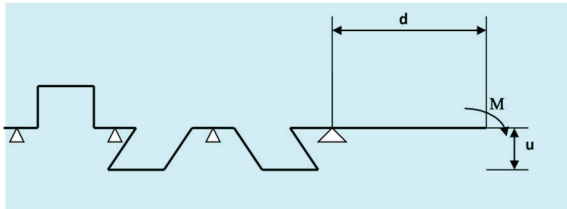

Figure 11. Definition of the Bending Stiffness

Unlike classical whirl in rotor dynamics [7], in the internal combustion engine the crankshaft can be excited not just by first order forces (imbalance), but by any higher order as well. In particular, the second order caused by piston reciprocating motion may be significant. Therefore, a good practice is to keep reverse frequency resonance with second order above engine operating range, including overspeed conditions as shown in Figure 12.

A true dynamic analysis is only done at stage 4 as a design validation step. For this level of analysis Cummins has chosen AVL Excite multi-body simulation code [12]. Figure 13 shows a typical representation of the crankshaft model within Excite.

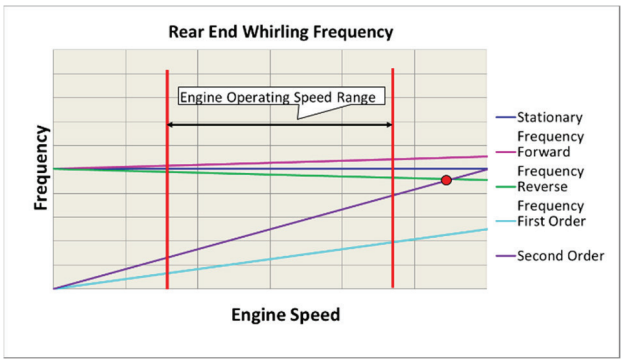

Figure 12. Simplified Flywheel Whirl Assessment

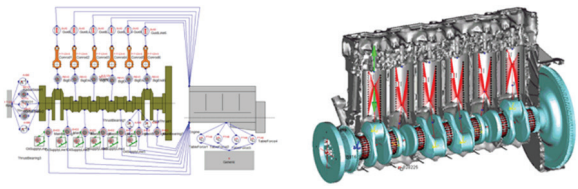

Figure 13. Simplified Flywheel Whirl Assessment

The same approach – Combined Stress Analysis (COMS) based on Unit Load Cases can be used here

for recovering stress from the dynamic analysis with one difference explained in Figure 14.

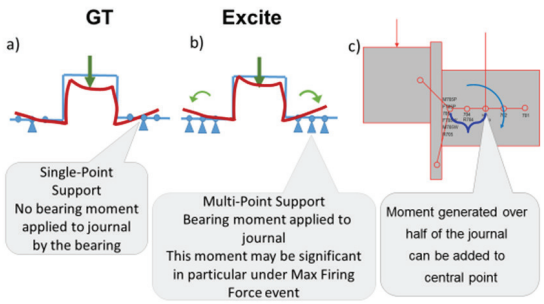

Figure 14. Bearing Moment

In quasi-static analysis with GT, COMS approach assumes that crankshaft is supported at a single point in the main journal and no moment is applied by the bearing as shown in Figure 14a. However, in Excite the Elasto-Hydrodynamic bearing model is used. Bearing loads are applied at multiple nodes along the journal as shown in Figure 14b and this generates bending moment which should be taken into account. This moment can be simply added to the internal moment at the central node (Figure 14c) and then standard COMS procedure can be enabled.

Comparison between combined (quasi-static bending + dynamic torsional) and truly dynamic analysis in Excite for rated condition for one of Cummins' 6 cylinder engine is shown in Figure 15.

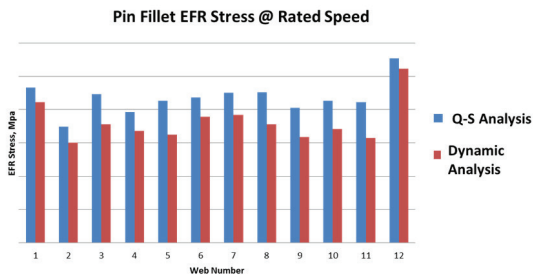

Figure 15. Comparison between Q-S and Dynamic Analysis

It can be seen that, in general, results from quasi-static analysis are higher than that from the dynamic analysis with Excite. This is primarily explained by ignoring the unloading action of the bearing moments. Particularly under firing events, the throw tends to bend and as a result the effective reaction load moves toward the inner edge of the main bearing which effectively reduces throw bending moment and the associated stress in the dynamic analysis. However, at some conditions dynamic stress may become higher than the static stress. This was found for a 6 cylinder heavy duty engine experimentally and this case was used as an opportunity for validation of simulated results.

EXPERIMENTAL VALIDATION OF SIMULATION RESULTS

Real time strain measurements were performed on a 6 cylinder heavy duty engine installed in the truck. This was a cast crank with rolled fillets. Strain gages were placed in the pin fillets and at some other locations, as shown in Figure 16. Apart from these gages, cylinder pressure on cylinder #1 was also measured. For all the gages wires were pulled to the front of the engine and data was collected through an amplifier and slip ring assembly. Data from all the gages was recorded at high speed (min. 12 kHz).

Figure 17 shows results of the strain measurement in the last pin fillet. It can be seen that Peak-to-Peak strain is reaching a maximum at an interim speed. At rated speed there is another peak, but it is not as high as at the interim speed. A waterfall diagram shows that at the interim speed 4th order becomes dominant and causes increase in the value of P-P strain. It is interesting to note, that though the amplitudes of low harmonics at higher speeds is similar to 4th order amplitudes at the interim speed, they do not produce as high total strain level due to the phasing of these harmonics.

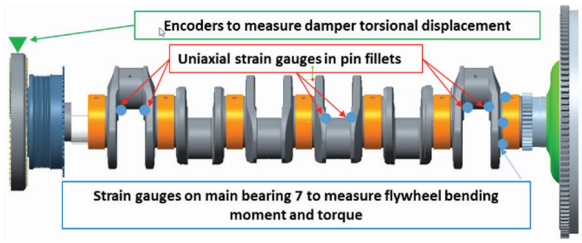

Figure 16. Strain Gage Placement in the Crankshaft

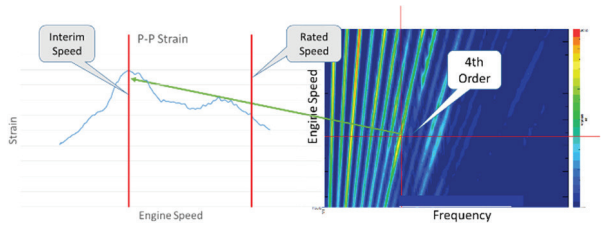

Figure 17. Strain Measurements for the Last Pin Fillet

To compare measured data against simulation the strain values were recovered from Excite models using the same technique as for stress recovery, except for in this case the unit load cases were solved for strain in the fillet in the toroidal system [13] as shown in Figure 18. Third principal strain in this case will align with the gage direction. The fillet was meshed so that node #7 is close to the middle of the strain gage and 3 nodes (6, 7 and 8) span the distance approximately equal to the gage length. Since a small fillet radius results in a significant strain gradient, simulated strain should be averaged over the length for of the gage. This can be done approximately using the following formula:

average strain = $(S_6+2S_7+S_8)/4$ (8)

where S_i is nodal strain from FEM model.

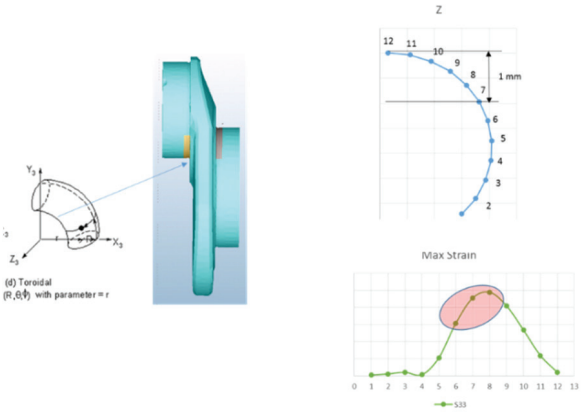

Figure 18. Strain Averaging

Peak-to-Peak averaged strain was calculated for multiple speeds and compared to measured data as shown in Figures 19. The waterfall diagrams are compared in Figure 20. It can be seen that simulated data match experimental results reasonably well with the difference at the peak within 10%. Both measured and simulated data highlight 4th order resonance at the interim speed as shown in Figure 20.

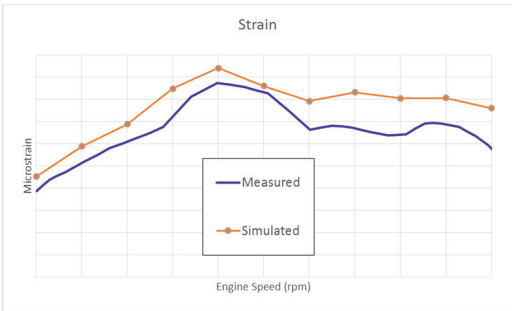

Figure 19. Measured and Simulated Results

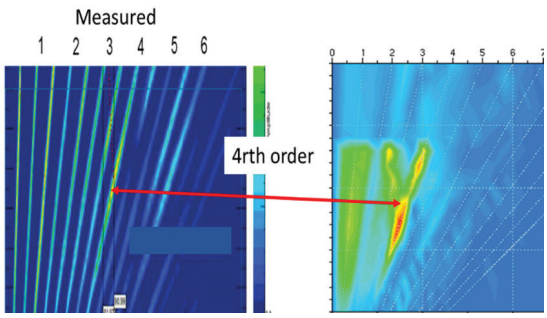

Figure 20. Measured and Simulated Waterfall Data

ADDITIONAL COMMENTS

It is interesting to note that stress and strain can be easily calculated using the statically determinate bending scheme as required by [1] and then combined with the dynamic torque using the same methodology (COMS). The results from such calculations are compared to the statically indeterminate results and the dynamic stress for the last pin fillet for a wide range of speeds in Figure 21. Figure 22 shows simplified flywheel whirl analysis results with the addition of higher orders.

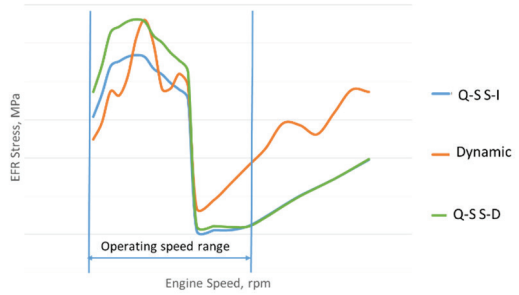

Figure 21. Last Pin Fillet EFR Stress

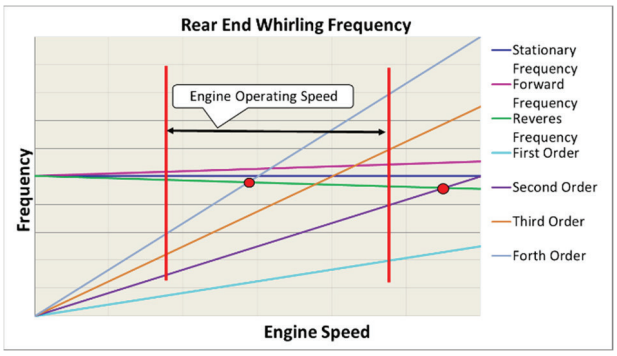

Figure 22. Simplified Flywheel Whirl Assessment

It can be seen that

- Dynamic stress from Excite when away from resonance is generally below that from quasi-static analysis due to the unloading effect of the bearing moments.
- At high speeds, stress from dynamic analysis in Excite is higher than in quasi-static analysis due to the flywheel dynamic moment.
- At resonance, calculated dynamic stress may be higher than from Q-S Analysis. The frequency of these resonances are heavily influenced by flywheel/clutch assembly mass and inertia.
- Maximum stress from S-D scheme matches well with the maximum dynamic stress from Excite. As was already mentioned, S-D scheme is known to be conservative and is the recommended method for marine engines (M53 from IACS [1]). S-D scheme has been historically considered to be conservative due to neglecting internal moments in the crankshaft journals and hydrodynamic moments in the bearings. However, dynamic moments at the ends of the crankshaft may

offset the positive effect of those moments and potentially completely cancel or even overweigh them. Therefore dynamic analysis should be recommended as the final, validation step of the crankshaft development process.

- Simplified flywheel whirl analysis is correctly predicting resonance frequencies, however is unable to predict amplitudes and therefore can be only used as a screening tool.

CONCLUSIONS

The crankshaft development process requires models of different fidelity level at various stages of the crankshaft development process. The crankshaft optimization stage makes it necessary to use simplified models to satisfy various design requirements efficiently. Use of a quasi-static analysis, along with historical guidelines, proved to be sufficient at this stage. A more detailed (combined bending and dynamic torsional analysis) is required to optimize web shape and oil hole geometry. A complete system dynamic analysis is necessary to validate the design against potential resonance issues.

NOMENCLATURE

f	Shear force
I	Moment of inertia
k	Support stiffness
m	Bending moment
P	Support transfer matrix
Q	External load
R	Reaction force
r	Crankshaft radius
S	Nodal strain
T	Object transfer matrix
u	Linear displacement
Z	State vector
ϕ	Angular displacement
Ω	Rotational velocity
ω	Natural frequency

REFERENCES

1. Calculation of Crankshafts for I.C. Engines, International Association of Classification Societies, Document M53, 1986
2. Welsh W.A., Booker J.F., Dynamic Analysis of Engine Bearing System, 1983 SAE International Congress, Detroit, MI, 1983, Paper No 830065.
3. Selim, M., Main Bearing Loads Calculated with the Crankshaft Carried on Flexible Supports having non-linear spring Characteristics, Rapp Inst. Farbrannigmot., NTH, Univ. Trondheim, No 8, 1972, pp.1-73.
4. Booker J.F., "Dynamically-loaded Journal Bearings: Numerical application of the Mobility Method", Trans. ASME, Journal of Lubrication Technology, Series F, Vol.93, No 1, January 1971, pp.168-176.
5. Goenka P.K., "Analytical Curve Fits for Solution Parameters of Dynamically Loaded Journal Bearings", Trans. ASME, Journal of Tribology, Vol.106, October 1984, pp 421-428.
6. Piraner I.L., Meleshenko N.G., Istomin P.A., Increase of Effectiveness of Multisupport Crankshaft Quasi-static Calculations, Dvigatelestrojenie, No 9, 1986, pp.24-26.
7. Piraner I.L., Rodriguez J., Okarmus M., Erogbogbo S, Keribar R., Validation, Benchmarking and Deployment of GT-Crank at Cummins, GT User Conference, 2007.
8. Swanson E., Powell C.D., Weissman S., A Practical Review of Rotating Machinery Critical Speeds and Modes, Sound and Vibration, May 2005.
9. Kobayashi S., Hakomoto K., et al., Whirl of Crankshaft Rear End, Part 1: an L6-Cylinder Diesel Engine:, SAE Int. J. Engines 10(4):2017.
10. Parikyan T., Complex Modes Analysis for Powertrain and Driveline Applications, Proceeding of ISMA 2016
11. J. P. Den Hartog, Mechanical Vibration. Dover Publications, Inc. New York.
12. N.N., "EXCITE Power Unit, software package for flexible multi-body dynamics", AVL List GmbH
13. ANSYS Modeling and Meshing Guide.

АНАЛИЗ КОЛЕНЧАТОГО ВАЛА И ПОДШИПНИКОВ И ПРОЦЕСС ОПТИМИЗАЦИИ КОНСТРУКЦИИ

Илья Л. Пиранер, Дзивей Лю, Амит Габале
Камминс инк., Колумбус, США

АННОТАЦИЯ

Проектирование коленчатого вала современного дизельного двигателя представляет определенные трудности, связанные с противоречивыми требованиями, предьявляемыми к его надежности и габаритам. Первоначальные размеры определяются на основе приближенного анализа, исходя из рамеров двигателя, скорости вращения коленчатого вала и максимального давления в цилиндре двигателя. На следующем этапе производится оптимизация основных размеров коленчатого вала на основе более точных расчетов. Многочисленные условия должны быть

удовлетворены для достижения нужных показателей надежности коленчатого вала и подшипников. В приведенной статье описывается процесс оптимизации, разработанный в компании Камминс, где минимизация трения в подшипниках служит целью оптимизации, в то время как критерии надежности используются в качестве ограничений. Поскольку оптимизация предполагает расчет большого числа вариантов, относительно упрощенные схемы расчета используются на этом этапе. Квази-статическая совместная модель вала и подшипников позволяет быстро найти основные показатели системы. Такая схема позволяет также высокую степень параметризации модели. Это, в свою очередь, позволяет проведение расчетов на основе планирования экспериментов и построение аналитических аппроксимаций для основных показателей работы вала и подшипников. Эти апрокимации используются для быстрой оптимизации конструкции для различных условий работы двигателя. После выбора наилучшей конструкции она проверяется на основе обьемной конечно-элементной модели с использованием результатов анализа крутильных колебаний. Окончательная проверка производится на основе динамического расчета коленчатого вала с использованием современных программных средств для исследования упругих динамических систем.

Proceedings of the 1st International Conference MES-2018 / ИРМ-2018
MECHANICAL ENGINEERING SOLUTIONS
Design, Simulation, Testing and Manufacturing
September 17-19, 2018, Yerevan, ARMENIA

MES2018-30

Optimization of gas engines for transient loads to stabilize local grids

Clemens FRANK[1] and Günther HERDIN[2] and Rüdiger HERDIN[3]

[1]PGES GmbH, Vienna, AUT, e-Mail: c.frank@prof-ges.com

[2]PGES GmbH, Jenbach, AUT, e-Mail: g.herdin@prof-ges.com

[3]PGES GmbH, Vienna, AUT, e-mail: r.herdin@prof-ges.com

ABSTRACT

Large gas engines are mainly used in stationary operation to provide heat and electricity. Therefore the design focus is on high efficiency, high power density and low emissions. This leads to disadvantages during transient loads due to the inertia of the turbocharger. With a new system the load gradients should increase significantly to expand the scope of application, especially in the balancing energy field. The gas engine will be enlarged by a compressed air system and a rotary blower, which are integrated in the intake section of the engine.

To show the potential of the system a physical model of the concept was created and simulated. This method enables the testing of the system to find concepts for control, select suitable components and test various versions. The results of the simulations show the potential of the system and the ramp-up time is decreased significantly.

INTRODUCTION

This introduction should explain the actual applications and the design of gas engines as well as the regulations of new fields of applications to understand the possible opportunities and recent problems. What is the definition of a large stationary gas engine and the actual operation purpose? In general these gas engines are four-stroke Otto engines with turbocharging and a lean combustion concept which operate at a constant generator rotation speed. The common fuel is natural gas, beside that many alternative gases can be used like hydrogen, biogas or landfill gas [12]. The major operation purpose is to produce heat and electricity in CHP (*combined heat and power*) plants or in the waste industry. Therefore the engines are designed for high efficiency and high power density with low emissions. To achieve this target at the best the engines have few large turbochargers. Due to their size and moment of inertia as well as the inertia of the flow through the engine and the charging system, it takes relatively long to increase the turbocharger rotation speed and thus to raise the boost pressure and engine load [8]. Modern high performance class engines have a ramp-up time from idle load points to full power of a few minutes (For example GE 920/10.4MW-120s to full power [1]). In comparison with similar performance class machines gas engines have advantages in terms of emissions to diesel engines and a higher efficiency than gas turbines. [12]

Due to variations in the supply and demand in the power grid, a deviation of the grid frequency occurs. Large deviations can lead to wide-area blackouts [7]. To prevent such scenarios the delivery of balancing power is needed. In the Central European grid the load-frequency control is divided into different stages. The first stage is the primary control. Therefore the deviation of the grid frequency has to be detected automatically and the needed balancing power has to be delivered within 30s. The power has to be available in both directions. Positive primary control means to feed energy into the grid. To provide negative primary control power has to be drawn from the grid or the power output has to be reduced. The next stage is secondary control and the reaction time for this stage is 5min [10].

In Europe the major part of the primary regulation energy is actually delivered by large power plants [3]. With new technologies in the electricity production these are going to be replaced by renewable energy sources [11]. Furthermore renewable sources have a fluctuating power output due to influences of nature [6]. In combination with new forms of primary electric production new ways to provide balancing power have to be found [2].

The target is to use gas engines for primary control. The reaction time of modern gas engines is too slow due to their actual design. Large state of the art gas engines can provide secondary control but cannot reach full power within 30s. The PGES Company has a patented system to reduce the ramp-up time of large gas engines. This paper shows extracts and special results of a master thesis which covers the elaboration of a patent [5]. This thesis shows the first step from the scratch of an idea to a final concept for a prototype plant by means of a simulation and configuration of the components. The aims are to significantly increase the response behavior coupled with a high efficiency at stationary operation, while undertaking minimal modifications of the basic structure of the gas engine. Additionally the system should need less energy and a small compressed air reservoir to increase the ramp up time efficiently. Therefore a physical model of the whole system with the gas engine is created. The simulations enabled the testing of the system and to invent concepts for the control and the system configuration.

NOMENCLATURE

A_{DK}	Free flow cross-section of the throttle valve (m²)
I	Mass moment of inertia (kgm²)
P_{An}	Input power (W)
P_{Ab}	Output power (W)
P_E	Rotary blower electric drive power (kW)
P_M	Engine power output (kW)
P_{Sys}	System power output (kW)
P_V	Compressor capacity (kW)
R_G	Ideal gas constant of the mixture (J/(kg*K))
SM	Surge margin
SM_B	Target surge margin
$\overline{T}_B$	Average container temperature (K)
T_2	Temperature upstream of the turbocharger compressor (K)
T_7	Temperature upstream of the throttle valve (K)
T_{10}	Exhaust temperature (K)
V_B	Container volume (m³)
c_{pG}	Isobaric heat capacity of the mixture (J/(kgK))
$\dot{m}_A$	Inlet container mass flows (kg/s)
$\dot{m}_B$	Outlet container mass flows (kg/s)
$\dot{m}_{DK}$	Throttle valve mass flows (kg/s)
$\dot{m}_G$	Rotary blower mass flow (kg/s)
$\dot{m}_M$	Engine mass flow (kg/s)
$\dot{m}_V$	Turbocharger compressor mass flow (kg/s)
$\dot{m}_{VSurge}$	Turbocharger compressor surge mass flow (kg/s)
$\dot{m}_T$	Turbocharger turbine mass flow (kg/s)
$\dot{m}_5$	Rotary blower mass flow (kg/s)
$\dot{m}_{5B}$	Target rotary blower mass flow (kg/s)
n_G	Rotary blower rotation speed (U/min)
n_{TL}	Turbocharger rotation speed (U/s)
p_B	Container pressure (Pa)
p_4	Pressure upstream of the blower (Pa)
p_5	Pressure after the blower (Pa)
p_7	Pressure upstream of the throttle valve (Pa)
p_{7B}	Target pressure upstream of the throttle valve (Pa)
p_9	Intake manifold pressure (Pa)
t_{Step}	Actual time step (s)
x_{DV}	Opening of the control valve
α_{DK}	Throttle valve opening
γ_{TB}	Turbocharger bypass valve opening
Δh_{Vs}	Specific isentropic enthalpy of the turbocharger compressor (J/kg)
Δp_G	Pressure difference of the rotary blower (Pa)
Δp_{45B}	Target pressure difference of the rotary blower (Pa)
Δp_{67}	Pressure difference of the bypass valve (Pa)
Δp_{67B}	Target pressure difference of the bypass valve 2 (Pa)
η_G	Rotary blower efficiency
η_M	Engine efficiency
η_V	Turbocharger compressor efficiency
η_T	Turbocharger turbine efficiency
κ_G	Isentropic exponent of the mixture
λ_B	Air-fuel ratio
Π_{DK}	Pressure ratio of the throttle valve
Π_V	Pressure ratio of the turbocharger compressor
Π_{VSurge}	Surge pressure ratio of the turbocharger compressor
Π_T	Pressure ratio of the turbocharger turbine
Ψ_{DK}	Flow coefficient of the throttle valve
φ_{BK1}	Bypass valve 1 opening
ω	Angular velocity (rad/s)

ACRONYMS

$OLCV$	Open loop control value
$CLCV$	Closed loop control value

SYSTEM EXPLANATION

The introduction shows the need of a concept to reduce the ramp-up time of gas engines. The system should provide a suitable solution to reduce the ramp-up times of gas engines for primary control. This section should explain the basic function of the system. The name of the new system is BOOST. The structure of the gas engine with the BOOST-system is shown in the figure below (**Figure 1**). The numbers show the boundaries of each component. The base is the gas engine (*R*) with intake manifold (*O)*, exhaust pipes (*Q*), turbocharger (compressor C, turbine V), air filter (*A*), exhaust system (*W*), throttle valve (*S*), gas mixer 1 (*B*), intercooler 1 (*D*) and generator (*P*). The BOOST-system complements the basic structure with a rotary blower (*G*), an electric motor for the rotary blower (*H*), a compressed air reservoir (*J*), a flow control valve (*K*), bypass valves 1 (*U)* and 2 (N), an additional gas mixer 2 (*L*) and an additional intercooler 2 (*I*). Additional components are: turbocharger bypass (*E*), supply line (*F)*, return line (*M*), collector (*T*).

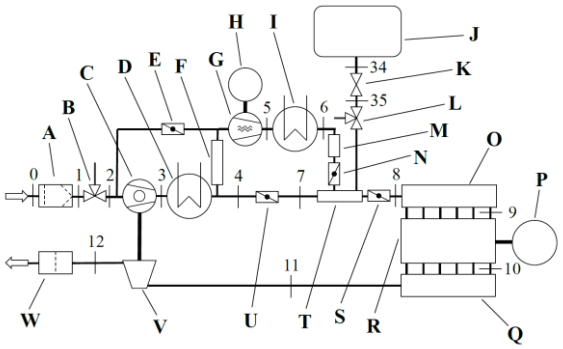

Figure 1. Structure of the BOOST-system

This section explains the basic function of the BOOST-system. As already explained, the ramp-up time is limited by the inertia of the turbocharger and the inertia of the charging system itself to build up the necessary boost pressure. In the concept the large high efficient turbocharger will not be replaced. To increase the load gradient compressed air is blown into the collector upstream of the throttle valve. Thus the pressure in the intake manifold as well as the engine load can be increased easily and instantly. The flow control valve controls the pressure in the collector and the compressed air is formed to mixture in the gas mixer 2. Due to the usage of the compressed air system a rotary blower is needed. The pressure after the compressor increases and so the pressure ratio. The engine mass flow is divided by the compressor and the compressed air system. Without the rotary blower the compressor operating point would get closer to the surge line due to the low mass flow and the high compression ratio. At fast load changes the compressor is highly endangered to surge. To prevent compressor surging, the rotary blower increases the compressor outlet pressure to the necessary intake manifold pressure. Due to this reduction of the pressure ratio of the compressor the operating point is shifted away from the surge line into a save operating range. Thus the load gradient is only depending on the reaction time of the rotary blower and flow control valve. The inertia of the turbocharger is not the limiting factor anymore. The bypass valves have the function to couple and decouple the BOOST-system during a stationary operation of the engine. With a fully opened bypass valve 1 the BOOST-system has minimal effects on the basic engine. The turbocharger bypass is needed for stabilization of fast positive load changes and to prevent engine surge at steep negative load gradients.

PHYSICAL MODEL

The majority of the used model is based on the approach of Skorjanz [9]. Therefore a physical model of the system is created. The whole system consists of the engine parts and the new components. The system is disassembled in the described major components (*A-W*) and coupled with specified parameters at the boundaries (*0-12/34-35*). The behavior of each component is described by algebraic equations, differential equations or by interpolations of measurement or characteristic map data. In general the real component behavior is way more complex and so simplified descriptions are used. The link between the components is done by parameters like pressure, temperature, mass flow, power output and other special parameters. This modelling is used because it is the best approach to describe the gas engine itself as well as all other new components. The simulation is done by an object-oriented numeric program with a variable time step.

General

The ambient conditions are defined by DIN ISO 3046-1. The system power output P_{Sys} is the gas engine power output P_M minus the electric drive power of the rotary blower P_E (1).

$$P_{Sys} = P_M - P_E \tag{1}$$

For the modelling of the turbocharger and the rotary blower shaft a simple mechanical model is used. The change of the rotary speed is driven by the changes of the in- and output power of the shaft. With an approach as a difference equation the following relation between rotary speed and power is found for each time step (2).

$$\omega_i = \frac{(\sum P_{An} - \sum P_{Ab})t_{Step}}{I\omega_{(i-1)}} + \omega_{(i-1)} \tag{2}$$

The system has many controllers which are modelled as simple PI-controllers. Due to the usage of measurement data and the complexity of the whole system the adjustment of the controller settings is done by an empirical process.

Gas Engine

The gas engine itself is modeled with characteristic map data of an engine test bench measurement. The gas engine has a rated power of 550kW. The engine map contains special parameters of different load points which are depending on the intake manifold pressure of the engine p_9 (3). The value of the air-fuel ratio λ_B is fixed by map data. It will be assumed that the gas mixture system provides the adjusted air-fuel ratio at all load points. The system has no effects on the combustion behavior (knocking and flammability limits) of the engine and no further consideration of this issue is done.

$$[P_M, \dot{m}_M, T_{10}, \eta_M] = f(p_9) \tag{3}$$

Container Model

Parts like the exhaust manifold or the intercooler are components with partly big volumes. Due to a change of the incoming and outgoing mass flow the container pressure p_B changes (4).

$$p_B = \frac{R_G \overline{T}_B}{V_B} \int (\dot{m}_A - \dot{m}_B) dt \tag{4}$$

The following parts are modeled with this concept: intercooler 1 and 2, supply line, collector, intake manifold, return line and exhaust pipes. Additionally, some components have implemented a simplified pressure loss, partly by characteristic map data or with a simple incompressible flow resistance. The air filter with gas mixer 1 and the exhaust system are components with a simple pressure loss and are not modelled with the container concept.

Flap Valves

The system contains flap valves, like the throttle valve, the turbocharger bypass or the bypass valves. These components are modelled with an approach of an isotropic escape of a container. This description has serious deviations in relation to the real behavior depending on the boundary conditions. Still this model is commonly used to describe throttle valves in physical models of engines [8, 4]. The result of the approach is a direct link between the pressure ratio Π_{DK}, the valve opening α_{DK} and the valve mass flow $\dot{m}_{DK}$. In the equation below the described relation is shown exemplary for the throttle valve (5). The flow coefficient Ψ_{DK} is a function of the pressure ratio Π_{DK} and the isotopic exponent κ_G of the mixture. The opening area A_{DK} is dependent of the opening α_{DK} and a leakage area.

$$\dot{m}_{DK} = \frac{p_7}{\sqrt{R_G T_7}} A_{DK}(\alpha_{DK}) \Psi_{DK}(\Pi_{DK}) \tag{5}$$

Turbocharger

The turbocharger of the modeled engine consists of a radial compressor and a radial turbine. Both components are modeled with characteristic maps. Due to the actual pressure ratio $\Pi_{V,T}$ and turbocharger rotation speed n_{TL} the mass flow $\dot{m}_{V,T}$ and the efficiency $\eta_{V,T}$ of the component are interpolated.

$$\dot{m}_{V,T} = f(\Pi_{V,T}, n_{TL}) \tag{6}$$

$$\eta_{V,T} = f(\Pi_{V,T}, n_{TL}) \tag{7}$$

The change of the turbocharger rotation speed is calculated with the basic equation for a rotating shaft (2). The component load itself is calculated with a specific isotropic enthalpy approach. This is shown exemplary in equation (8) and (9) for the turbocharger compressor.

$$\Delta h_{Vs} = c_{pG} T_2 \left[\Pi_V^{\frac{\kappa_G - 1}{\kappa_G}} - 1 \right] \tag{8}$$

$$P_V = \frac{\dot{m}_V \Delta h_{Vs}}{\eta_V} \tag{9}$$

One important value is the surge margin of the turbocharger compressor. The data of the surge line are depending on the actual turbocharger rotation speed and were implemented by map data.

$$SM = \frac{\frac{\Pi_{VSurge}}{\dot{m}_{VSurge}}}{\frac{\Pi_V}{\dot{m}_V}} - 1 \tag{10}$$

Rotary blower

The modelling of the rotary blower is similar to the components of the turbocharger. The actual mass flow $\dot{m}_G$ and the efficiency η_G of the rotary blower are driven by the pressure difference Δp_G and the blower rotation speed n_G (11), (12).

$$\dot{m}_G = f(\Delta p_G, n_G) \tag{11}$$

$$\eta_G = f(\Delta p_G, n_G) \tag{12}$$

The change of the rotation speed is calculated with the input power of the electric motor and the needed power of the rotary blower with equation (2). The power of the rotary blower itself is calculated with the described equations in the turbocharger section (8), (9).

BOOST-System components

The remaining components of the BOOST-system are the compressed air reservoir, the flow control valve and the gas mixer 2. The compressed air reservoir is modelled with the container model. The flow control valve is calculated with equations inspired by DIN EN 60534. This calculation is mainly used for valve design. The gas mixer 2 is modelled as a component with a simple pressure loss and the mass flow increases by adding of natural gas to the air flow of the flow control valve.

CONTROL OF THE BOOST-SYSTEM

This part of the paper describes the control algorithm at a load increase with or without the BOOST-system. Starting point is an already coupled BOOST-system. A figure of the system and the current state is shown below (**Figure 2**). The closed loop control value (*CLCV)* boxes show controlled variable = reference variables and the open loop control value (*OLCV)* boxes show the fixed control variable for the open loop control.

The first case considers a stable or transient engine load without the BOOST-system activated. The load ramp of the engine is only depending on the inertia of the turbocharger. Still the BOOST-system is coupled into the system and the algorithm ensures a stable operation and a change of the BOOST-system load point itself due to the engine load point.

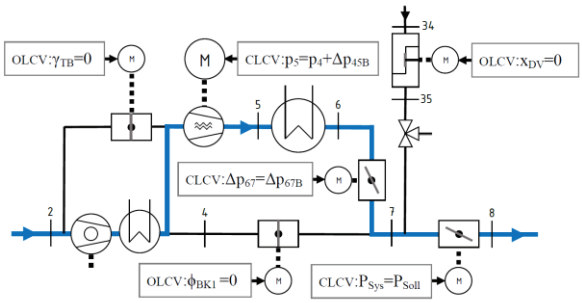

Figure 2. Structure for coupled BOOST-system and steady engine load

The system load P_{Sys} is regulated by the throttle valve and the reference value is the set load P_{Soll}. The following components turbocharger bypass, bypass valve 1 and flow control valve remain closed by the control. The bypass valve 2 regulates an adjusted pressure difference Δp_{67}. The controller of the rotary blower electric motor controls the pressure p_5 after the rotary blower. The reference variable is defined with a configured pressure difference Δp_{45} based on the pressure after the intercooler 1 p_4. This configuration ensures a stable operation and avoids a backflow during the coupling of the BOOST-components. Additionally it keeps a required minimum pressure difference for the rotary blower. In case of a load increase the pressure after the intercooler 1 increases and with that the mass flow. This leads to a higher pressure after the rotary blower and a change of the bypass valve 2 opening to ensure the adjusted pressure difference. To increase the power the throttle valve opens. With this configuration the load gradient of the used engine is max. 3%/s.

To increase the load gradient the pressure system components are activated. This event is called BOOSTup. The structure of this state is shown in figure below (**Figure 3**).

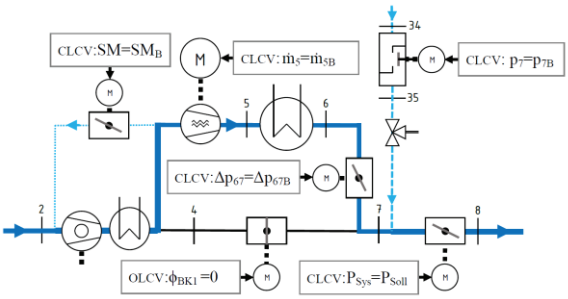

Figure 3. Structure for coupled BOOST-system and large load gradients with BOOST-system

At the BOOSTup-case the maximum load ramp increases to 10%/s. To achieve this gradient the flow control valve opens and the pressure upstream of the throttle valve p_7 increases. The reference variable of the flow control valve p_{7B} is defined by characteristic map data dependent on the set power output P_{Soll}. The mass flow to the engine is divided in the mass flow of the turbocharger compressor and the mass flow of the pressure system. With the activation of the BOOSTup-case the control of the rotary blower electric motor changes to a mass flow controller. Therefore the reference variable of the mass flow $\dot{m}_5$ is depending on a map data mass flow $\dot{m}_{5B}$ which is connected to the set power output. Additionally, the turbocharger bypass is activated and opens if the surge margin of the compressor reaches a critical level. The bypass valve 1 remains closed. If the set power output is stable, the control valve is closed and the mass flows of the rotary blower as well as the system power output have reached its set level, the system switches back to the first case (**Figure 2**).

SIMULATION RESULTS

This chapter contains selected results of the simulation and validation of the model. Measurement data of the reference engine without the BOOST-system are available and used for the validation of the model. The first diagram shows the comparison between measured and simulated power output of the engine (**Figure 4).** The measured ramp-up time is significantly longer compared with those used in the following simulations. The deviation of the chart lines is small except during the start of the simulation. At this stage the parameters need a few seconds to stabilize. The used model is suitable to describe the behavior of the engine for flat load ramps without the BOOST-system.

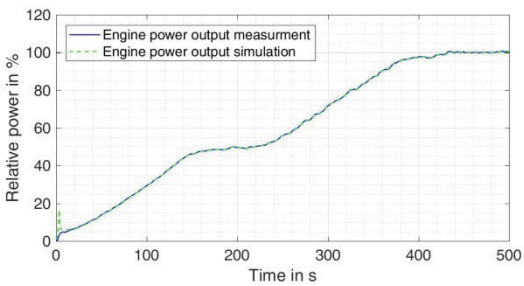

Figure 4. Comparison between measurement and simulation data for engine without BOOST-system

The following charts show selected results of the simulation model with the activated BOOST-system. The next diagram shows the different load ramps with or without the BOOST-system (**Figure 5**). The steepest possible load ramp without the boost system and a stable operation behavior is 3%/s. The steeper ramp with the BOOST-system has a gradient of 10%/s. The engine can achieve full power within 10s from an idle load point.

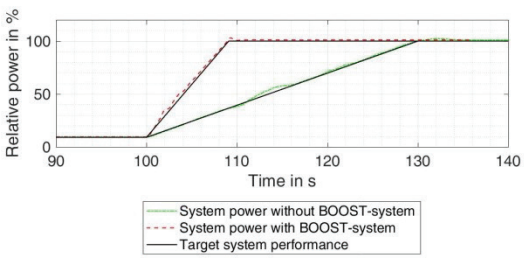

Figure 5. Comparison of relative engine power between load ramp with or without BOOST-system

The next charts show selected parameters of the engine and the system during a fast load change of 10%/s which is printed in the previous figure (**Figure 5**). These figures present the described BOOSTup-case. The opening of the valves is shown in figure below (**Figure 6**).

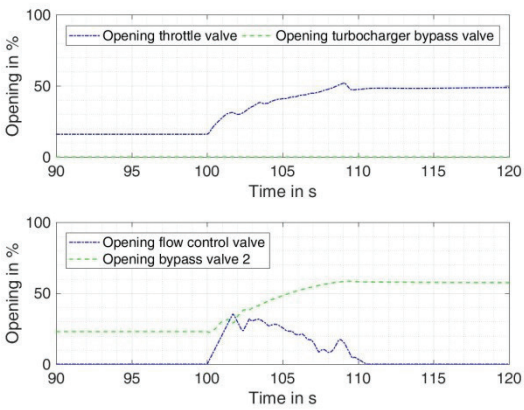

Figure 6. Selected engine und system parameters – BOOSTup-load ramp

The throttle valve opens fast according to the rising set power output. The turbocharger bypass valve remains closed because the value of the surge margin does not reach the critical value. The bypass valve 2 opens with the increasing mass flow to provide the set pressure difference. The flow control valve opens quickly to 35% and closes slowly during the BOOSTup-process. The used compressed air mass is 0.7kg.

The following chart shows selected parameters of the turbocharger (**Figure 7**).

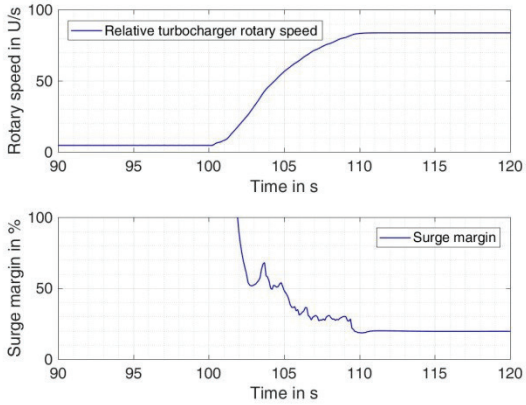

Figure 7. Selected turbocharger parameters – BOOSTup-load ramp

The rotary speed increases fast due to the load increase of the engine and in tandem with the increase of the turbine power output. The surge margin decreases fast with the increasing power output. At the idle load point and at low load steps the surge margin is more than 100%. The definition of the surge margin has a maximum of 100%. The reason for this exceeding is that the characteristic compressor and turbine map are extrapolated in low level operation points. This has no effect on the functionality of the concept. In the low load points of the engine the pressure ratio of the compressor is close to 1 with a suitable distance to the surge line (SM=0%).

The last diagram shows selected parameters of the rotary blower (**Figure 8**). With the start of the BOOSTup-load ramp the electric drive power increases fast to speed up the blower. The rotary blower accelerates and the pressure difference increases. The value of the pressure difference stays inside the operation window. The operation window is limited by the maximum pressure difference of the machine and a minimum one to ensure a stable operation.

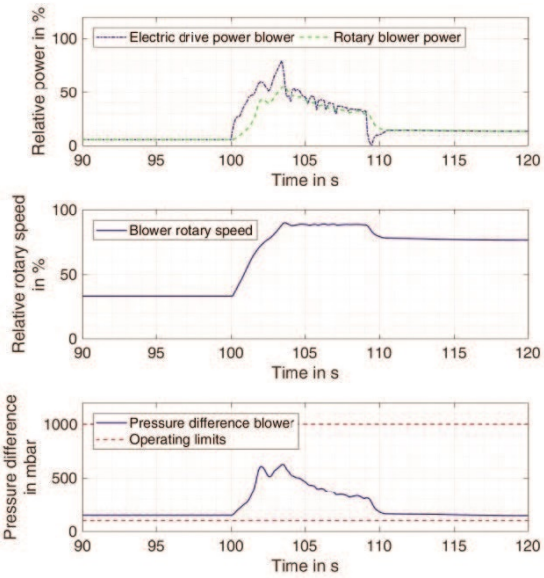

Figure 8. Selected blower parameters – BOOSTup-load ramp

CONCLUSION

The simulation results show that the used model is a suitable description of the gas engine's and the additional BOOST-system's behavior. Despite the simplifications the base engine and different expansions can be simulated and different system configurations can be tested. The diagrams show that the system has a stable operating behavior. Still some parameters like the electric drive power of the rotary blower show the potential for improvements of the control.

The main target of the system is to reduce the ramp-up time significantly. The gradient of the load ramp can be tripled from 3%/s to 10%/s. The energy consumption of the rotary blower is related to the system power, between 5% at idle and 1.1% at full power. The decrease of the electric efficiency is between 1.1%points and 0.5%points. The needed air mass for a large load step from an idle load point to full power is just 0.7kg. Thus the decrease of the efficiency is low and for primary control a compressed air tank of less than 1m³ is needed. Additionally the decoupled system has no effects on the maximum efficiency of the engine. The rotary blower meets the operating limits and the compressor is operated in a stable operating point with an adequate distance to the surge line.

It should be noted that the used gas engine can reach full power within 30s. Due to its relatively small power output the reaction time is quite fast. With larger gas engines the reaction time is longer due to their size and inertia of the larger turbochargers. Therefore and due to the requirements for balancing power the system is more suitable for large gas engines with a power output of two or more megawatts.

REFERENCES

1. Birgel A. Böwing R. Trapp C. Wimmer A., "GE's J920 Gas Engine – 10.4MW Power and more than 50% Efficiency", *MTZ industrial* (2017)
2. Brauner G., "Nachhaltige zentrale und dezentrale Versorgungskonzepte", *e&i Elektrotechnik und Informationstechnik 132*, (2015)
3. BDEW Bundesverband der Energie- und Wasserversorgung. "Bereitstellung von (System-) Dienstleistung im Stromversorgungssystem" (2016)
4. Carlsoon P., "Flow Through a Throttle Body", Linköping Universitet, *Master thesis* (2007)
5. Frank C., *Innovatives Aufladungskonzept von Gasmotoren*, TU Wien, *Master Thesis* (2018)
6. Jarass A. Jarass L., "Integration von erneuerbarem Strom", *BoB – Books on Demand* (2016)
7. Niederhausen H. Burkert A.: "Elektrischer Strom", 1st Edition, *Springer Vieweg* (2014)
8. Puchner H. Zinner K., "Aufladung von Verbrennungsmotoren", 4th Edition, *Springer* Vieweg (2012)
9. Skorjanz P., "Physikalische Modellierung eines Großgasmotors und regelungstechnische Anwendungen", Dissertation, *TU Wien* (2001)
10. UCTE. "Continental Europe Operation Handbook" (2004)
11. Wietschel M. Ullrich S. Markewitz P. Schulte F. Genoese F., "Energietechnologien der Zukunft", 1st Edition, *Springer Vieweg* (2015)
12. Zacharias F., "Gasmotoren", 1st Edition, *Vogel* (2001)

ОПТИМИЗАЦИЯ ГАЗОВЫХ ДВИГАТЕЛЕЙ ПРИ ПЕРЕХОДНЫХ НАГРУЗКАХ ДЛЯ СТАБИЛИЗАЦИИ ЛОКАЛЬНЫХ СЕТЕЙ

Клеменс ФРАНК, Гюнтер ХЕРДИН и Рюдигер ХЕРДИН

ПГЕС ГмбХ, Вена и Йенбах, Австрия

АННОТАЦИЯ

Большие газовые двигатели в основном используются как стационарные установки для обеспечения тепла и электричества. Поэтому основное внимание в их проектировании уделяется высокой эффективности, высокой плотности мощности и низким выбросам. Это приводит к недостаткам при переходных нагрузках из-за инерции турбокомпрессора. С применением новой системы градиенты нагрузки должны значительно увеличиться, чтобы расширить область применения, особенно в балансирующем энергетическом поле. Газовый двигатель снабжается системой сжатого воздуха и роторной воздуходувкой, которые встроены во впускную часть двигателя.

Чтобы показать потенциальные возможности системы, была создана и смоделирована физическая модель прототипа. Этот метод позволяет тестировать систему для поиска схемы управления, выбора подходящих компонентов и тестирования различных версий. Результаты моделирования показывают потенциальные возможности системы, и время разбега значительно уменьшается.

SECTION B

Mechanisms / Robots / Biomechanics

Proceedings of the 1st International Conference MES-2018 / ИРМ-2018
MECHANICAL ENGINEERING SOLUTIONS
Design, Simulation, Testing and Manufacturing
September 17-19, 2018, Yerevan, ARMENIA

MES2018-K2

EVOLUTION, DEVELOPMENT TRENDS AND PERSPECTIVES OF MACHINE AND MECHANISM SCIENCE IN ARMENIA

Yuri Sargsyan

National Polytechnic University of Armenia, Yerevan, Armenia, e-mail: yusarg@seua.am

ABSTRACT

A brief historical overview is given on the genesis and evolution of the Theory of Mechanisms and Machines (TMM) and related research fields united under the term "Mechanism and Machine Science (MMS)" in Armenia. Main achievements of Armenian MMS in research and education are highlighted. The role and stimulating influence of the International Federation of Theory of Mechanism and Machines (IFToMM) on the development of MMS in Armenia are underlined. Based on the critical analysis of the present situation in MMS its main development trends and challenges are identified. The paper concludes with an outline of the priority directions and prospects for the further development of MMS in the context of the revitalization and innovative development of industrial machinery in Armenia.

INTRODUCTION

Armenia has developed one of the most advanced science and technology systems in the former Soviet Union which served with distinction the interests of the Union. Science in Armenia has been strongly affected by generic transitional problems inherited partly from the Soviet model of the science organization. As a result, S@T capacities of the country have declined, due to the drastic reduction of state investments and slow and inadequate restructuring of the sector accompanied by heavy brain drain and worsening of material conditions for research [1]. As a part of the Armenian science system MMS also passed through Soviet and post-Soviet periods in its history and has suffered much from the transition hardships, especially from losing its industrial base as a result of the collapse of industrial machinery in Armenia.

We start the paper with the quotation to the founder of quantum mechanics W. Heisenberg: "To grasp the progress of science as a whole, it is useful to compare contemporary problems of science with the problems of the preceding epoch and to investigate the specific changes that one or another problem has undergone over decades and even centuries". To assess objectively the present situation of MMS in Armenia and outline the prospects of its further development we will first present a short historical overview of MMS and outline its main achievements in research and education. The present review is based essentially on our previous paper [2] and attempts to compliment and update the analysis given there.

HISTORICAL OVERVIEW

The history of MMS in Armenia cannot be regarded independently of its Soviet context. Similar to the every major field of the Soviet science complex, MMS once had a centralized organizational framework, including regular all-Union conferences on contemporary problems of TMM and related areas of MMS, a year-round central TMM seminar with an extensive network of regional branches, MMS-focused state framework programs and a unified Soviet IFToMM Committee coordinating all international activities in MMS all over the Union.

The first attempts of MMS scientific activity in Armenia can be referred to the early 1950s when at Yerevan State University and Yerevan Polytechnic Institute (YPI), now National Polytechnic University of Armenia (NPUA), investigations started in kinematic synthesis of spatial linkages [3] and design of mechanisms with optimum force transmission characteristics. Later the first Armenian digital computers "Gohar" were used for the approximate synthesis of path generating four-bar mechanisms [4].

In 1971 the Armenian Branch of the all-Union TMM seminar was established at YPI which has become the main center of MMS research activities in Armenia. The decisive role of academician I.I. Artobolevski in the formation and development of the Armenian MMS scientific school is unquestionable.

Since its foundation IFToMM has been another important driving force for developing MMS in Armenia, being a unique "window" to the west and a rare opportunity for the internationalization of research activities and establishing contacts with western scientists in the Soviet period. Forms of involvement of Armenian scientists in IFToMM activities have included participation in the IFToMM World Congresses beginning from the 4-th Congress in 1975 and IFToMM sponsored conferences (Syrom, Romansy, etc.), publications in IFToMM official journals and editions, membership in the IFToMM Executive Counsel and Soviet National IFToMM Committee (1992-1995), IFToMM PC-s and TC-s. In 1998, Armenia has officially become an IFToMM member country and has its IFToMM National Committee coordinating MMS international activities in Armenia.

In line with the rapid technological progress of industrial machinery in Soviet Armenia, new scientific schools, research infrastructures and international collaboration links have been established in different areas of MMS based on the respective units of YPI, National Academy of Sciences (NAS) and other higher education and research institutions of Armenia. The main research activities have been implemented within a series of state supported projects, international collaboration programs and research labs with state institutional funding. As shown below, some of the results of the MMS research implemented in the Soviet and post-Soviet periods can be qualified as achievements. On the whole, MMS has been and still is one of the most active and high ranked technical sciences of Armenia which had a considerable contribution in creating the science base and research workforce for the national machine building industry.

ACHIEVEMENTS IN MMS RESEARCH

In what follows, we present the main achievements in some traditionally active research areas of Armenian MMS scientists.

Synthesis of mechanisms. The most active research area of TMM in the starting period has been synthesis of mechanisms. Armenian scientists – mostly followers and co-workers of Prof. N. Levitski – developed and popularized his method which was based on least square approximations of given motions and used as algebraic deviation functions in the motion approximation problems of mechanism synthesis polynomial expressions of loop closure equations (weighed differences) written for any desired number of the given design positions.

Due to the growing internationalization process in the field initiated by IFToMM, in the early 1970s, cooperation links were established between the researchers from Soviet Armenia – followers of Chebishev's algebraic approach in the mechanism synthesis theory and their American counterparts who followed a classical geometrical approach based on the Burmester theory. A collaborative research project implemented at Stanford University in 1971-1972 resulted in "cross fertilization" of two traditionally opposable directions in mechanism synthesis and a new synthetic approach combining the algebraic method of mechanism synthesis based on least square approximations with the geometric notions of the Burmester theory emerged [5].

In [6], the kinematic geometry associated with planar motion approximations [5] was extended to spherical and spatial motions. The geometrical theory developed in [5] may be regarded as a generalization of the Burmester theory to an unlimited number of design positions. In follow-up papers [7–9] of the same authors a general theory for Chebishev (or minimax) approximations of given rigid body position sets in its planar, spherical and spatial motion was developed and applied to the kinematic synthesis of planar and spatial rigid body guidance mechanisms. The first of these works was honored with the Best Paper Award at the 11-th ASME conference on mechanisms in 1968.

By these studies a theoretical foundation was laid for the new branch in kinematic geometry – approximational (approximation based) kinematic geometry which has become an active area of investigations in Armenia and internationally. A systematic description of the theory, computational methods and design applications of approximational kinematic geometry is given in [16] and in keynote lecture [11] at the 8-th World IFToMM Congress (1991,Prague).

Further developments in this area have been connected with extensions of the developed methods to spherical motions [12], approximations by second order curves and surfaces [13], minimax problems of mechanism synthesis with bound variables [14], computational aspects of approximational kinematic geometry [15,16] and minimax problems of dynamic synthesis of mechanisms [17,18].

In a series of recent works [19–22], the geometrical theory created for single motion (single position set) approximations was extended to the case of multiple motions (multiple positions sets) of a rigid body and a new class of kinematic approximation problems was set to determine the special points and lines in a moving body which in alternating sets of its given finite positions approximate best concentric circles and spheres, coaxial cylinders, cones and line congruences describing the constraints imposed on the moving body by adjustable dyads with different topologies attached to the moving body.

To apply these results in the mechanism synthesis a unified modular principle for the approximate synthesis of parallel mechanisms of arbitrary structure has been developed based on the methods of approximational kinematic geometry. Regardless the kinematic function and topology, parallel mechanisms approximately generating the given rigid body motions are built of independently synthesized structural units (modules) connecting the

moving body with the frame. The motions which should be generated are described either by some continuous functions of rigid body generalized coordinates or by ordered sets of its finite displacements. The structural modules of the sought-for motion generator mechanisms impose on the prescribed rigid body motion a certain number of constraints which force some points, lines or other rigid body elements to stay on curves, surfaces and more complex geometric objects, which can be easily mechanized.

The binary links are the simplest and most practical modules for design applications. The proposed approach permits to decompose the complex computational process of kinematic synthesis into a number of local blocks-procedures synthesizing structural modules of the mechanism. The methodology and numerical methods for the realization of the described modular principle are given in [10], [23, 24].

Theory and biomedical applications of robot-manipulators. In parallel and in connection with mechanism synthesis, in the late 1970's, extensive research has started in robot-manipulator mechanics and design applications. Since then this area has become a priority for the investigations of Armenian MMS scientists. Some of the main results of these investigations are shown below.

New theoretical concepts and computational methods have been developed for the structural and approximation based parametric synthesis of lower mobility parallel robotic mechanism, including parallel mechanisms generating spatial translatory motions [25], 3D angular orientation devices [26] used as structural modules of multi-link flexible robots which imitate the motions of an elephant trunk, modular discrete manipulators with a minimum number of DOF [27] and robotic mechanisms for generating motions which are not completely specified [28].

New principles of structural synthesis of reconfigurable manipulators with variable structure and geometry to realize multiple kinematic tasks with a minimum number of actuators have been developed [29]. A task based methodology of structural-parametric synthesis of reconfigurable parallel robotic mechanisms made of two and three link adjustable structural modules has been created and tested for differentdesign applications [24].

In the last decade, intensive research works have been implemented in rehabilitation robotics. New types and structures of robotic rehabilitation synthesis with improved portability, versatility, energy efficiency and other functional characteristics ,methods of their conceptual design, dynamic modeling and balancing have been created [30–34].

Tribology and Reliability studies of Machines. The beginning of tribological research in Armenia goes as far back as the early 1960's when investigations on wear resistance and durability of cutting tools were set up in YPI. One of the fruitful directions of tribological studies established later has been the development of new friction materials and friction joints on the basis of self-lubricating polymer composites [35]. Current research issues in this area include investigations of tribomechanical and physicomechanical properties of mineral filled polymer composites [36], development of new self-lubricating composites with the use of Armenian minerals and filters [37], tribological study of plastic lubricants with bentonite thickeners [38] and other issues. Triblogical studies and related international activities in Armenia have been coordinated by the Armenian Tribology Committee established in 1974.

Reliability studies of machines and machine components started in the 1960s by the joint efforts of researchers from YPI and Armenian Academy of Sciences. The main direction of research in this area was the study of the fatigue resistance and durability of machine components based on statistical estimation methods of fracture mechanics [39–41].

Industrial research and inventive activities. A large amount of MMS research in Soviet times was influenced by the demands of industrial machinery and implemented through research contracts with industry. Interaction with industry promoted also broad scale inventive activities in all main areas of MMS. Over 150 inventions, many of them patented abroad, have been registered for new devices, automation systems, robot-manipulators, new materials and research methods. Many of these inventions have been addressed to concrete industrial applications, but the lack of financial resources, protective patent regimes and innovation infrastructures prevented to convert them into marketable products.

ACHIEVEMENTS IN MMS EDUCATION

MMS has also a rather high status in the higher engineering education of Armenia. In 1995, the first MMS based study program "Dynamics and Strength of Machines" was established in SEUA at Bachelor's, Master's and Doctoral (Candidate of Science) levels reorganized later into a broader program of Applied Mechanics which has produced over 300 graduates with BE and ME degrees. In the same period, over 70 postgraduates prepared and defined their doctoral (Candidate of Science) dissertations in MMS. On the other hand, MMS has been and still remains as one of the core courses in all Mechanical Engineering degree programs, while a general Applied Mechanics course is included in all engineering curricula of NPUA.

The progress of MMS research and education in Armenia and growing trends of their internationalization required to develop and update the Armenian terminology of MMS based on the English and Russian master versions of IFToMM terminology.

In 2009, the English-Armenian-Russian glossary of MMS has been published [42] with its on-line version installed in the website of NPUA.

DEVELOPMENT TRENDS AND CRITICAL PROBLEMS

We consider the last decade as the modern period for the MMS history in Armenia. This period was marked by the economic stabilization of the country and some positive developments in the science sphere.

Three main trends are characteristic for the present state of MMS:

- Natural experiments requiring expensive modern instruments and equipment are substituted often by computer simulations and virtual experiments. On the other hand, most of MMS research today is implemented with the use of information technologies and computer oriented approaches while the doctoral dissertations are concluded as a rule by developing application software packages.
- Growing internationalization of research activities influenced greatly by IFT0MM is another major trend in MMS development. International cooperation is playing and has to play a role of cardinal importance for Armenian MMS as a key to sound adaptation with international standards and a rare source for non- statutory funding. Mechanisms and channels used are many, including bilateral and multilateral programs, collective and individual grants, joint projects and publications with international participation.
- New targets and non traditional applications for MMS research have emerged, such as medical devices, Microsystems and new friction materials, which require interdisciplinary studies, integration of concepts and methods from different fields.

There are some critical problems and preventive factors hindering the further development of MMS in Armenia which are mainly typical for the whole science sector of the country.

* Since early 90's a continuing outflow of young MMS researchers has been taking place motivated by the lack of job opportunities and appropriate conditions for research. Generally, the brain drain process has two forms. The first is the external brain drain of scientists, mostly of a high level, who leave the country to work abroad in better conditions. The second is the internal brain drain of those who leave their academic/research careers to work elsewhere. MMS has suffered from both forms, although the former can be a way to establish links with the international scientific community which has been used to same extent. Since the most talented postgraduates are no longer attracted by the possibility of a university career, MMS faces a serious problem how to preserve and reproduce its science potential.
* Lack of state support and other funds for international academic mobility restricts strongly the participation of the Armenian MMS scientists in international conferences and their more active involvement in international research collaboration programs. Moreover, in some MMS areas publications of Armenian authors are mostly in Russian which prevents popularization and dissemination of the published results at the international level.
* The existing research infrastructures of MMS – facilities, equipment, scientific instruments are outdated and need urgent modernization. This is a precondition for the competitiveness in those research areas which require mainly experimental studies.
* Another major problem that MMS encounters today is its disconnection from industry, because industrial machinery, once a powerful branch of the national economy, was disintegrated mainly in the transition period. Lack of industrial research projects and R&D contracts with enterprises had an obvious negative influence on practical aspects of MMS restricting applied research works and innovative/inventive activities.

EXPECTATIONS AND PERSPECTIVES

Expectations for a sustained and predictable future of MMS in Armenia depend on how and to what extent the above-mentioned problems will be solved.

- Changes are necessary in the educational field to train a new generation of innovation oriented MMS researchers who are able to transform their research results and original technical ideas into marketable products. To achieve this aim the existing MMS based study programs and courses need to be brought in line with the demands of potential employment markets. A competency based curricular modernization is necessary to solve this task. One of the main targets here should be the creation of a new MMS doctoral program responding adequately to the current needs and demands of the emerging research workforce market and able to attract more students ready to start their science and academic careers in MMS.
- To prevent the continuing brain drain from Armenian MMS it is important to continue organizing more research labs in priority areas of MMS with state institutional funding that will open job opportunities for the early stage researchers and doctoral students. On the other hand, it is today's imperative to rejuvenate the teaching staff of MMS in NPUA and engineering units of other universities by recruiting the best graduates of MMS doctoral programs and creating favorable conditions for their further research work.
- Further internationalization of research and educational activities in MMS is a good resource to be used effectively. A key issue is to establish efficient financial mechanisms for benefiting from international cooperation. There is a need also to develop and implement joint degree programs at doctoral level with EU universities through Erasmus and other schemes to support international mobility of Armenian scientists and doctoral students and new initiatives for their

international research cooperation. In this regard, it is important to use effectively the existing links with the Armenian MMS scientists who work abroad. The continuing fruitful cooperation between the respective constituencies of NPUA and INSA (Rennes, France) established due to the consistent efforts of Prof. V.Arakelyan is a good example and model to follow.

- Innovation should become the main priority for the future developments in MMS and a source of opportunities yet to come. There should be more and more activity and attention to the specific problems and research needs of modern machinery, intersection with other disciplines and hybridization of technology, applications and solutions for unusual technical problems and new needs of machinery. From this viewpoint, it is believed that the present situation, trends and perspectives for MMS will not be much different from the rest of the world.
- Meanwhile, it is expected that the Armenian MMS community will contribute more in the process of revitalization and modernization of industrial machinery in Armenia. Coordinated efforts are required for the commercialization of R&D results and new technical ideas and development of innovation oriented start-ups. Building efficient research activities in the existing enterprises is also necessary. It cannot take place overnight, since the enterprises need first to become profitable to find then a possibility and interest to start innovative industrial research. In this respect, MES-18 can be a good platform to discuss new directions and targets of future MMS research addressed to the real needs and demands of industrial machinery in Armenia.

CONCLUSIONS

The present review could cover only the most significant developments and achievements of MMS in Armenia. There is much important work done that deserved mention but could not be reflected due to space limitations. In particular, very little of the very large volume of research work implemented in the last decade has been touched upon. We tried to concentrate more on the development trends and expected future of MMS related to its mission in revitalization and innovative development of industrial machinery in Armenia.

Renewal of the existing scientific potential and its reorientation to the new technological needs and demands of the country are the main challenges for Armenian MMS community. They require further internationalization of research activities and a competency based modernization of the existing study programs for preparing mechanical engineers and researchers. Specific programs directed towards young scientists to prevent brain drain should be initiated as a priority. MES-18 offers a rare opportunity to discuss these issues and find solutions for them.

REFERENCES

1. Sarkissyan Y.L. Guidelines of Science Policy and Research Management in Armenia // NATO ASI series 4.–1995.–Vol. 2.–P. 165–171.
2. Sarkissyan Y.L. MMS and IFToMM in Armenia history, present trends and perspectives. Technology Developments, the Role of Mechanism and Machine Science and IFToMM, Springer, 2010.– pp. 221–233.
3. Levitski, N.I., Shahbazian, K.K.: Synthesis of four-element spatial mechanisms with lower pairs (translated from Russian original, 1954) // Int. J. Mech. Sci.– 1960. Vol. 2, –P.76–92.
4. Edilyan, M.B.: Application of digital computers to the synthesis of path generating mechanisms (in Russian). // Proc. Armenian Acad. Sci. Phys. Math Ser.,–1961.–XIV, №5, – P.12–20.
5. Sarkissyan, Y.L., Gupta, K.C., Roth, B.: Kinematic geometry associated with the least square approximation of a given motion // ASME J. Eng. Fir Industry. 1973. –Vol.95, №2, P.503–510.
6. Sarkissyan, Y.L., Gupta, K.C., Roth B.: Spatial least square approximations of a given motion // Proceedings of IFToMM International Symposium Linkages and Computer Design Methods, Bucharest, 7–13 June 1973, vol. B, P. 512–521.
7. Sarkissyan, Y.L., Gupta, K.C., Roth, B.: Chebishev approximations of finite point sets with application to planar kinematic synthesis // ASME J. Mech. Design.–1979. Vol. 101, №1, P.32–40.
8. Sarkissian, Y.L., Gupta, K.C., Roth, B.: Chebishev approximations of spatial point sets using spheres and planes // ASME J. Mech. Design. – 1979.– Vol. 101, №3, – P. 499–503.
9. Sarkissyan, Y.L., Gupta, K.C., Roth, B. Chebishev Approximations on Finite Line Sets as a Tool in Kinematic Synthesis // Proceedings of 5th World Congress on the Theory of Machines and Mechanisms, Montreal, Canada, July 8–13 1979. P. 13–16.
10. Sarkissyan, Y.L.: Approximational Synthesis of Mechanisms.– Moscow: Nauka, 1982. – 304 p. (in Russian)
11. Sarkissyan, Y.L. Approximation problems in kinematic synthesis of spatial mechanisms. // Proceedings of 8th IFToMM World Congress on the Theory of Machines and Mechanisms, Prague, Czechoslovakia, August 26–31, 1991, Vol. 1, P. 13–17.
12. Sarkissyan, Y.L., Shahparonyan, S.S., Gupta, K.C., Roth, B. Some geometrical problems of Chebishev approximation with application to the synthesis of spherical mechanisms // Mechanica Machine. – 1983. – Vol. 60, P. 57–66 (in Russian)
13. Sarkissyan, Y.L., Stepanyan, K.G., Shahparonyan, S.S. Some problems of the approximation by curves and surfaces of the second order in kinematic geometry of 2 and 3D Motion // Proceedings of 6th World Congress on Theory of Machines and Mechanisms. – New Deli, India, December 15–20, 1983, Vol. 1, P. 303–307.
14. Sarkissyan, Y.L., Stepanyan, K.G., Shahparonyan, S.S. Minimax problems with bound

variables in synthesis of mechanisms // Proceedings of 7th World Congress on theory of machines and mechanisms, Sevilla, Spain, 1987. – Vol. 1, P. 151–154.
15. Sarkissyan, Y.L., Djavakhyan, R.P., Stepanyan, K.G., Shahparonyan, S.S. To the theory of nonlinear minimax problems in synthesis of mechanisms // Mashinovedenie. – 1983, –№1. – P. 52–60 (in Russian)
16. Sarkissyan, Y.L., Stepanyan, K.G., Shahparonyan, S.S., Karapetyan G.P. Computation algorithms for the approximation problems of mechanism synthesis with bilinear deviation functions // Transactions of the 4th IFToMM International Symposium on Theory and Practice of Mechanisms (Syrom-85), –Bucharest, Romania, 1985. – Vol. I-2, – P. 397–404.
17. Sarkissyan, Y.L., Stepanyan, K.G., Martirosyan, A.O. Approximate dynamic synthesis of linkages with elastic links // Proceedings of 9th World Congress on Theory of Machines and Mechanisms, Milan, Italy, 1995. – Vol. 2, P. 1571–1574.
18. Sarkissyan, Y.L., Stepanyan, K.G., Ohanjanyan A. Chebishev approximations in dynamic synthesis of mechanisms // Proceedings of the 11th World Congress on Mechanism and Machine Science.– Tianjin, Chine, April 1–4, 2004, Vol. 2, P. 609–611.
19. Sarkissyan Y.L., Stepanyan K.G., Verlinski S.V. Rigid body points approximating concentric circles in given sets of its planar displacements. Proceeding of the IFToMM 2015 World Congress, Oct. 25-30, 2015 Taipei, Taiwan, P. 57-61
20. Sarkissyan Yu.L. Rigid body points approximating concentric spheres in alternating sets of its given positions, Reports, NAS RA, №2, 2015, P. 110–118.
21. Sarkissyan Yu.L. Rigid body points approximating coaxial cylinders in alternating sets of its positions // Proceedings of National Polytechnic University of Armenia, Mechanics, Machine Science, Machine Building, №2,–Yerevan 2016, P.45–52.
22. Sarkissyan Yu.L. Least square approximations on finite sets of lines as applied to the synthesis of adjustable robotic mechanisms. // Proceedings of National Polytechnic University of Armenia, Mechanics, Machine Science, Machine Building, №2,–Yerevan 2017, P.31–42.
23. Sarkissyan Yu.L., Darbinyan H. Unified task based conceptual and parametric design methodology. Proc. of 14th IFToMM World Congress, Taipei, Taiwan, 25–30 October, 2015, P.806–811.
24. Sarkissyan Yu.L., Stepanyan K.G., Harutyunyan M.G., Verlisnki S.V. Methodology of block-modular structural-parametric synthesis of adjustable parallel robotic mechanisms. // Proceeding of National Polytechnic University of Armenia, Series "Mechanics, Machine science, machine-building ". - 2016. - Issue 15, N 1.- P. 28-38 (in Russian).
25. Sarkissyan, Y.L., Parikyan, T.F.: Principles of construction of spatial translational mechanisms // Mashinovedenie.–1988. – №4, P.12–20 (in Russian).
26. Sarkissyan Yu.L. Stepanyan K.G. Study and design of angular orientation mechanisms of multi-link manipulators. In "Robotic systems".– Kiev, Mashinostroenie, 1980 (In Russian).
27. Sarkissyan, Y.L., Egishyan, K.M., Kharatyan, A.G.: Synthesis of discrete manipulators with minimum number of DoF (in Russian) // Proceedings of Polish Conference of TMM. – Warsaw, Poland, 1984. P. 357–362.
28. Sarkissyan Yu.L., Parikyan T.F., Stepanyan K.G., Kharatyan A.G. Approximate synthesis of parallel manipulators for not completely specified positions of output links // Proc. of NAS and NPUA, Series of Tech. Sc., 2008,–Vol.XI, №2 (in Russian).
29. Sarkissyan, Y.L., Kharatyan, A.G., Egishyan, K.M., Parikyan T.F. Synthesis of mechanisms with variable structure and geometry for reconfigurable manipulation systems // Proceedings of ASME/IFToMM International Conference on Reconfigurable Mechanisms and Robots (ReMar - 2009). – London, UK, 2009. – P. 195–199.
30. Arakelyan, V., Ghazaryan, S.: Improvement of balancing accuracy of robotic systems: application to leg orthosis for rehabilitation devices // International Journal of Mechanisms and Machine Theory.– 2008. – Vol. 45(5), P.565–575.
31. A.L. Danielyan, K.G. Stepanyan, M.G. Harutyunyan, Yu.L. Sargsyan. Optimal control with moving ends for robotic rehabilitation devices of human extremities // Proceeding of State Engineering University of Armenia, Series "Mechanics, Machine science, machine-building ". – 2012. – Issue 15, N 1.– P. 34–41 (in Russian).
32. M.G. Harutyunyan, K.G. Stepanyan, Yu.L. Sargsyan. To the design of robotic rehabilitation systems // "Science Intensive Technologies in Mechanical Engineering", M. - Mashinostroenie – 2012, N 6. P. 41–48 (in Russian).
33. M.G. Harutyunyan, Yu.L. Sargsyan, S. Sargsyan, V. Arakelyan. Conceptual design of rehabilitation devices with artificial muscles // Coll. works XIX XXIII international scientific and technical conference "Machine Building and Technosphere in XXI century". Doneck–Sevastopol, 2012, Volume 1, pp.40-43 (in Russian).
34. N.B. Zakaryan, M.G. Harutyunyan, Y.L. Sarkissyan. Optimal design of active orthosis with redundant composite polymer-metal controllable stiffness actuators. // Coll. works XXIII international scientific and technical conference "Machine Building and Technosphere in XXI century". – Doneck–Sevastopol, 2016.– Volume 1–. P. 86-91.
35. Pogosian, A.K.: Tribology in Armenia // Proceedings of the First World Congress of Armenian Engineers, Scientists and Industrialists, – Los Angeles, USA, August 3–5, 1989, P. 195–197.
36. Pogosyan, A.K., Bahadur, S., Hovhannisyan, K.V. Investigation of the tribochemical // Physico-mechanical processes in sliding of mineral-filled

formaldehyde copolymer composites against steel. – 2006. – Vol. 260, №6, P. 662–668.
37. Cho, M.H., Behadur, S., Pogosian, A.K.: Observation on the effectiveness of some surface treatments of mineral particles and inorganic compounds from Armenia as the fillers in polyphenylene sulfide for tribological performance // Tribology International.– 2006. – Vol. 39, №3, –P. 249–260.
38. Pogosian, A.K., Martirosyan, T.R. Tribological properties of bentonite thickener-containing greases // Journal of Friction and Wear. – 2008. – Vol. 29, №3. –P. 205–209.
39. Stakyan, M.G., Galechyan, N.A.: Complex investigation and diagnosing of fatigue fractured shafts (in Russian). Proc. Nat. Acad. Sci. Ser. Technol. Sci. 54(2), 325–333 (2001)
40. Stakyan, M.G., Manukyan, M.A., Ramazyan, A.G. Statistical estimation of factors influencing crack development in shafts // Proc. Nat. Acad. Sci. Ser. Technol. Sci. –2005. –Vol. 58, №3, – P.420–425 (in Russian).
41. Gasparyan, S.H. Determination of residual stresses in metallic composites // Journal of Materials Processing Technology.– 2006. – № 178, – P.14–18(in Russian).
42. Sarkissyan, Y.L., Hovumyan, N.G., Petrosyan, H.T. English-Armenian-Russian Terminology of the Theory of Mechanisms and Machines. – Yerevan: SEUA, 2009. – 390 p.

ЭВОЛЮЦИЯ, ТЕНДЕНЦИИ И ПЕРСПЕКТИВЫ РАЗВИТИЯ НАУКИ О МАШИНАХ И МЕХАНИЗМАХ В АРМЕНИИ

Юрий Саркисян

Национальный политехнический университет Армении, Ереван, АРМЕНИЯ

АННОТАЦИЯ

Приводится краткий исторический обзор возникновения и развития теории механизмов и машин (ТММ)» и связанных с ней областей науки, объединенных под названием «Наука о механизмах и машинах (НММ)» в Армении. Представлены основные достижения армянских ученых-машиноведов в науке и образовании. Подчеркнуты роль и стимулирующее влияние Международной федерации теории механизмов и машин (IFToMM) на развитие НММ в Армении. На основе критического анализа текущего состояния НММ определены основные тенденции и проблемы ее развития. Статья завершается обсуждением приоритетных направлений и перспектив дальнейшего развития НММ в контексте возрождения и инновационного развития машиностроения в Армении.

Proceedings of the 1st International Conference MES-2018 / ИРМ-2018
MECHANICAL ENGINEERING SOLUTIONS
Design, Simulation, Testing and Manufacturing
September 17-19, 2018, Yerevan, ARMENIA

MES2018-04

THE TASK BASED METHOD OF CONCEPTUAL DESIGN AND ITS APPLICATION TO SOLAR ENERGY DEVICES OF INDOOR USAGE

Hrayr DARBINYAN

Shanghai Kunjek Hand Tool & Hardware Co.Ltd, Shanghai, China, hvdarbin@yahoo.com

ABSTRACT

Usage of solar energy in Armenia lacking in natural power resources is an actual objective as well an attractive perspective to access endless ecologically clean energy. Experience of more than two decade creation of mirror-covered parabolic plates shows definite limitation of usage because of its outdoor location and safety, usage convenience concerns. A novel conceptual design (CD) methodology applicable for large variety of mechanical devices is used for setting objective, analyzing resources and coming to optimal structural solutions for mirror-covered parabolic plates. This methodology is advantageously singled out from known CD methods by multifunctional synthesis, application of a standard set of design environment modification tools, possibility of building intermediate mechanical-functional models, development and usage of flexible evaluation charts. In the current paper attention is paid to more formalized mathematical description of key steps of suggested Conceptual Design process: description and growth of mechanical and functional entities, development of models and charts for evaluation and making decision. Application of developed and multiply proven design methodology for mirror-covered parabolic plates helps to reveal ways for coming to most effective designs and set guidelines for their everyday application.

INTRODUCTION

Conceptual design in mechanical engineering is the most challenging and least understood part of the whole design process. Various methods and approaches are developed and are being developed to set rules, starting points, and procedures leading to a novel conceptual solution. Most of the methods are grouped around the fundamental idea of separating function from mechanism [1], leading to abstraction of the physical and kinematical diagram of mechanism into topological categories and arranging combinational search of novel conceptual design through combinational search. Such an approach is followed and developed by [2], [3],etc. A block using approach [4] allows to build design modules responsible for definite movement and to arrange combination of different movements for getting different functions. The synthesis is solely based on the previous knowledge and new features are searched by proper modification of structure of existing mechanisms. Currently application of genetic algorithms is widely used in conceptual design and particularly in automated conceptual design. In study [5] different modular robotic structures have been considered, the variety of these structures is generated by combinational method. Each new generation of robots is evaluated by means of numerated features, and the direction of further synthesis tactics is defined by means of a genetic algorithm. More traditional approaches [6] rely on practical knowledge rather than formalized methodology of mechanism synthesis, the conceptual solution is searched as a structure addition to the current design by chains from a database having the demanded mechanical properties.

Widely popularized method of TIPS (Theory of Inventive Problem Solving) suggests a procedure of VEPOL (a Russian abbreviation of Substance + Field) formation to reveal and neutralize harmful functions. Massive matrix of contradictions serves a large number of design scenarios, without development of compact models to express a set of demands and organize search of novel concept design solutions[7].

Anyhow difficulties of building mathematical and logical models supporting and describing the CD process are still obstacles slowing down the efficiency of the conceptual design process.
A novel concept design method [8] approved and confirmed for numerous products developed by the author during a long term engineering career is suggested where the main idea is formulated as search, isolation and general consideration of sets from both functional and mechanical entities, where mechanical means define the nature of functions and functions are provided by the mechanical means isolated from a mechanical entity. In other words this kind of modification of both entities can be considered as modelling and the process of conceptual design is dealing with models of limited contents, more compact and flexible than the entire functional and mechanical entities are.

Starting from the idea of separating function from mechanism attempts were directed to substitute a large scale and exhausting search of a conceptual solution by a directed and targeted search. Previous strategies for accomplishing this idea have focused on consideration of specific fragments of mechanical and functional entities, when both fields should be presented in a way allowing consideration of their specific and limited parts. So the objective was formulated as description and modification of mechanical and functional entities and setting of rules for combined usage of components from those entities. A general point is adopted for this purpose, according to which a parent link may serve as origin for daughter link, with further equal status for consideration of both. And a parent function may serve origin for daughter function, with later definition of function status and weight. For the case of links relation particularly can be a specific kinematical joint. In the case of a function, generation of a daughter function is important from point of its satisfaction by mechanical means. Most CD approaches [1, 2, 3] are not considering multifunctional synthesis of mechanism. Usually one function is considered as main one, while others are considered as limitations. The fact of granting both the links and functions all equal and adequate categories allows buildup of homogenous mechanical and functional fields, with possibility of their unified modification. Function discrimination is applicable on the evaluation stage of conceptual design by means of weighing, limitation and cancelation of functions.

TASKS AND OBJECTIVES

First task of this paper is to build a mathematical and logical model for basic steps of a task based conceptual design process. The next task is to show implementation of developed models on an example of novel solution for a device using solar energy for indoor application.

KEY MODEL AND MAIN COMPONENTS OF TASK BASED CONCEPTUAL DESIGN

Key model is connecting links x_1 and x_2 in a way to allow implementation of function F_{12} by this connection (1). The connection expresses a standard kinematical joint as well it can express more general types of link contact, thus enlarging scope of functions involved and setting base of more comprehensive conceptual design with manifold functions.

$$M_{1,2} = \begin{bmatrix} x_1 & a_{12} & x_2 \\ (x_1) & F_{12} & (x_2) \end{bmatrix} = \begin{bmatrix} x_1 & a_{12} \\ F_{12} & x_2 \end{bmatrix} \qquad (1)$$

Topologically this fact can be visualized by two vertices and two edges of graph where vertices are related to two original links of start of conceptual design and one edge relates to the function subject to implementation, and the other edge relates to the type of joint between those two links. Same can be shown in a specific 3 x 2 matrix presentation as well as in a standard 2 x 2 square matrix, with numeration of links along rows and columns and with indication of their relation in intersection cells. Self-relation of links gives empty cells $a_{m,n} = 0$, if $m = n$. Elements of upper right diagonal area are for link relation, and elements in the lower left diagonal area are for functions. So:

$$a_{m,n} = a_{n,m} = F_{i,j} \qquad (2)$$

A mechanism subject to conceptual design needs to include two sets of categories m, n – the links and $a_{m,n}$ relations, related in a way to satisfy given set of functions:

$$M = \{m, n / Q(a_{m,n})\} \qquad (3)$$

Therefore the objective of CD is to find a required set of links connected in a way to satisfy given set of functions:

$$M_{m,n} = M \begin{bmatrix} m, n \\ a_{m,n} \end{bmatrix} \qquad (4)$$

The initial objective of a novel CD approach should be description of expandable entities for both mechanical and functional categories.

Description of Mechanical Entity

Components of mechanical entity arranged in a square matrix:

$$M_{m,n} = M \begin{bmatrix} m, n \\ a_{m,n} \end{bmatrix} = \begin{bmatrix} a_{11} & \cdots & a_{1n} \\ \vdots & \ddots & \vdots \\ a_{m1} & \cdots & a_{mn} \end{bmatrix} \qquad (5)$$

Set of links m, n related in a way to satisfy a property-feature-function $Q(a_{m,n})$:

$$M_{m,n} = \{m, n / Q(a_{m,n})\} \qquad (6)$$

Where:

m, n - numeration of links (set of links)

$a_{m,n}$ - relation of links,

$a_{n,m}$ - kinematic or other joint

$a_{m,n} = 1$, if links are related

$a_{m,n} = 0$, if the links are not related

If $m = n$, then $a_{mn} = 0$

Where number of links varies within range (7). $M = N$ is maximum number of links.

$$M = \begin{bmatrix} 1 \le m, n \le M, N \\ a_{1 \le m, n \le M, N} \end{bmatrix} \qquad (7)$$

Two integers (numbers) m and n are used to designate links, to allow identification of relation between different links m, n of mechanical entity so self-relation of a link is disregarded.

Description of Functional Entity

Components of functional entity also can be arranged in a square matrix: (8)

$$F_{i,j} = F\begin{bmatrix} i, j \\ f_{i,j} \end{bmatrix} = \begin{bmatrix} f_{11} & \cdots & f_{1j} \\ \vdots & \ddots & \vdots \\ f_{i1} & \cdots & f_{ij} \end{bmatrix} \qquad (8)$$

Set of function i, j translated from each other in a way to satisfy function generation or creation rule $Q\left(f_{i,j}\right)$:

$$F_{i,j} = \left\{ i, j / Q(f_{i,j}) \right\} \qquad (9)$$

Where:

i, j - numeration of functions

$f_{i,j}$ - function translation between i and j

$f_{i,j} = 1$, if functions are translated

$f_{i,j} = 0$, if there is no relation between functions

If $i = j$, then $f_{i,j} = 0$

Where number of links varies within range (10).

$I = J$: is the maximum number of links.

$$F\begin{bmatrix} 1 \le i, j \le I, J \\ f_{1 \le i, j \le I, J} \end{bmatrix} \qquad (10)$$

Growth of Mechanical Entity

Growth of mechanical entity is stipulated by necessity and possibility of function satisfaction by getting a satisfactory number of links:

$$M_{m,n}\begin{bmatrix} m, n \\ a_{m,n} \end{bmatrix} \Rightarrow M_{m+\Delta m, n+\Delta n}\begin{bmatrix} m+\Delta m, n+\Delta n \\ a_{m+\Delta m, n+\Delta n} \end{bmatrix} \qquad (11)$$

Growth is measured by number of links Δm added to original number of links m . Range of both values is specified in (12)

$$\begin{bmatrix} 1 \le m \le M \\ 1 \le \Delta m \le M - 1 \end{bmatrix} \qquad (12)$$

The mechanical entity can be squeezed down as well as opposite procedure to growth. The combined description of both growth/squeezing action will read:

$$M_{m,n}\begin{bmatrix} m, n \\ a_{m,n} \end{bmatrix} \Rightarrow M_{m \pm \Delta m, n \mp \Delta n}\begin{bmatrix} m \pm \Delta m, n \pm \Delta n \\ a_{m \pm \Delta m, n \pm \Delta n} \end{bmatrix} \qquad (13)$$

Once entity modification is done link and relation designations are getting their original values:

$$m \pm \Delta m \rightarrow m\,,\ a_{m \pm \Delta m} \rightarrow a_m \qquad (14)$$

Growth of Functional Entity

Growth of functional entity is stipulated by necessity and possibility of translation function into an "understandable" one that could be implemented by mechanical entity:

$$F_{i,j}\begin{bmatrix} i, j \\ f_{i,j} \end{bmatrix} \Rightarrow F_{i+\Delta i, j+\Delta j}\begin{bmatrix} i+\Delta i, j+\Delta j \\ f_{i+\Delta i, j+\Delta j} \end{bmatrix} \qquad (15)$$

Growth is measured by number of functions Δi consecutively translated from original function i .

Range of both values is specified in (16)

$$\begin{bmatrix} 1 \le i \le I \\ 1 \le \Delta i \le I - 1 \end{bmatrix} \qquad (16)$$

Analogously to the mechanical entity the functional entity also can be squeezed down. The combined description of both growth/squeezing action is:

$$F_{i,j}\begin{bmatrix} i, j \\ f_{i,j} \end{bmatrix} \Rightarrow F_{i \pm \Delta i, j \pm \Delta j}\begin{bmatrix} i \pm \Delta i, j \pm \Delta j \\ f_{i \pm \Delta i, j \pm \Delta j} \end{bmatrix} \qquad (17)$$

Once entity modification is done, function and translation designations are getting their original values:

$$i \pm \Delta i \to i\,,\ f_{i\pm\Delta i} \to f_i \qquad (18)$$

Combined Description of Mechanical and Functional Entities

The methodical value of including function in the matrix of mechanical entity is firstly in planning and secondly supporting to function satisfaction (19, 20):

$$M_{m,n}\begin{bmatrix} m,n \\ a_{m,n} \\ a_{n,m} \end{bmatrix} \Leftrightarrow F_{i,j}\begin{bmatrix} i,j \\ f_{i,j} \end{bmatrix} \qquad (19)$$

$$M_{m,n}^{i,j}\begin{bmatrix} m,n \\ a_{m,n} \\ a_{n,m} \Leftrightarrow F_{i,j} \end{bmatrix} \Leftrightarrow M_{m,n}^{i,j}\begin{bmatrix} m,n \\ a_{m,n} \Leftrightarrow R_{m,n} \\ a_{n,m} \Leftrightarrow F_{i,j} \end{bmatrix} \qquad (20)$$

Mirror $a_{n,m}$ position of relation $a_{m,n}$ to kinematical joint cell $R_{m,n}$ is given to function $F_{i,j}$ subject to satisfaction.

Modification and Creation of Models

Methodical value of choice of a fragment g_M (21) in mechanical entity is in isolation of the fragment best suitable for planning and implementation of specific set of functions:

$$M\begin{bmatrix} m,n \\ a_{m,n} \end{bmatrix}\begin{bmatrix} 1 \le m,n \le M,N \\ a_{1\le m,n\le M,N} \end{bmatrix} \Rightarrow g_M\begin{bmatrix} m,n \\ a_{m,n} \end{bmatrix} \qquad (21)$$

Choice of a fragment g_F (22) in functional entity is subject to implementation by fragment g_M (21) in mechanical entity.

$$F\begin{bmatrix} i,j \\ f_{i,j} \end{bmatrix}\begin{bmatrix} 1 \le i,j \le I,J \\ f_{1\le i,j\le I,J} \end{bmatrix} \Rightarrow g_F\begin{bmatrix} i,j \\ f_{i,j} \end{bmatrix} \qquad (22)$$

$$g\left\{g_M, g_F\right\} \qquad (24)$$

Set (26) can be called the mechanical-functional model of conceptual design. Modification of both entities (21and 22) are doable by procedures described in chapters “Growth of Mechanical Entity” and “Growth of Functional Entity” above.

Evaluation of Conceptual Solutions

Functional $F_{i,j}$ entity stores capability for qualitative evaluation of conceptual design solutions at a single step as well for the final solution. The summarizing indicator (25) depends on presence or absence of a challenged function and its weight.

$$E_{i,j} = \sum_{i.j=1}^{I,J} W_{i,j}F_{i,j} \qquad (25)$$

$F_{i,j} = 1$, if function is satisfied

$F_{i,j} = 0$, if function is not satisfied

$0 \le W_{i,j} \le 1$, function weight and its range

Two conceptual solutions can be compared and evaluated by summarizing indicators:

$$E_{i,j} = \sum_{i.j=1}^{I,J} W_{i,j}F_{i,j} \Leftrightarrow \bar{E}_{i,j} = \sum_{i.j=1}^{I,J} \bar{W}_{i,j}\,\bar{F}_{i,j} \qquad (26)$$

APPLICATION OF CONCEPTUAL DESIGN METHOD TO INDOOR USAGE SOLAR DEVICES

Parabolic antennas are used for focusing solar energy from a distant source to a focus point. Starting from the early 90’s there were continuous attempts in Armenia for using mirror-covered parabolic dishes (Fig.1) as an energy source for everyday purposes. Unlike tube collectors those devices require close approach of the user to the focus point where the hot area is located. This makes usage quite complicated dealing with movement of large scale counterweight-balanced mirror-plated parabolic dishes. Such parabolic dishes should be used outdoors only, while tube collectors allow transfer of heated water indoors for much comfortable application. So the task of concept current design is to synthesize a solar energy usage device capable to transfer heating energy indoors for comfortable and safe application (Fig.2).

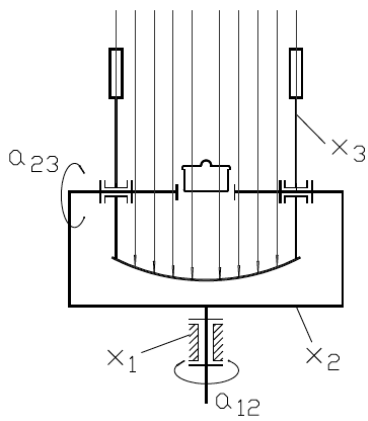

Figure 1.Outdoor usage parabolic plate solar device

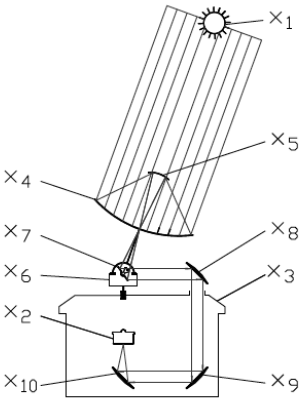

Figure 2. Indoor usage parabolic plate solar device

Table 1.Set of conceptual design actions

1.Set of functions as task on CD	2.Isolation of a function
$\begin{bmatrix} i,j \\ f_{i,j} \end{bmatrix} = \begin{bmatrix} \{1,..,6\} \\ f_{1,..,6}=0 \end{bmatrix}$	$\begin{bmatrix} i,j \\ f_{i,j} \end{bmatrix} = \begin{bmatrix} \{6\} \\ f_{1,..,6}=0 \end{bmatrix}$

	i_1	i_2	i_3	i_4	i_5	i_6	i_7	i_8
j_1	0	0	0	0	0	0	0	0
j_2	0	0	0	0	0	0	0	0
j_3	0	0	0	0	0	0	0	0
j_4	0	0	0	0	0	0	0	0
j_5	0	0	0	0	0	0	0	0
j_6	0	0	0	0	0	0	0	0
j_7	0	0	0	0	0	0	0	0
j_8	0	0	0	0	0	0	0	0

	i_1	i_2	i_3	i_4	i_5	i_6	i_7	i_8
j_1	0	0	0	0	0	0	0	0
j_2	0	0	0	0	0	0	0	0
j_3	0	0	0	0	0	0	0	0
j_4	0	0	0	0	0	0	0	0
j_5	0	0	0	0	0	0	0	0
j_6	0	0	0	0	0	0	0	0
j_7	0	0	0	0	0	0	0	0
j_8	0	0	0	0	0	0	0	0

3. Translation of a function	4.Set of links and function planning
$\begin{bmatrix} i,j \\ f_{i,j} \end{bmatrix} = \begin{bmatrix} \{5,6\} \\ f_{56}=1 \end{bmatrix}$	$\begin{bmatrix} m,n \\ a_{m,n} \end{bmatrix} = \begin{bmatrix} \{1,2,3\} \\ a_{1,2}a_{2,3} \end{bmatrix}$

	i_1	i_2	i_3	i_4	i_5	i_6	i_7	i_8
j_1	0	0	0	0	0	0	0	0
j_2	0	0	0	0	0	0	0	0
j_3	0	0	0	0	0	0	0	0
j_4	0	0	0	0	0	0	0	0
j_5	0	0	0	0	0	△	0	0
j_6	0	0	0	0	△	0	0	0
j_7	0	0	0	0	0	0	0	0
j_8	0	0	0	0	0	0	0	0

	n_1	n_2	n_3	n_4	n_5	n_6	n_7	n_8
m_1	0	○	0	0	0	0	0	0
m_2	□	0	○	0	0	0	0	0
m_3	0	□	0	0	0	0	0	0
m_4	0	0	0	0	0	0	0	0
m_5	0	0	0	0	0	0	0	0
m_6	0	0	0	0	0	0	0	0
m_7	0	0	0	0	0	0	0	0
m_8	0	0	0	0	0	0	0	0

5. Synthesis: input of joints	6.Evaluation of a single cycle of conceptual design
$\begin{bmatrix} m,n \\ a_{m,n} \end{bmatrix} = \begin{bmatrix} \{1,2,3\} \\ R_{1,2}R_{2,3} \end{bmatrix}$	$\begin{bmatrix} i,j \\ f_{i,j} \end{bmatrix} = \begin{bmatrix} \{6,7,8\} \\ f_{6,7,8}=0 \end{bmatrix}$

	n_1	n_2	n_3	n_4	n_5	n_6	n_7	n_8
m_1	0	▲	0	0	0	0	0	0
m_2	□	0	▲	0	0	0	0	0
m_3	0	□	0	0	0	0	0	0
m_4	0	0	0	0	0	0	0	0
m_5	0	0	0	0	0	0	0	0
m_6	0	0	0	0	0	0	0	0
m_7	0	0	0	0	0	0	0	0
m_8	0	0	0	0	0	0	0	0

	i_1	i_2	i_3	i_4	i_5	i_6	i_7	i_8	Wi	Ei
j_1	0	0	0	0	0	0	0	0	0	0
j_2	0	0	0	0	0	0	0	0	0	0
j_3	0	0	0	0	0	0	0	0	0	0
j_4	0	0	0	0	0	0	0	0	0	0
j_5	0	0	0	0	0	0	0	0	0	0
j_6	0	0	0	0	0	0	0	0	W_6	E_6
j_7	0	0	0	0	0	0	0	0	W_7	E_7
j_8	0	0	0	0	0	0	0	0	W_8	E_8

Table3.Symbols used in Table2

Symbols	Nomenclature	Category
■	m,n	Links of mechanical entity
□	i,j	Numeration of functions
□	$F_{i,j}$	Set of functions
△	$f_{i,j}$	Translation of a function
○	$a_{m,n}$	Kinematical or other relation(planned)
▲	$R_{m,n}$	Kinematical or other joint(relation)

Table2.Set of conceptual design steps

K1.Set of functions	K2.Concentrate rays
$\begin{bmatrix} m,n \\ a_{m,n} \end{bmatrix} = \begin{bmatrix} \{1,2,3\} \\ a_{1,2}a_{2,3} \end{bmatrix}$	$\begin{bmatrix} m,n \\ a_{m,n} \end{bmatrix} = \begin{bmatrix} \{1,...,5\} \\ a_{m,n} \end{bmatrix}$
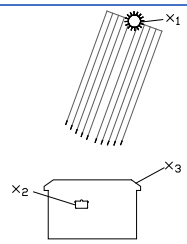	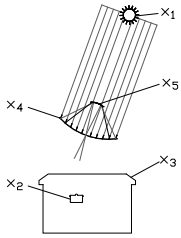
K3. Track the Sun	**K4.Guide the ray**
$\begin{bmatrix} m,n \\ a_{m,n} \end{bmatrix} = \begin{bmatrix} \{1,...,6\} \\ a_{1,2}...a_{5,6} \end{bmatrix}$	$\begin{bmatrix} m,n \\ a_{m,n} \end{bmatrix} = \begin{bmatrix} \{4,5,7\} \\ a_{4,5}a_{5,7} \end{bmatrix}$
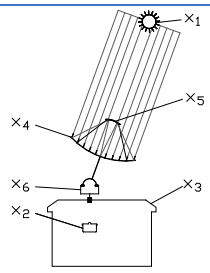	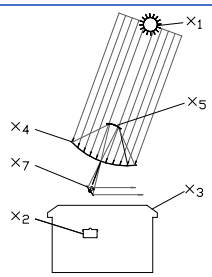
K5.Track the Sun	**K6.Guide rays indoors**
$\begin{bmatrix} m,n \\ a_{m,n} \end{bmatrix} = \begin{bmatrix} \{3,6,4\} \\ a_{3,6}a_{6,4} \end{bmatrix}$	$\begin{bmatrix} m,n \\ a_{m,n} \end{bmatrix} = \begin{bmatrix} \{7,8,9\} \\ a_{7,8}a_{8,9} \end{bmatrix}$

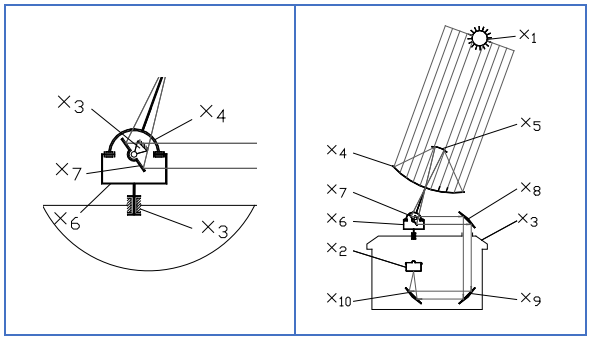

Table4.Nomenclature of components

Nomenclature of Components	
x_1 : Sun	x_6 : Azimuth track
x_2 : Pot	x_7 : Receiver
x_3 : House	x_8 : Top plate
x_4 : Reflector(Parabolic plate)	x_9 : Bottom plate
x_5 : Sub reflector	x_{10} : Cook plate

CONCLUSION

1. Developed mathematical models for description of the main components of conceptual design process, making another step toward creation of interactive designer/system environment.
2. Developed means of mathematical and physical description support such steps of CD process as description, combined consideration of both mechanical and functional entities, modification and usage of accumulated knowledge from database, application of modification tools, getting and evaluation of result after each step of cyclically organized CD process.
3. Method is applied for conceptual design for a device for indoor usage of solar energy
4. Future work and actions. Further develop the mathematical base and software components for creation of interactive designer-CD system environment. Complete physical design and test physically the device conceptually developed and presented in this paper.

REFERENCES

1. Freudenstein F, Maki E.R., "The Creation of Mechanisms According to Kinematic Structure and Function", Environment and Planning B., Vol.6, 375-391 (1979).
2. Tsai L.W., *Mechanism Design: Enumeration of Kinematic Structures According Function*, CRC Press, New York (2000).
3. Yan Hong-Sen, "A Methodology for Creative Mechanism Design", Mech.Mach. Theory, Vol.27, No.3, 235-242 (1992).
4. Kota, Shean-Juinn Chiou, "Conceptual Design of Mechanisms Based on Computational Synthesis and Simulation of Kinematic Building Blocks", Research in Engineering Design, Springer-Verlag, NY, Vol.4,75-87 (1992).
5. Farritor S., Dubowsky S., "On Modular Design of Field Robotic Systems", University of Nebraska Publications (2001).
6. Pahl G., Beitz W., *Engineering Design, A Systematic Approach*, Springer, NY (1995).
7. Альтшуллер Г.С., *Творчество как точная наука. Теория решения изобретательских задач*. - Сов. радио, Кибернетика, М.,(1979).
8. Darbinyan H.V., "Task Based Conceptual Design Method" in Proceedings of 13th World Congress in Mechanism and Machine Science, A23-559. Guanajuato, Mexico (2011).

ПРИНЦИП КОНСТРУИРОВАНИЯ СОЛНЕЧНЫХ ЭНЕРГЕТИЧЕСКИХ УСТРОЙСТВ ДОМАШНЕГО ИСПОЛЬЗОВАНИЯ

Г. Дарбинян
Шанхай Кунджек ручные инструменты и оборудование Ко. Лтд., Шанхай, Китай

АННОТАЦИЯ

Использование солнечной энергии в небогатой энергоносителями Армении является актуальной проблемой, а также хорошей перспективой доступа к бесконечной и экологически чистой энергии. Более чем двадцатилетний опыт создания устройств с параболическими тарелками, покрытыми зеркалами, выявил ограниченность их применения из-за необходимости размещения вне жилого помещения и проблем безопасности использования. Новая методология концептуального проектирования (КП), применяемая для большого разнообразия механических устройств, включает постановку задачи, анализ доступных ресурсов и достижение оптимального структурного решения для параболических тарелок, покрытых зеркалами. Данная методология выгодно отличается от известных методов КП многофункциональным синтезом, применением стандартного набора инструментов модификации среды проектирования, возможностью создания промежуточных механико-механико-функциональных моделей, разработкой и использованием гибких оценочных таблиц. В настоящей статье внимание уделено

более формализованному математическому описанию ключевых этапов предлагаемого метода концептуального проектирования: описанию и росту механических и функциональных объектов, разработке моделей и таблиц для оценки результата и принятия решения. Применение разработанной и многократно проверенной методологии проектирования для случая установок с параболическими тарелками, покрытыми зеркалами, дает возможность раскрыть наиболее эффективное концептуальное решение и наметить пути для их каждодневного использования.

Proceedings of the 1st International Conference MES-2018 / ИРМ-2018
MECHANICAL ENGINEERING SOLUTIONS
Design, Simulation, Testing and Manufacturing
September 17-19, 2018, Yerevan, ARMENIA

MES2018-14

MODELING AND DESIGNING OF THE HYDRAULIC STEWART PLATFORM CONTROL SYSTEM IN MATLAB

Azatuhi ULIKYAN[1], Markar GASPAROV[2], Amalya MKHITARYAN[3], Astghik HAKOBYAN[4]

[1]NPUA, Yerevan, Armenia, e-mail: azatuhi.ulikyan@gmail.com

[2] Ltd «Urartu», Samara, Russia, e-mail: info@urartusystems.ru

[3]NPUA, Yerevan, Armenia, e-mail: amalya.mkhitaryan@gmail.com

[4]NPUA, Yerevan, Armenia, e-mail: astghikhakobyan@gmail.com

ABSTRACT

The Stewart platform on hydraulic motors is investigated. The dynamic model for the system investigation was created in Simulink (Sims cape) environment for physical simulation. The created model allows to reconfigure the system by inserting numeric parameters. The PID controller for getting stabile and observable responses for given inputs is designed.

The changes in the length of each leg of the Stewart platform were obtained by use of the inverse kinematics problem.

The software allows to explore the behavior of the system for a given input signal.

INTRODUCTION

During the last decades hexapods and in particular Stewart platform [1] have been widely used in control applications including vibro-insulation systems, big telescopic secondary mirror control systems, laboratory's research devices and etc.

In this paper, Stewart platform is considered as a multidimensional hydraulic control system [1].

Structurally, a hexapod is a mobile platform with a payload. The platform is situated on six legs - hydraulic actuators, each of which can change its length. In the terms of dynamic analysis, the given configuration makes the problem much more complex.

The structural scheme of multidimensional system is given. **(Figure 1).**:

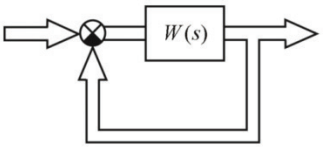

Figure 1. The structural scheme of Stewart platform

The kinematic scheme of hexapod as a multidimensional hydraulic system is given **(Figure 2)**:

All legs of the platform are hydraulic actuators.

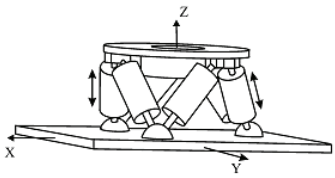

Figure 2. The kinematic scheme of the hexapod

The control system of the Stewart platform is aimed to provide the desired position of the platform.

The control of the position and direction can be implemented by use of inverse kinematics task and trajectory design algorithm through control of length of the legs [2]. The inverse kinematics task for investigated object can be formulated as following: to find out pump length (force or position) for each of the six hydraulic actuators.

Each leg (one axis hydraulic actuator) is represented by the pump and the cylinder, connected

by prismatic node. The multidirectional Stewart platform consists of 6 subsystems.

At the first stage, coordinates of the connection of actuators (legs), platform and its base are calculated. Despite diversion of 60 degrees the platform and the base differ from each other only by size, that's why the analysis for both are done by the same way. The layout of the coordinates of the platform and base nodes has been constructed in MATLAB environment.

For the initial position of the base we have chosen an alignment in which its centre coincides with the origin of the coordinate system and one of the long edges is perpendicular to the X axis, with the crossing point in the positive direction. In this configuration the centre of the platform coincides with the centre of the base in the X,Y plane and the platform is rotated by 60^0 along its centre relative to the base.

With this initial state configuration and chosen physical dimensions we have calculated the coordinates of all nodes.

The coordinates of the nodes in the X, Y plane are shown **(Figure 3)**.

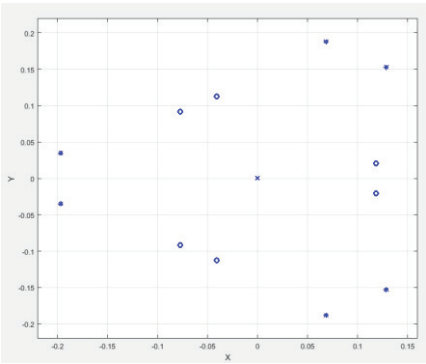

Figure 3. Coordinates of Stewart platform joints in the X,Y plane

In the graph the coordinates of the base nodes are indicated by *, o - the platform, and x - the coordinates of the middle point. The view of the model in three-dimensional space is given(**Figure 4**) for Z = 0.4m value.

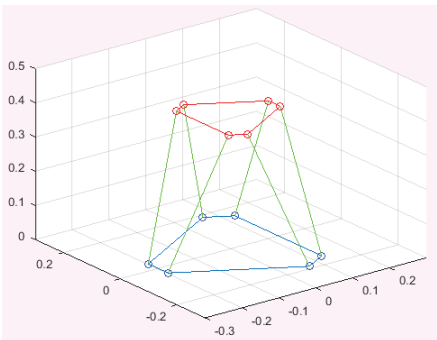

Figure 4. The node coordinates in three-dimensional space (Z=0.4m)

The coordinates of the nodes of the platform are 169.0370 45.2933; 123.7437 123.7437; -123.7437 123.7437; -169.0370 45.2933; -45.2933 -169.0370; 45.2933 -169.0370 and 20 mm width.

The coordinates of the nodes of the base are 193.1852 51.7638; 141.4214 141.4214; -141.4214 141.4214; -193.1852 51.7638; -51.7638 -193.1852; 51.7638 -193.1852 and 20 mm width.

The Stewart top and bottom platforms for given coordinates are built by use of Multibody blocks.

All six legs of the platform are connected by spherical nodes. As a result, the dynamic model of the Stewart platform and its appearances are received **(Figure 5, Figure 6)**.

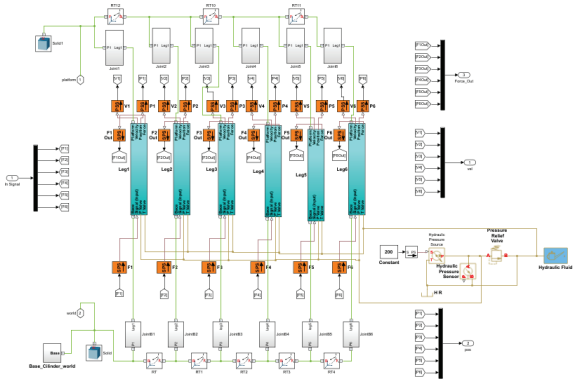

Figure 5. Dynamic model of the Stewart platform

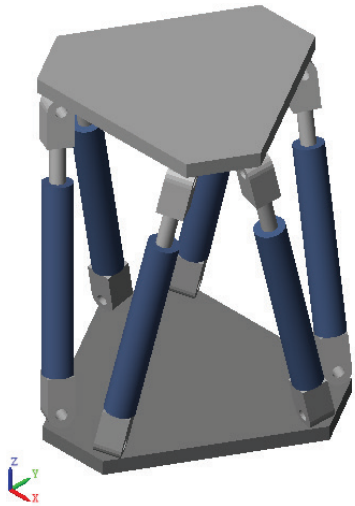

Figure 6. The 3D model of the Stewart platform

The position and speed for each leg are received as an output response to the given input signals to all actuators. The determination of the full input matrix of the system rotation toward the bottom platform is necessity:

$$
{}^{P}R_B = R_z(\psi)\cdot R_y(\theta)\cdot R_x(\varphi) =
$$

$$
= \begin{pmatrix} c\psi c\theta & -s\psi c\varphi + c\psi s\theta s\varphi & s\psi s\varphi + c\psi s\theta c\varphi \\ s\psi c\theta & c\psi c\varphi + s\psi s\theta s\varphi & -c\psi s\varphi + s\psi s\theta c\varphi \\ -s\theta & c\theta s\varphi & c\theta c\varphi \end{pmatrix}
$$

The length of each of actuators (legs) are determined by the following equation:

$$L_i = \sqrt{{l_x}^2 + {l_y}^2 + {l_z}^2}:$$

The received non-linear system is linearized by Linear Analysis Tool. For the closed loop system, the time response curve has been obtained. The curves have indicated the instability of the system and necessity to design a regulator. The structural scheme and model of the Stewart platform closed loop system with PID controller are given [3] **(Figure 7, Figure 8).**

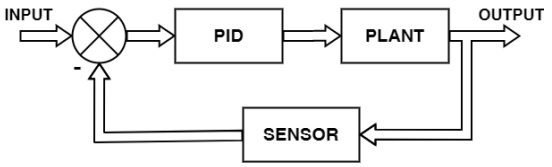

Figure 7. The structural scheme of the control system of the Stewart platform

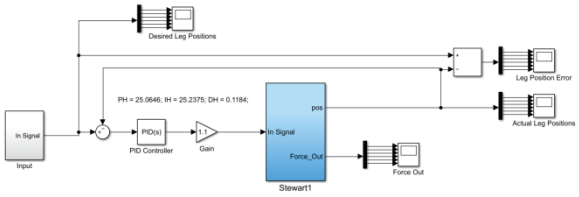

Figure 8. The model of control system of the Stewart platform

By use of MATLAB Response Optimization section possibilities, the PID controller parameters are found.

Determination of the parameters are done as a solution of the optimization problem by the gradient method. The PID controller parameters as arguments are specified.

P, I and D parameters of PID controller have been transferred to MATLAB workspace or registered in the configuration file. Through giving the change boundaries of the input signal in Design Optimization window, the parameters of the PID controller P=25.0646, I=25.2375, D=0.1184 were obtained for the given physical characteristics of the system.

The model developed in the MATLAB Simulink environment [4-5] does not allow to have analytical expressions of differential equations of the system. The MATLAB Simulink model provides an opportunity to get almost any characteristic through simulation, including movements, rotations, speeds, accelerations, forces, torques, and other characteristics.

Let's consider the system's response to 0.05m step displacement only along Z axis. We also consider rotation angles around the axes equal to 0 degree. The motion of the each of the legs toward input signal as well as the error of the output signal toward input have the appearance shown **(Figure 9)**.

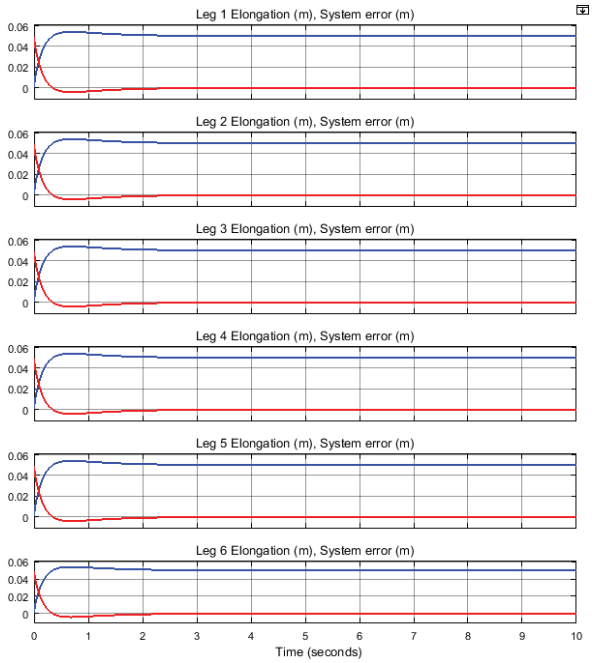

Figure 9. The elongation of each leg (blue) and error of the system (red) for given step signal

For the time response parameters we have obtained following values: overshooting - $\delta = 8.5\%$ and settling time - $t_s = 3.012$ min:

Let's create harmonic signal in the input with 0.01m amplitude and 5rad/s frequency for getting vibrating system. The elongation of each length of the leg and the error in the system is following **(Figure 10)**.

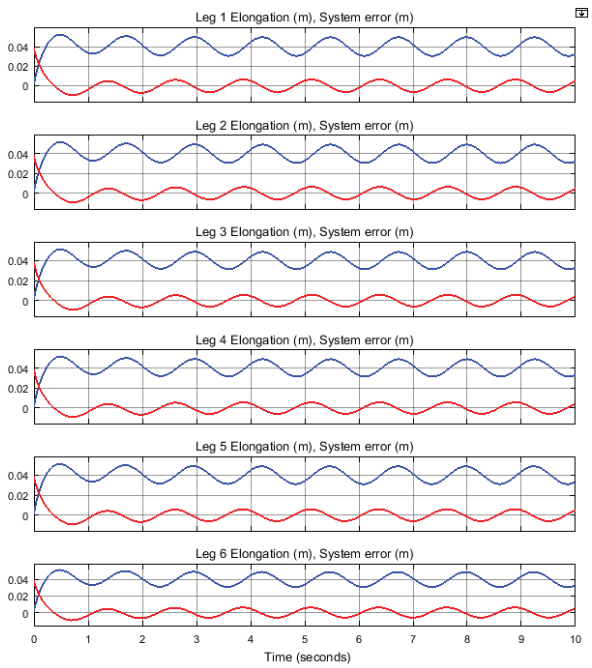

Figure 10. The elongation of each leg (blue) and error of the system (red) for given harmonic signal

Similarly, the system's behavior when rotation angles around the axes are not 0 degree is given.

The rotation angles around the X and Z axes are given as a sine signals with opposite sign 0.08 m amplitude and 10 radar/s frequensy. The angle of rotation around the Y axis is given as a harmonic signal with same amplitude and frequency, but with π/2 phase deviation. The output parameters of the hydraulic system are elongation and error of the corresponding legs **(Figure 11)**.

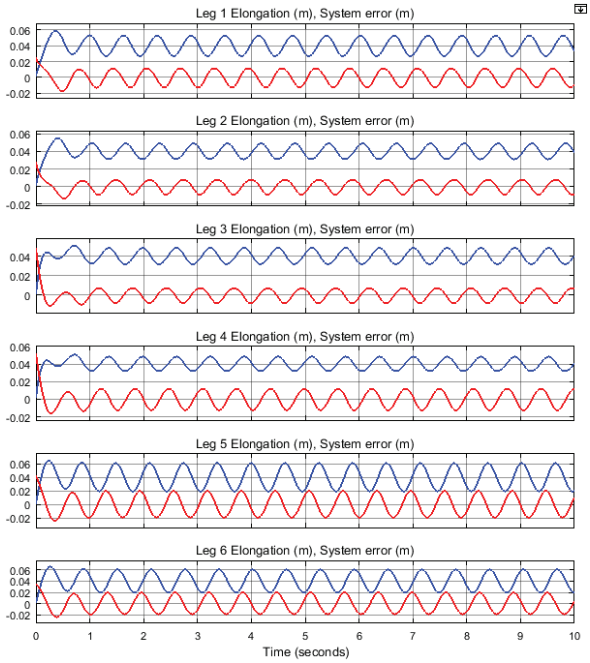

Figure 11. The elongation of each leg (blue) and error of the system (red) for given harmonic signal for corresponding positions and angles

As in previous cases, for a similar input signal, the system is stable and controllable.

MAIN HEADING

P	Proportional coefficient;
I	Integral coefficient;
D	Differential coefficient;
$t_н$	Rise time;
t_y	Establishment time;
δ	Overshooting;
φ	Rotation around the x-axis (roll);
θ	Rotation around the y-axis (pitch);
ψ	Rotation around the z-axis (yaw);
$c\varphi$	$cos(\varphi)$;
$c\theta$	$cos(\theta)$;
$c\psi$	$cos(\psi)$;
$s\varphi$	$sin(\varphi)$;
$s\theta$	$sin(\theta)$;
$s\psi$	$sin(\psi)$;
${}^{P}R_{B}$	Full rotation matrix of the Platform relative to the Base;
$R_x(\varphi)$	Rotation matrix around the x-axis;
$R_y(\theta)$	Rotation matrix around the y-axis;
$R_z(\psi)$	Rotation matrix around the z-axis;
L_i	Length of each leg.

CONCLUSION

The dynamic model of the system is created in Simulink environment. The control system of mechanism is created and investigated based on the model. The PID controller is designed. The system is linearized. All obtained results are checked and confirmed their compliance with the given task.

All experimental work has been done at ANEL within scope of “Hydraulic Vibro-stand” scientific project's grant.

REFERENCES

1. Filip, Szufnarowski. *Stewart platform with fixed rotary actuators: a low cost design study*.- 2013. - 11 p,
2. Afzulpurkar N.V. *Kinematics, design, programming and control of a robotic platform for sattellite tracking and other applications*.- Christchurch, New Zealand, 1990.- 213 p.
3. Nise, Norman S. *Control Systems Engineering Seventh edition* / California state Polytechnic University.- Ponama, Wiley, Print ISBN-10: 1118170512 Print ISBN-13: 978-1118170519. - 2015.- 944 p.
4. *Simulink® Control Design™ Getting Started Guide*, The MathWorks, Inc. 2004-2017.- 48 p.
5. *Simscape™ Fluids™ User's Guide*, The MathWorks, Inc. 2006-2017.- 96p.

МОДЕЛИРОВАНИЕ И ПРОЕКТИРОВАНИЕ ГИДРАВЛИЧЕСКОЙ СИСТЕМЫ УПРАВЛЕНИЯ ПЛАТФОРМОЙ СТЮАРТА В СРЕДЕ MATLAB

А.Т. Уликян, А.Л. Мхитарян, А.А. Акопян
НПУА, Ереван, Армения

М.С. Гаспаров
ООО «УРАРТУ», Самара, Россия

АННОТАЦИЯ

Рассмотрена платформа Стюарта на гидромоторах. Для исследования системы была создана динамическая модель для физического моделирования в среде Simulink (Simscape). Данная система позволяет перенастроить систему, меняя числовые параметры. Разработан ПИД-регулятор для получения устойчивых и наблюдаемых откликов для выходных сигналов на заданные входные.

С использованием обратной задачи кинематики были получены изменения длины каждой ноги платформы Стюарта.

Программное обеспечение позволяет исследовать систему для заданных входных сигналов.

Proceedings of the 1st International Conference MES-2018 / ИРМ-2018
MECHANICAL ENGINEERING SOLUTIONS
Design, Simulation, Testing and Manufacturing
September 17-19, 2018, Yerevan, ARMENIA

MES2018-16

DESIGN OF HIGH-SPEED ROBOT MANIPULATORS WITH REDUCED CENTER OF MASS ACCELERATION

Vigen ARAKELIAN[1, 2]

[1] MECAPROCE, INSA, 20 avenue des Buttes de Coësmes, CS 70839, 35708 Rennes cedex 7, France
e-mail: vigen.arakelyan@insa-rennes.fr

[2] LS2N, UMR CNRS 6004, 1 rue de la Noë, 44300 Nantes, France
e-mail: vigen.arakelyan@ls2n.fr

ABSTRACT

This paper deals with the problem of shaking force balancing of high-speed robot manipulators. The known solutions of this problem are carried out by an optimal redistribution of moving masses which allows the cancellation or the reduction of the variable loads on the manipulator frame. However, one of the most promising methods is the optimal control of the robot links center of masses. Such a motion control allows the reduction of the maximum value of the center of mass acceleration and, consequently, the reduction in the shaking force. The present paper is an overview of this approach developed for serial and parallel manipulators. The suggested balancing technique is illustrated through computer simulations. The results obtained via ADAMS simulations showed the efficiency of such a solution.

INTRODUCTION

Many industrial manipulators face the problem of frame vibrations during high-speed motion. Such a vibration can result from a number of conditions, acting alone or in combination. One of the main reasons is the unbalanced inertia forces leading to the increase of shaking force and shaking moment. It is known that a mechanical system with unbalance shaking force and shaking moment transmits substantial vibration to the frame. Thus, a primary objective of the balancing is to cancel or reduce the variable dynamic loads transmitted to the frame and surrounding structures. The balancing of manipulators is generally can be achieved in two steps: i) the cancellation (or reduction) of the shaking force and ii) the cancellation (or reduction) of the shaking moment.

A considerable amount of research on balancing of shaking force and shaking moment in 1-dof mechanisms has been carried out in the past [1]. A new field for their application is the design of fast parallel manipulators, which are very efficient for advanced robotic applications. However, the practical applications of the developed methods face serious obstacles due to the increase in the total mass of the manipulators and its dimensions. The shaking force can be cancelled or reduced by adding of supplementary masses.

However, the added masses lead to the increase of the overall size of the robot-manipulator, the total mass and the efforts in joints [2-6]. They can also be cancelled or reduced by auxiliary structures [7], [8]. However, such a balancing can be reached by creating quite complex mechanical system and by an unavoidable increase of manipulator's size.

The study [9] deals with the synthesis of the balanced five-bar mechanism via changing the geometric and kinematic parameters of the mechanical structure. The shaking force balancing leads to the conditions which are usually satisfied by the redistribution of moving masses. In the mentioned study, the mass of the link is considered unchanged, then, the length and the mass center of the links are

determined in order to achieve the shaking force balancing. Thus, a new kinematic structure is obtained which is fully force balanced. With regard to the trajectory planning, the authors propose to estimate the given positions of the end-effector of the mechanism by the controllers of servomotors. The inconvenience of practical application of this principle lies in the fact that designers rarely have the possibility to fix the values of moving masses and then find the kinematic parameters with geometric constraints.

It should be noted that the various numerical optimization methods were also developed [10], [11] to perform the counterweight balancing. Standard nonlinear optimization algorithms that provide the best local solution to the problem have been performed [12], [13]. However, this solution is generally not the global one and the reformulation of the optimization problem into a convex program leads to the global optimum [14]. In [15], the shaking force acting on the frame of the 5R planar manipulator has been minimized by an optimal choice of mass parameters of all moving links. The conditions of the balancing of the five-bar linkage are expressed as seven equations and three inequalities, with twelve linkage parameters. Then the shaking force balancing of mechanism is formulated and solved as a numerical optimization problem. The dynamic balancing of 5R planar manipulators has also been formulated as an optimization problem such that a sum-squared values of bearing forces, driving torques, shaking moment are minimized [16]. This method has been performed using a numerical procedure based on dimensionality reduction through velocity transformation [17]. It is obvious that for certain cases they lead to quite satisfactory results. However, they are numerical optimization approaches, which cannot easily be applied on 3-RRR manipulators. Furthermore, it is unreliable to affirm that such solutions are optimal and efficient for any manipulator with arbitrary parameters. In this sense, it is much better to obtain optimal The proposedsolutions in explicit balancing tform.echnique is achieved by optimal trajectory planning of the common center of mass of the manipulator by "bang-bang" profile. In such a way, the minimization of the magnitude of the acceleration of the center of mass of the manipulator brings about a minimization of shaking force.

Let us consider the balancing of 2R serial robots, as well as 5R and 3RRR parallel manipulators.

SHAKING FORCE MINIMIZATION OF 2R SERIAL MANIPULATORS

The shaking forces $\mathbf{f}^{sh}$ of a manipulator can be written in the form:

$$\mathbf{f}^{\mathrm{sh}} = \sum m_i \ddot{\mathbf{x}}_S \tag{1}$$

where $\sum m_i$ is the total mass of the moving links of the manipulator and $\ddot{\mathbf{x}}_S$ is the acceleration of the total mass centre. The classical balancing approach consists in adding counterweights in order to keep the total mass centre of moving links stationary. In this case, $\ddot{\mathbf{x}}_S = 0$ for any configuration of the mechanical system. But, as a consequence, the total mass of the manipulator is considerably increased. Thus, in order to avoid this drawback, in the present study, a new approach is proposed, which consists of the optimal control of the total mass centre of moving links. Such an optimal motion planning allows the reduction of the total mass centre acceleration and, consequently, the reduction of the shaking force.

Classically, manipulator displacements are defined considering either articular coordinates $\mathbf{q}$ or Cartesian variables $\mathbf{x}$. Knowing the initial and final manipulator configurations at time t_0 and t_f, denoted as $\mathbf{q_0} = \mathbf{q}(t_0)$ and $\mathbf{q_f} = \mathbf{q}(t_f)$, or $\mathbf{x_0} = \mathbf{x}(t_0)$ and $\mathbf{x_f} = \mathbf{x}(t_f)$, in the case of the control of the Cartesian variables, the classical displacement law may be written in the form:

$$\mathbf{q}(t) = s_q(t)\left(\mathbf{q_f} - \mathbf{q_0}\right) + \mathbf{q_0} \tag{2a}$$

or

$$\mathbf{x}(t) = s_x(t)\left(\mathbf{x_f} - \mathbf{x_0}\right) + \mathbf{x_0} \tag{2b}$$

where $s_q(t)$ and $s_x(t)$ may be polynomial (of orders 3, 5 and higher), sinusoidal, bang-bang, etc. motion profiles.

From expression (1), we can see that the shaking force, in terms of norm, is minimized if the norm $\|\ddot{\mathbf{x}}_S\|$ of the masses centre acceleration is minimized along the trajectory. This means that if the displacement $\mathbf{x}_S$ of the manipulator centre of masses is optimally controlled, the shaking force will be minimized. As a result, the first problem is to define the optimal trajectory for the displacement $\mathbf{x}_S$ of the manipulator centre of masses.

For this purpose, let us consider the displacement $\mathbf{x}_S$ of a point S in the Cartesian space. First, in order to minimize the masses centre acceleration, the length of the path followed by S should be minimized, i.e. point S should move along a straight line passing through its initial and final positions, denoted as $\mathbf{x}_{S0}$ and $\mathbf{x}_{Sf}$, respectively.

Then, the motion profile used on this path should be optimized. It is assumed that, at any moment during the displacement, the norm of the maximal admissible acceleration the point S can reach is constant and denoted as $\ddot{x}_S^{\max}$. Taking this maximal value for the acceleration into consideration, it is known that the motion profile that minimizes the time interval (t_0, t_f) for going from position $\mathbf{x_{S0}} = \mathbf{x_S}(t_0)$ to position $\mathbf{x_{Sf}} = \mathbf{x_S}(t_f)$ is the "bang-bang" profile [18], given by (Fig. 1a)

$$\begin{cases} \mathbf{x}_S(t) = s(t)(\mathbf{x}_{Sf} - \mathbf{x}_{S0}) + \mathbf{x}_{S0} \\ \dot{\mathbf{x}}_S(t) = \dot{s}(t)(\mathbf{x}_{Sf} - \mathbf{x}_{S0}) \\ \ddot{\mathbf{x}}_S(t) = \ddot{s}(t)(\mathbf{x}_{Sf} - \mathbf{x}_{S0}) \end{cases} \quad (3)$$

with

$$\ddot{s}(t) = \frac{1}{\left\|\mathbf{x}_{Sf} - \mathbf{x}_{S0}\right\|} \begin{cases} \ddot{x}_S^{\max} & for\ t \le (t_f - t_0)/2 \\ -\ddot{x}_S^{\max} & for\ t \ge (t_f - t_0)/2 \end{cases} \quad (4)$$

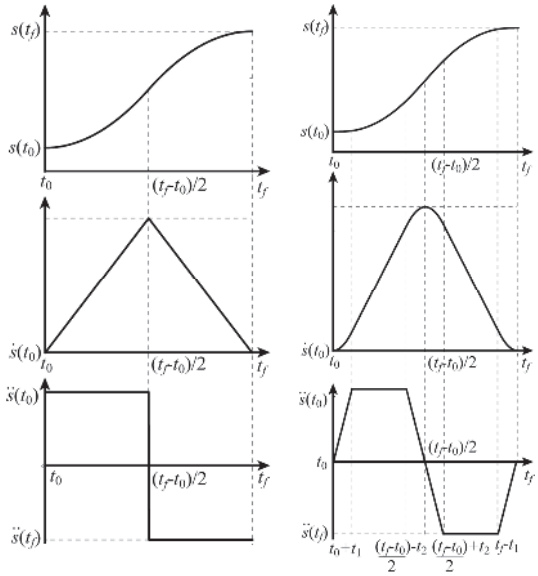

(a) "Bang-bang" profile (b) Trapezoidal profile

Figure 1. Motion profiles used for the shaking force minimization.

Consequently, if the time interval (t_0, t_f) for the displacement between positions $\mathbf{x}_{S0}$ and $\mathbf{x}_{Sf}$ is fixed, the "bang-bang" profile is the trajectory that minimizes the value of the maximal acceleration $\ddot{x}_S^{\max}$. Thus, in order to minimize $\left\|\ddot{\mathbf{x}}_S\right\|$ for a displacement during the fixed time interval (t_0, t_f), the "bang-bang" profile has to be applied on the displacement $\mathbf{x}_S$ on the manipulator total mass centre.

Once the displacement of the manipulator centre of masses is defined, the second problem is to find the articular (or Cartesian) coordinates corresponding to this displacement. For this purpose, let us consider a manipulator composed of n links. The mass of the link i is denoted as m_i (i = 1, …, n) and the position of its centre of masses as $\mathbf{x}_{Si}$. Once the articular coordinates $\mathbf{q}$ or Cartesian variables $\mathbf{x}$ are known, the values of $\mathbf{x}_{Si}$ may easily be obtained using the manipulator kinematics relationships. As a result, the position of the manipulator centre of masses, defined as

$$\mathbf{x}_S = \frac{1}{m_{tot}} \sum_{i=1}^{n} m_i \mathbf{x}_{Si}\ , \quad (7)$$

where $m_{tot} = \sum_{i=1}^{n} m_i$, may be expressed as a function of $\mathbf{x}$ or $\mathbf{q}$. But, in order to control the manipulator, the inverse problem should be solved, i.e. it is necessary to express variables $\mathbf{q}$ or $\mathbf{x}$ as a function of $\mathbf{x}_S$. Here, two cases should be distinguished:

(i) dim($\mathbf{x}_S$) = dim($\mathbf{q}$), i.e. the manipulator has got as many actuators as controlled variables for the displacements $\mathbf{x}_S$ of the centre of masses (two variables for planar cases, three variables for spatial problems). In such case, the variables $\mathbf{q}$ or $\mathbf{x}$ can be directly expressed as a function of $\mathbf{x}_S$ using (7), i.e. $\mathbf{q} = \mathbf{f}(\mathbf{x}_S)$.

(ii) dim($\mathbf{x}_S$) < dim($\mathbf{q}$), i.e. the manipulator has got more actuators than controlled variables. In such case, the problem is under-determined as there are more parameters in variables $\mathbf{q}$ or $\mathbf{x}$ than in $\mathbf{x}_S$. In order to solve it, let us consider that p_0 parameters of vector $\mathbf{q_0}$ (or $\mathbf{x_0}$) and p_f parameters of vector $\mathbf{q_f}$ (or $\mathbf{x_f}$) are fixed. In a first task, it is necessary to define the m–p_0 and m–p_f other parameters of the initial and final manipulator configurations (m = dim($\mathbf{q}$)). The way to fix it is to find the manipulator initial and final configurations, taking into account the p_0 initial and p_f final fixed parameters, that will allow minimizing the norm of the vector $\mathbf{x}_{Sf} - \mathbf{x}_{S0}$, i.e. the length of the displacement of the manipulator centre of masses. Then, the second task is to choose m–k articular variables among the m possible of vector $\mathbf{q}$ (k = dim($\mathbf{x}_S$)). These m–k variables, denoted as $\mathbf{q_{m-k}}$ will be controlled using some classical displacement law given at (2) or can be used in order to minimize some other performance criteria, such as the shaking moments or some other interesting performance criterion (see section 3.2). The k other variables, denoted as $\mathbf{q_k}$, should be expressed as a function of $\mathbf{x}_S$ and $\mathbf{q_{m-k}}$ using (7), i.e. $\mathbf{q_k} = \mathbf{f}(\mathbf{x}_S, \mathbf{q_{m-k}})$.

The numerical simulations carried out in [19] have showed that that the optimal trajectory planning ("bang-bang profile") allows the reduction of the shaking force from 36% up to 76.7 %.

However, despite the obvious advantages, observations and attempts of practical implementations showed that the approach described above also has some drawbacks. It is difficult to control a robot-manipulator based on the kinematic parameters of a virtual point as a center of masses. As a result, measurements and refinements of the displacements of the total mass center of moving links becomes pretty complex. Another imperfection of the mentioned method is the fact that the end-effector trajectory becomes a derivative of the trajectory of the center of masses, i.e. by using the known balancing method mentioned above it is possible to ensure only initial and final positions of the end-effector but not a straight line trajectory between them.

To eliminate these drawbacks, the studies [20], [21] propose to combine the balancing through mass redistribution and the balancing via center of mass acceleration control. This allows one to reach more efficient balancing results, i.e. to increase the shaking force balancing rates and to control the displacements of the total mass center of moving links via the end-effector trajectory.

Let us consider the shaking forces balancing of 5R and 3RRR parallel manipulators.

SHAKING FORCE MINIMIZATION OF PARALLEL MANIPULATORS

A kinematic scheme of the 5R planar manipulator is shown in Fig. 2. The output axis $P(x,y)$, which corresponds to the axis of the end-effector, is connected to the base by two legs, each of which consists of three revolute joints and two links. The two legs are connected to a common axis P with the common revolute joint at the end of each leg. In each of the two legs, the revolute joint connected to the base is actuated. Such a manipulator can position the end-effector freely in a plane.

In the given planar 5R parallel mechanism each actuated joint is denoted as A_i $(i=1,2)$, the other end of each actuated link is denoted as B_i and the common joint of the two legs is denoted as P, which is also the axis of the end-effector. A fixed global reference system Oxy is located at the center of A_1A_2 with the y-axis normal to A_1A_2 and the x-axis directed along A_1A_2. The lengths of links are denoted as $l_1 = A_1B_1$, $l_2 = A_2B_2$, $l_3 = B_1P$, $l_4 = B_2P$ and $l_0 = OA_1 = OA_2$. The locations of the centers of mass are denoted as $r_1 = l_{A_1S_1}$, $r_2 = l_{A_2S_2}$, $r_3 = l_{B_1S_3}$ and $r_4 = l_{B_2S_4}$.

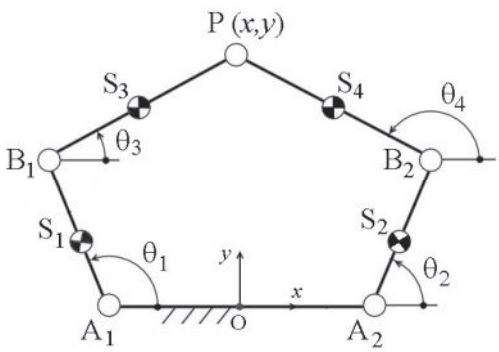

Figure 2. The planar 5R parallel manipulator.

The complete shaking force balancing of such a mechanism can be reached by adding 3 or 4 counterweights making the common center of mass stationary [1]. However, as mentioned above, such a solution leads to the increase of the total mass and the overall size of the robot-manipulator. Therefore, let us consider a partial balancing of the 5R mechanism via optimal redistribution of moving masses and reduction of the center of mass acceleration. Two steps will be considered: *i*) optimal redistribution of the masses of input links to ensure the similarity of the output trajectory and the common center of mass trajectory; *ii*) optimal control of the acceleration of the end-effector.

Let us consider the reaching similar accelerations of the end-effector of the 5R planar parallel manipulator and its common center of mass.

The coordinates of the common center of mass of the 5R planar manipulator can be expressed as:

$$x_S = \frac{m_1 x_{S_1} + m_2 x_{S_2} + m_3 x_{S_3} + m_4 x_{S_4}}{m}$$
$$y_S = \frac{m_1 y_{S_1} + m_2 y_{S_2} + m_3 y_{S_3} + m_4 y_{S_4}}{m} \tag{8}$$

with

$m = m_1 + m_2 + m_3 + m_4$; $x_{S_1} = r_1 \cos\theta_1 - l_0$;
$y_{S_1} = r_1 \sin\theta_1$; $x_{S_2} = r_2 \cos\theta_2 + l_0$; $y_{S_2} = r_2 \sin\theta_2$;
$x_{S_3} = l_1 \cos\theta_1 + r_3 \cos\theta_3 - l_0$; $y_{S_3} = l_1 \sin\theta_1 + r_3 \sin\theta_3$;
$x_{S_4} = l_2 \cos\theta_2 + r_4 \cos\theta_4 + l_0$,
$y_{S_4} = l_2 \sin\theta_2 + r_4 \sin\theta_4$

where, m_i (i = 1,2,3,4) are the masses of moving links.

Given that the following relationships between angles θ_3, θ_4 and x, y can be established:

$$\sin\theta_3 = (y - l_1 \sin\theta_1)/l_3$$
$$\cos\theta_3 = (x - l_1 \cos\theta_1 + l_0)/l_3$$
$$\sin\theta_4 = (y - l_2 \sin\theta_2)/l_4$$
$$\cos\theta_4 = (x - l_2 \cos\theta_2 - l_0)/l_4$$

the coordinates of the common center of mass of the 5R planar manipulator can be rewritten as:

$$x_S = k_1 \cos\theta_1 + k_2 \cos\theta_2 + k_3 x + k_0$$
$$y_S = k_1 \sin\theta_1 + k_2 \sin\theta_2 + k_3 y \tag{9}$$

where,

$$k_1 = (m_1 r_1 + m_3 l_1 - m_3 r_3 l_1 / l_3)/m$$
$$k_2 = (m_2 r_2 + m_4 l_2 - m_4 r_4 l_2 / l_4)/m$$
$$k_3 = (m_3 r_3 / l_3 + m_4 r_4 / l_4)/m$$
$$k_0 = l_0 (-m_1 + m_2 - m_3 + m_4 + m_3 r_3 / l_3 - m_4 r_4 / l_4)/m$$

Now, it is easy to see that the mass redistribution of links connected directly to the frame can ensure the condition $k_1 = k_2 = 0$ which, in turn, leads to the

following expressions for the coordinates of the common center of mass of the 5R planar manipulator:

$$x_S = k_3 x + k_0$$
$$y_S = k_3 y$$

As a result, acceleration of the common center of mass of the 5R planar manipulator will be:

$$\ddot{x}_S = k_3 \ddot{x}$$
$$\ddot{y}_S = k_3 \ddot{y}$$

This means that the acceleration of the end-effector of the manipulator and its common center of mass are similar, i.e. the minimization of the acceleration of the end-effector leads to the proportional minimization of the acceleration of the common center of mass of the manipulator.

The shaking forces F_{sh} of the planar 5R parallel manipulator with $k_1 = k_2 = 0$ can be written in the form:

$$F_{sh} = m\ddot{s} = m\sqrt{\ddot{x}_S^2 + \ddot{y}_S^2} = mk_3\ddot{s}_P = mk_3\sqrt{\ddot{x}^2 + \ddot{y}^2}$$

where, $\ddot{s}$ is the acceleration of the common center of mass of the manipulator, $\ddot{x}_S$ is the acceleration of the common center of mass of the manipulator along x axis, $\ddot{y}_S$ is the acceleration of the common center of mass of the manipulator along y axis, $\ddot{s}_P$ is the acceleration of the end-effector of the manipulator, $\ddot{x}$ is the acceleration of the end-effector of the manipulator along x axis and $\ddot{y}$ is the acceleration of the end-effector of the manipulator along y axis.

As was mention above the shaking force, in terms of norm, is minimized if the norm of the center of masses acceleration is minimized along the generated trajectory. This means that if the displacement of the manipulator center of masses is optimally controlled, the shaking force will be minimized. For this purpose has been proposed to apply the "bang-bang" law ensuring two identical phases with constant acceleration and deceleration (Fig. 1).

Let us consider an illustrative example.

To create a CAD model, the following geometric parameters of the 5R planar manipulator have been used: $l_1 = l_2 = L_1 = 0.36\text{m}$; $l_3 = l_4 = L_2 = 0.3\text{m}$; $l_0 = 0.24\text{m}$. The masses and the locations of the centers of mass of the moving links 3 and 4 are the following: $m_3 = m_4 = 1kg$, $r_3 = r_4 = 0.15\text{m}$. Now, taking into consideration the condition $k_1 = k_2 = 0$ and assuming $r_1 = r_2 = -0.06\text{m}$, the masses of the links 1 and 2 can be determined: $m_1 = m_2 = 3\text{kg}$.

The trajectory of the end-effector P is given by a straight line limited between the initial position P_i with the coordinates $x_i = -0.06\text{m}$, $y_i = 0.45\text{m}$ and the final position P_f with the coordinates $x_f = 0.1364\text{m}$, $y_f = 0.4878\text{m}$.

The input angles θ_1 and θ_2 will be determined from following expressions:

$$\theta_i = 2\tan^{-1}(z_i), \quad i = 1,2$$

where

$$z_i = \frac{-b_i + \sigma_i\sqrt{b_i^2 - 4a_i c_i}}{2a_i}, \quad i = 1,2$$

with

$\sigma_i = \pm 1 \ (i = 1,2)$;

$a_1 = L_1^2 + y^2 + (x + l_0)^2 - L_2^2 + 2(x + l_0)L_1$;

$b_1 = b_2 = -4yL_1$;

$c_1 = L_1^2 + y^2 + (x + l_0)^2 - L_2^2 - 2(x + l_0)L_1$;

$a_2 = L_1^2 + y^2 + (x - l_0)^2 - L_2^2 +$

$2(x - l_0)L_1$; $c_2 = L_1^2 + y^2 + (x - l_0)^2 - L_2^2 - 2(x - l_0)L_1$.

The chosen configuration for simulations corresponds to $\sigma_1 = 1$ and $\sigma_2 = -1$. Thus, for given coordinates $x_i = -0.06\text{m}$, $y_i = 0.45\text{m}$ of the initial position P_i, the input angles are $\theta_1^i = 1.856$, $\theta_2^i = 1.609$ and for the final position P_f with $x_f = 0.1364\text{m}$, $y_f = 0.4878\text{m}$, the input angles are $\theta_1^f = 1.247$, $\theta_2^f = 1.141$.

Now, let us apply a "bang-bang" motion profile to the end-effector P with parameters $s = 0.2\text{m}$ and $t = 0.02\text{s}$.

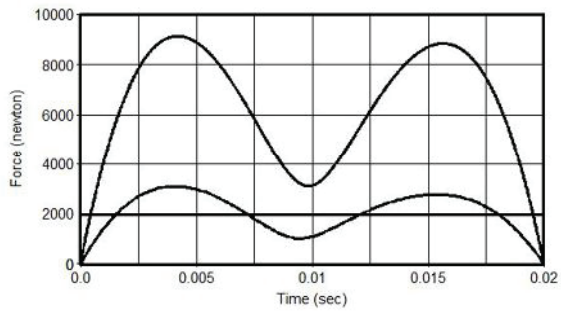

Figure 3. Shaking forces for three simulated cases.

To show the efficiency of the developed method, three 5R planar parallel manipulators are compared: a) an unbalanced manipulator, i.e. $r_1 = r_2 = 0.18\text{m}$ and $m_1 = m_2 = 1.2\text{kg}$, with generation of input motions via five-order polynomial laws; b) the manipulator designed by suggested approach; c) the manipulator with the same parameters as "b" but with generation of input motions via five-order polynomial laws.

In Fig. 3, the variations of the shaking forces for three simulated cases are presented. The obtained results showed that by suggested approach, the reduction of the maximal value of the shaking force is about 78% related to the case "a" and 36% related to the case "c".

Such an approach has also been applied on 3RRR parallel manipulators [21]. The results obtained via ADAMS simulations showed that a reduction in the maximum value of the shaking force of 60% has been obtained.

CONCLUSION

In this paper, an overview of a new approach, based on an optimal trajectory planning, which allows the considerable reduction of the shaking force, has been presented. This simple and effective balancing method is based on the optimal control of the acceleration of the manipulator center of masses. For this purpose, the "bang-bang" profile has been used.

It should be mentioned that such a solution is also very favorable for reduction of input torques because it is carried out without adding counterweights or adding counterweights on the links linked with the frame. The proposed balancing method has been illustrated via numerical examples.

REFERENCES

1. V. Arakelian, S. Briot, *Balancing of linkages and robot manipulators. Advanced methods with illustrative examples*. Springer, Switzerland, 2015. – 291p.
2. S. Agrawal, A. Fattah, "Reactionless space and ground robots: novel design and concept studies," *Mech. Mach. Theory*, 39, 2004, pp.25–40.
3. T. Hess-Coelho, L. Yong, V. Alves, "Decoupling of dynamic equations by means of adaptive balancing of 2-dof open-loop mechanisms," *Mech. Mach. Theory*, 39(8), 2004, pp. 871–881.
4. A.G. Coutinho, T.A. Hess-Coelho, "A new approach for obtaining the dynamic balancing conditions in serial mechanisms," *International Journal of Mechanisms and Robotic Systems*, 3(1), 2016, pp. 32-47.
5. M. Acevedo. "Conditions for dynamic balancing of planar parallel manipulators using natural coordinates and their application," In *Proc. 14th IFToMM World Congress*, Taipei, Taiwan, October 25-30, 2015.
6. S. Briot, I. A Bonev, C. M Gosselin, V. Arakelian. "Complete shaking force and shaking moment balancing of planar parallel manipulators with prismatic pairs," *Journal of Multi-body Dynamics*, 222(1), 2009, pp.43-52.
7. A. Fattah, S. Agrawal. "Design arm simulation of a class of spatial reactionless manipulators," *Robotica*, 3, 2005, pp.75–81.
8. V. van der Wijk, J. Herder. Dynamic balancing of Clavel's delta robot. In the book «Computational Kinematics». Springer, 2009, pp. 315–322
9. P. Ouyang, W. Zhang. "Force balancing of robotic mechanisms based on adjustment of kinematic parameters," *J. Mech. Des. Trans. ASME* 127, 2005, pp.433–440.
10. C.A. Coello Coello, A.D. Christiansen, A.H. Aguirre, "Multiobjective Design Optimization of Counterweight Balancing of a Robot Arm using Genetic Algorithms," In *Proc. of the Seventh International Conference on Tools with Artificial Intelligence,* IEEE Computer Society Washington, DC, USA, 1995, pp. 20-23.
11. F. Xi, "Dynamic balancing of hexapods for high-speed applications," *Robotica,* 17, 1999, pp.335–342.
12. C. Gosselin, K. Vollmer, G. Côté and Y. Wu, "Synthesis and Design of Reactionless Three-Degree-of-Freedom Parallel Mechanisms," *IEEE Trans. Rob. Autom*., 20, 2004, pp. 191–199
13. S. Foucault, S., and C.M. Gosselin, "Synthesis, Design, and Prototyping of a Planar Three Degree-of-Freedom Reactionless Parallel Mechanism," *ASME J. Mech. Des.,* 126(6), 2004, pp. 992–999.
14. B. Demeulenaere, M. Verschure, J. Swevers and J.D. Schutter, "A General and Numerically Efficient Framework to Design Sector-Type and Cylindrical Counterweights for Balancing of Planar Linkages*," ASME J. Mech. Des*., 132(1), 2010, p. 011002.
15. D. Ilia, R. Sinatra, "A novel formulation of the dynamic balancing of five-bar linkages with applications to link optimization," *Multibody Syst. Dyn*., 21(2), 2009, pp.193–211.
16. G. Alici, B. Shirinzadeh, "Optimum dynamic balancing of planar parallel manipulators based on sensitivity analysis," *Mech. Mach. Theory*, 41, 2006, pp.1520-1532.
17. M. Buganza, M. Acevedo, "Dynamic balancing of a 2-DOF 2RR planar parallel manipulator by optimization," In *Proc. 13th IFToMM World Congress*, Guanajuato (Mexico) 19-25 June, 2011.
18. W. Khalil, and E. Dombre, Modeling, identification and control of robots. Hermes Sciences Europe, (2002).
19. S. Briot, V. Arakelian and J.P. Le Baron. Shaking force minimization of high-speed robots via centre of mass acceleration control. Mechanism and Machine Theory, Vol. 57, November, 2012, pp. 1-12.
20. V. Arakelian. Design of partially balanced 5R planar manipulators with reduced center of mass acceleration. In *Proc. of the 21st CISM IFToMM Symposium on Robot Design, Dynamics and Control*, June 20-23, Udine, Italy, 2016, pp. 113-122.
21. V. Arakelian, J. Geng and J.-P. Le Baron. Synthesis of balanced 3-RRR planar parallel manipulators. In *Proc. of the 19th International Conference on Robotics and Computer Integrated Manufacturing (ICRCIM'2017)*, September 4-5, Prague, Czech Republic, 4(9), 2017, pp. 37-43.

ПРОЕКТИРОВАНИЕ ВЫСОКОСКОРОСТНЫХ РОБОТ-МАНИПУЛЯТОРОВ С УМЕНЬШЕННЫМ УСКОРЕНИЕМ ОБЩЕГО ЦЕНТРА МАСС

Виген АРАКЕЛЯН [1, 2]

[1] МЕКАПРОС, Национальный институт прикладных наук (INSA), 20 avenue des Buttes de Coësmes, CS 70839, 35708 Rennes cedex 7, France e-mail: vigen.arakelyan@insa-rennes.fr

[2] Лаборатория LS2N UMR CNRS 6004, 1 rue de la Noë, 44300 Nantes, France e-mail: vigen.arakelyan@ls2n.fr

АННОТАЦИЯ

В данной статье рассматривается задача уравновешивания сил инерции высокоскоростных манипуляторов. Известные решения этой задачи осуществляются путем оптимального перераспределения движущихся масс, что позволяет уменьшить или аннулировать переменные нагрузки на стойку манипулятора. Однако, одним из наиболее перспективных методов уравновешивания является оптимальное управление общим центром масс манипулятора. Такое управление движением позволяет уменьшить максимальное значение ускорения общего центра масс и, следовательно, уменьшить силы инерции. Данная статья представляет собой обзор подобного подхода, разработанного для сериальных и параллельных манипуляторов. Предложенная методика уравновешивания проиллюстрирована с помощью компьютерного моделирования. Результаты, полученные с помощью программы ADAMS, показали эффективность такого решения.

Proceedings of the 1st International Conference MES-2018 / ИРМ-2018
MECHANICAL ENGINEERING SOLUTIONS
Design, Simulation, Testing and Manufacturing
September 17-19, 2018, Yerevan, ARMENIA

MES2018-27

An Optimized Method for a Pick and Drop waste-sorting System using a Parallel Mechanism

C. Kassis, R. Rizk

Lebanese University Faculty of engineering, *CRSI*, Lebanon
carine.kassis@ul.edu.lb; rrizk2@ul.edu.lb

ABSTRACT:
waste-sorting is an emerging worldwide problem. The task needs high frequency for light payload. The ideal solution for this pick-and-place problem is to use a parallel mechanism.
For fast operation, the trajectory optimization is a must. It can increase considerably the efficiency. In this paper, we consider a series of operations with two different goals. The objective is to minimize the global time of the waste-sorting process. The robot has to pick glass and plastic items from a conveyor and place them in two different containers. Since we have a series of operations, there is no interest in stopping the mechanism at the place time. As a result, the trajectory will not be planar anymore.
The trajectory is designed in the operational space; the control is in the joint space. Thus, the calculation of the inverse kinematic and differential model is a must. Finally, an experimental validation on a small prototype is presented.

NOMENCLATURE

$\{B\}$	fixed base Cartesian reference frame
$\{P\}$	moving platform Cartesian reference frame
${}^{R}_{i}R_{Z}$	Transformation matrix between frames $\{R_i\}$ and $\{R\}$
θ_i	Angle of the first upper arm attached to motor i
$\dot{\theta}_i$	angular velocity of the upper arm i
x,y,z	Cartesian variables of the platform center
$\dot{x},\dot{y},\dot{z}$	velocity variables of the platform center
l	length of arm
L	length of forearm
v_c	velocity of the conveyor
B_i,	hips of leg i
A_i	knee of leg i
P_i,	ankles of leg i
w_B	planar distance from $\{B\}$ to near base side
u_B	planar distance from $\{B\}$ to a base vertex
w_P	planar distance from $\{P\}$ to near platform side
u_p	planar distance from $\{P\}$ to a platform vertex
s_B	size of the base side
s_p	size of the moving platform side

I. INTRODUCTION

Parallel mechanisms are emerging in industry (for instance machine tools, high-speed pick-and-place robots, flight simulators, medical robots). A parallel mechanism can be defined as a mechanism with a closed kinematic chain. It is made up of an end-effector with N degrees of freedom and a fixed base connected to each other by at least two kinematic chains, the motorization being carried out by N actuators [1]. This allows parallel mechanisms to bear higher loads at higher speed and often with a higher repeatability [1]. Waste-sorting is a pick-and-place task. In this case, high speed manipulation is needed but the payload is not heavy. Thus, the parallel manipulator represents an ideal solution. However, with the high speed and accelerations, inertia becomes an important factor; it can lead to serious damages. That is why the motion strategy should be optimized. We search the fastest sorting, with the minimum internal loads. The travelled distance during each pick-and-place cycle should be minimized, as well as the highest acceleration, the velocity, and especially the actuation torque. Thus, an important part of our study is to design an algorithm that minimizes cycle duration. The robot works in waste-sorting, thus it has to be fast. It should also place each kind of waste in the specific container. An optimization process for the pick-and-place strategy, the order of the picked object, is essential.
In the following, a literature review about the parallel mechanisms used in the pick-and-place field is presented in Section II. The problem settings and the sorting stages are presented in Section III. The trajectory design for the moving platform and the optimization algorithm are

described in Section IV. The kinematics calculations of the delta robot, with the horary equations of the actuators are discussed in section V. To validate the algorithm, a small prototype is shown in Section VI. We finish with some conclusions and further works.

II. STATE OF THE ART

Pick-and-place operations are required in most light industry sectors such as waste-sorting, electronics, packaging, pharmacy and many others. Manipulated objects are light in weight and small in size, but in large amount. Since the charge is cumulative in a serial robot, the inertia becomes a serious load. The task load becomes negligible with respect to the inertia. That is why Clavel presented his invention of a 3 degree of freedom (DOF) translational parallel mechanism named Delta [2–6]: a fast parallel robot based on parallelogram mechanisms. Actuators are base-mounted, so they do not move. Low-mass links induce low global inertia. Thus the Delta robot is an ideal candidate for high-speed pick-and-place operations. The ratio between the link and parallelogram lengths governs the cylindrical workspace diameter/height ratio. The relevant literature along this line can be exemplified by recent publications [7–18] and many others. Extensive research activities have been directed towards analysis of the motion strategy [19–26]. In fact, for the same displacement, the maximum velocity and acceleration can vary significantly upon the motion strategy, which leads to inertia forces from the loads on the actuators. Large inertia forces lead to the use of heavy control and less accuracy [27].

This paper deals with the optimization of the pick-and-place operation. We present an algorithm to maximize the pick-and-place process. The duration depends mainly on the cycle time and the intermediate interval between two cycles. The order of the picked objects is also important. The algorithm tries to minimize the total duration of two consecutive cycles.

III. PROBLEM SETTINGS

Our goal is to robotize the waste-sorting. Thus, wastes are disposed on a conveyor. The first stage consists of an electro-magnet in order to retain all ferromagnetic wastes. In a second stage, all non-ferromagnetic metallic parts are ejected from the conveyor using an eddy-current system. In the third stage, plastics and glass are to be sorted by the robot (Figure 1). Finally, only organic wastes remain on the conveyor.

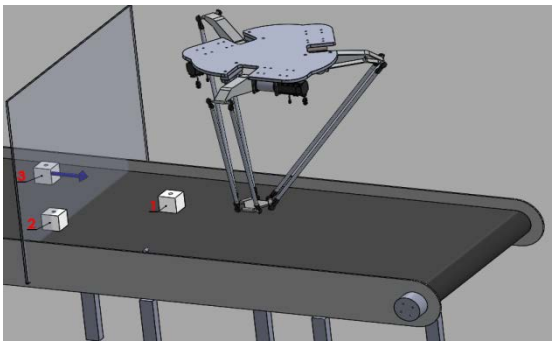

Figure 1: robotized waste-sorting system

A special infrared camera can detect the plastics and the glass on the conveyor (Figure 2). It gives also the y coordinate of the plastic or glass component.

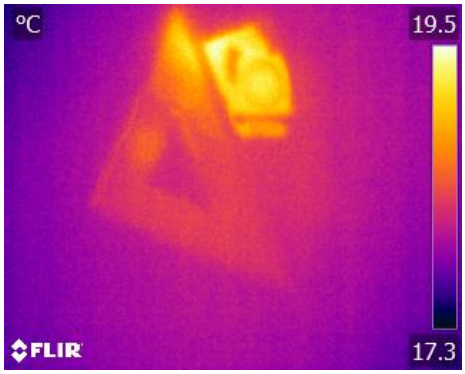

Figure 2: plastic and glass parts detected by Flir A35

The conveyor speed v_c is known and constant, which allows us to compute the x coordinate function of time. Therefore, the duration needed for the detected object to enter into the robot workspace can be calculated, as well as the duration inside the workspace.

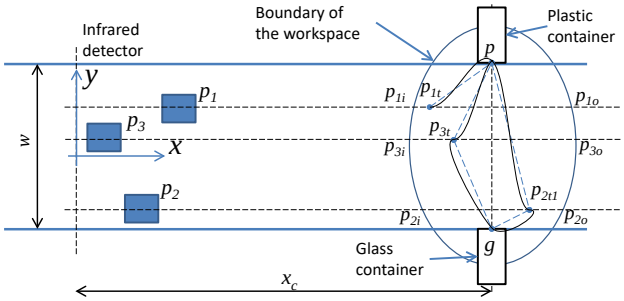

Figure 3: pick-and-place operation

In order to optimize the pick-and-place process, the objective is to maximize the number of pick-and-place cycles per minute. The constraint to respect is to pick the object before getting off the robot workspace (Figure 3). The positions $\{x_c, y_p, z_c\}$ and $\{x_c, y_g, z_c\}$ of the containers are used as inputs. Once an object passes through the detector, its y coordinate and its corresponding container are defined. The x coordinate becomes

$$x = v_c . t. \quad (1)$$

To explain the idea, let us consider three objects. The first detected object must be picked from the target position p_{1t}, the second from the target position p_{2t} and the third from the target position p_{3t}. If the detected object is plastic, the robot will place it at point p, otherwise at point g. To remove three objects, the moving platform has to carry out five travels, upon six choices:

- Travel 1 from p_{1t} to the corresponding container;
- Travel 2 from the previous container to p_{2t};
- Travel 3 from p_{2t} to the corresponding container.
- Travel 4 from the previous container to p_{3t}.
- Travel 5 from p_{3t} to the corresponding container.

Other choices are obtained by alternating the orders of the picked objects. (Figure 3)

In all cases there are three pick-and-place travels and two intermediate travels. Then, the algorithm searches for the target points, p_{1t}, p_{2t}, and p_{3t} that minimize the total duration of the five travels. A third vector variable ε is needed to determine the order of the picked objects. Let ΔT_1, ΔT_2 and ΔT_3 be the durations of the pick-and-place travels. Intermediate travel durations can make vector $\Delta T_i^T = (\Delta T_{i123} \quad \Delta T_{i132} \quad \Delta T_{i231} \quad \Delta T_{i213} \quad \Delta T_{i312} \quad \Delta T_{i321})^T$ where each component of this vector represents the total duration needed for the corresponding order. Vector ε is also six-dimensional, however five of its terms are zeros and the sixth is one. The term one gives the chosen order. The dot product $\varepsilon^T.\Delta T_i$ gives the duration of the intermediate travels.

IV TRAJECTORY DESIGN AND OPTIMIZATION

The manipulator has to pick the part from the target point and drop it into the container. Then, it has to lift up the part, move it until it reaches the container, and finally release it (Figure 4). In order to avoid any impact on the robot structure at the pick instant, the moving platform has got to have the conveyor velocity. In order to get the fastest work, we need continuity of velocity and acceleration and the pick-and-place points positions.

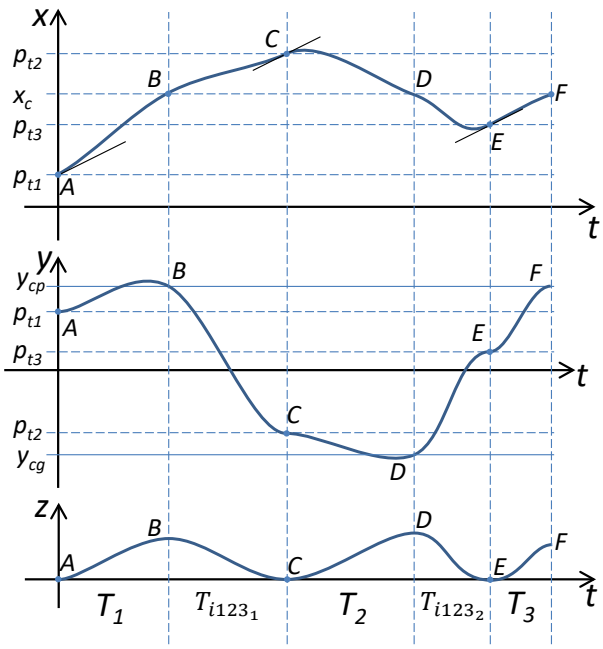

Figure 4: trajectory of the moving platform

$x_{p_{ti}}$ and $y_{p_{ti}}$ are the coordinates of the target point where the object number *i* is picked. Those values are determined by the infrared sensor, the conveyor velocity, and the optimization algorithm.

The motion design has to give the shortest time for the cycle with full respect to the initial conditions. The motion is designed as a function of time along *x*, *y* and *z* separately.

A. *Initial conditions:*

The path is divided into five periods (Figure 4). Periods *AB*,*CD* and *EF* are the periods when an object is hold by the mechanism. Periods *BC* and *DE* are intermediate between two objects (Figure 4). For all motions, we are going to use fifth degree polynomial function of time. For each two consecutive phases we have to respect the boundary conditions and the initial conditions along *x*,*y* and *z*. mainly at the pick of the item the manipulator has to have the same velocity and acceleration of the conveyor. Also the position, velocity, acceleration and jerk should be continuous between two consecutive phases. Since there are five phases, we have 30 unknowns along each dimension. However since the target and container's positions are known, and the velocity and accelerations at the pick are known (see appendix) it remains 19 linear equations with 19 unknowns along each direction. The resolution gives all the coefficients function of the periods $T_1, T_{i123_1}, T_2, T_{i123_2}, T_3$, the positions $x_{pt_1}, x_{pt_2}, x_{pt_3}, x_{cont}$ and the conveyor velocity v_c. Finally, we get an operational research problem with $x_{pt_1}, x_{pt_2}, x_{pt_3}$ as optimization variables, and the objective function to minimize is the total period:

$$T = T_1 + T_2 + T_3 + \varepsilon^T.\Delta T_i \tag{2}$$

Where ΔT_i is the total intermediate time during which the robot platform is free. The same calculations can be done for the *y* and *z* motions

T should be minimized under the following constraint: the three objects must be inside the workspace at the pick instant i.e.:

$$\begin{matrix} \frac{x_{p_{1i}}}{x_{p_{t1}}} - 1 < 0 & \frac{x_{p_{2i}}}{x_{p_{t2}}} - 1 < 0 & \frac{x_{p_{3i}}}{x_{p_{t3}}} - 1 < 0 \\ \frac{x_{p_{t1}}}{x_{p_{1o}}} - 1 < 0 & \frac{x_{p_{t2}}}{x_{p_{2o}}} - 1 < 0 & \frac{x_{p_{t3}}}{x_{p_{3o}}} - 1 < 0 \end{matrix} \tag{3}$$

In order to take equation (68) into consideration, the penalty method [29] is used. The penalized objective function is:

$$L = T + \lambda_1.sup\left(\left(\frac{x_{p_{1i}}}{x_{p_{t1}}} - 1\right), 0\right) + \lambda_2.sup\left(\left(\frac{x_{p_{2i}}}{x_{p_{t2}}} - 1\right), 0\right) + \lambda_3.sup\left(\left(\frac{x_{p_{3i}}}{x_{p_{t3}}} - 1\right), 0\right) + \lambda_4.sup\left(\left(\frac{x_{p_{t1}}}{x_{p_{1o}}} - 1\right), 0\right) + \lambda_5.sup\left(\left(\frac{x_{p_{t2}}}{x_{p_{2o}}} - 1\right), 0\right) + \lambda_6.sup\left(\left(\frac{x_{p_{t3}}}{x_{p_{3o}}} - 1\right), 0\right) \tag{4}$$

$\lambda_1, \lambda_2, \lambda_3, \lambda_4, \lambda_5, \lambda_6$ are penalty constant coefficients.

The algorithm becomes (Figure 5):

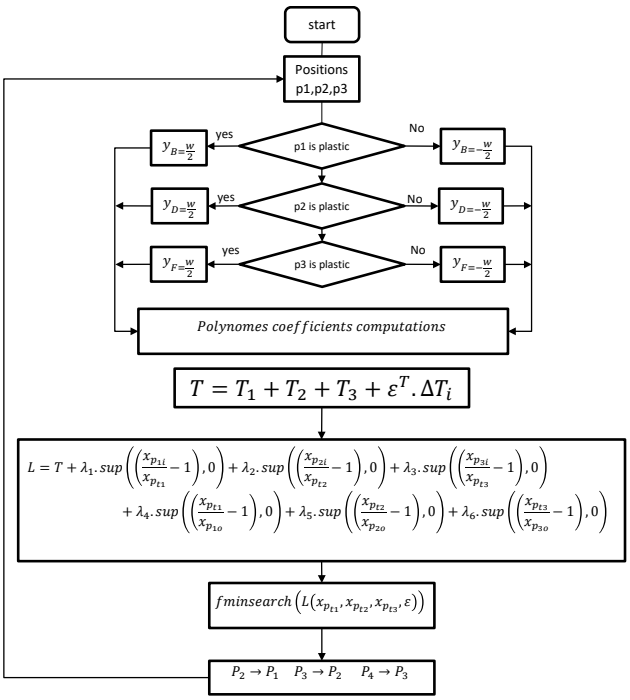

Figure 5: pick-and-place process optimization algorithm

Example

As first example, we consider a conveyor animated with a velocity $v_c = 1000mm/s$ the maximum acceleration of the manipulator was limited to $a_{max} = 27m/s^2$. Three objects were placed on the conveyor. The first and third object are plastics; the second one is glass. The second object is detected 0.7s after the first one, and the third 0.8s after the second. The objects were placed with:

$$y_{t_1} = \frac{L}{4}$$
$$y_{t_2} = -\frac{L}{3} \qquad (5)$$
$$y_{t_3} = \frac{L}{5}$$

Where *L=1200mm* is the conveyor width.

We carried out first a numerical simulation of the algorithm with MatLab. The first remark is, the algorithm cannot converge if the distance between the sensors and the containers is less than 300mm; physically the three objects cannot be removed from the conveyor. Indeed if the intermediate time is less than 0.3s the algorithm fails. That means on the real system we need this test also to find the maximum pick-and-place frequency. In fact, even with the trajectory optimization, the maximum velocity and acceleration of the robot limit the work frequency. To solve this issue we need to decrease the conveyor speed, or even better to use more than one robot. Hence as an object missed by the first robot is removed by the second one. After running the algorithm on MatLab, we got the trajectory shown in Figure 6.

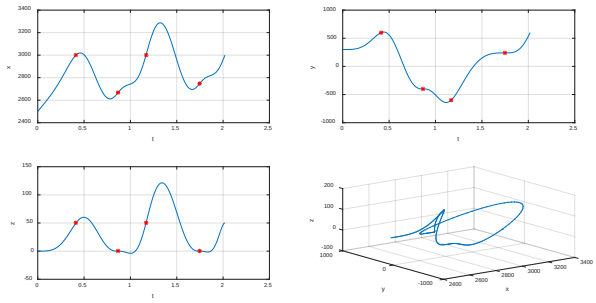

Figure 6: Numeric simulation

V. Kinematics

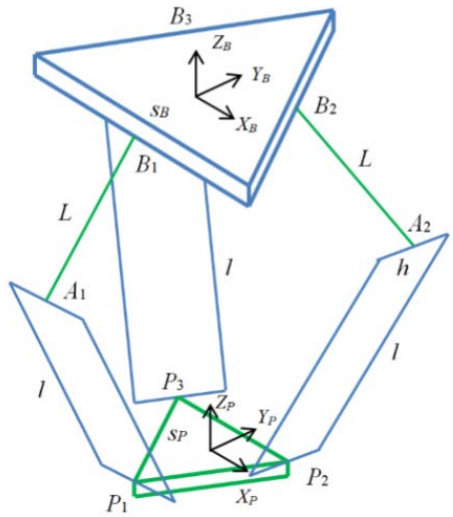

Figure 7: Delta robot kinematic diagram

The motion calculated is for the moving platform. However, the controller acts on the actuators.

Thus, the equations of the joint coordinate motions must be calculated. In this section, the inverse kinematics model is derived.

Then, it will be sufficient to replace *x*, *y* and *z* by their values to get the joint coordinates, θ_1, θ_2 and θ_3, as functions of time. The Delta robot has three DOF, thus it can carry out three translations for its moving platform in the workspace. It is the assembly of three kinematic chains where each one can be considered as a leg. The hip centers are the points B_i, the knee centers are A_i, and the ankle centers are P_i, for leg *i*. Hips are three revolute joints, thus the fixed platform will be considered as an equilateral triangle made by the three joint axes. The length of this triangle side is denoted by s_B. The moving platform is also an equilateral triangle but obtained by its three edges P_i. The length of this triangle side is denoted by s_p (Figure 7). The motion of the moving platform is only a translation, thus it has a constant orientation.

We associate the reference frame $\{B\}$ to the fixed platform with the origin at the base center. We associate the reference frame $\{P\}$ to the moving platform, with the origin at the center of the triangle $P_1P_2P_3$. The rotation matrix ${}^B_PR = I_3$ remains constant. The joint coordinates are $\{\theta_1, \theta_2, \theta_3\}^T$ and the operational coordinates are ${}^BP_P = \{x\ y\ z\}^T$. The design shown in Figure 8 and 9 presents the symmetry of the robot architecture.

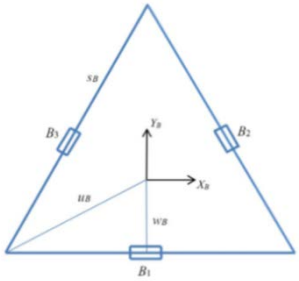

Figure 8: Delta robot fixed base details

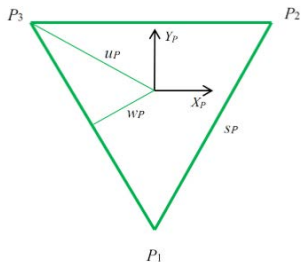

Figure 9: Delta robot moving platform details

The hip B_i coordinates are constant in the coordinate system $\{B\}$ and the ankle P_i coordinates are constant in the base frame $\{P\}$:

$$ {}^{B}B_1 = \begin{Bmatrix} 0 \\ -w_B \\ 0 \end{Bmatrix} \quad {}^{B}B_2 = \begin{Bmatrix} \frac{\sqrt{3}}{2} w_B \\ \frac{1}{2} w_B \\ 0 \end{Bmatrix} \quad {}^{B}B_3 = \begin{Bmatrix} -\frac{\sqrt{3}}{2} w_B \\ \frac{1}{2} w_B \\ 0 \end{Bmatrix} $$

$$ {}^{P}P_1 = \begin{Bmatrix} 0 \\ -u_P \\ 0 \end{Bmatrix} \quad {}^{P}P_2 = \begin{Bmatrix} \frac{s_P}{2} \\ w_P \\ 0 \end{Bmatrix} \quad {}^{P}P_3 = \begin{Bmatrix} -\frac{s_P}{2} \\ w_P \\ 0 \end{Bmatrix} \qquad (6) $$

$$ w_B = \frac{\sqrt{3}}{6} s_B \quad u_B = \frac{\sqrt{3}}{3} s_B $$

$$ w_P = \frac{\sqrt{3}}{6} s_P \quad u_P = \frac{\sqrt{3}}{3} s_P $$

N.B.: The upper left index is the base where the vector is described.

Since three kinematics chains exist (Figure 7), three vector-loop closure [28] equations should be elaborated:

$$ \{{}^{B}B_i\} + \{{}^{B}L_i\} + \{{}^{B}l_i\} = \{{}^{B}P_P\} + [{}^{B}_{P}R]\{{}^{P}P_i\} \qquad (7) $$

For $i = 1,2,3$.

The operational coordinates are ${}^{B}P_P = \{x\ y\ z\}^T$. Vectors $\{{}^{B}L_i\}$ depend on the joint coordinates:

$$ {}^{B}L_1 = \begin{Bmatrix} 0 \\ -L\cos\theta_1 \\ -L\sin\theta_1 \end{Bmatrix} $$

$$ {}^{B}L_2 = \begin{Bmatrix} \frac{\sqrt{3}}{2} L\cos\theta_2 \\ \frac{1}{2} L\cos\theta_2 \\ -L\sin\theta_2 \end{Bmatrix} \qquad (8) $$

$$ {}^{B}L_3 = \begin{Bmatrix} -\frac{\sqrt{3}}{2} L\cos\theta_3 \\ \frac{1}{2} L\cos\theta_3 \\ -L\sin\theta_3 \end{Bmatrix} $$

$$ \{{}^{B}l_1\} = \begin{Bmatrix} x \\ y + L\cos\theta_1 + a \\ z + L\sin\theta_1 \end{Bmatrix} $$

$$ \{{}^{B}l_2\} = \begin{Bmatrix} x - \frac{\sqrt{3}}{2} L\cos\theta_2 + b \\ y - \frac{1}{2} L\cos\theta_2 + c \\ z + L\sin\theta_2 \end{Bmatrix} $$

$$ \{{}^{B}l_3\} = \begin{Bmatrix} x + \frac{\sqrt{3}}{2} L\cos\theta_3 - b \\ y - \frac{1}{2} L\cos\theta_3 + c \\ z + L\sin\theta_3 \end{Bmatrix} $$

Where: $a = w_b - u_P$, $b = \frac{s_P}{2} - \frac{\sqrt{3}}{2} w_B$, $c = w_p - \frac{1}{2} w_B$ (see equation 70)

Equations (7) establish respectively the kinematics equations for the mechanism:

$$ 2L(y+a)\cos\theta_1 + 2zL\sin\theta_1 + x^2 + y^2 + z^2 + a^2 + L^2 + 2ya - l^2 = 0 \qquad (9) $$

$$ -L\left(\sqrt{3}(x+b) + y + c\right)\cos\theta_2 + 2zL\sin\theta_2 + x^2 + y^2 + z^2 + b^2 + c^2 + L^2 + 2xb + 2yc - l^2 = 0 \qquad (10) $$

$$ L\left(\sqrt{3}(x-b) - y - c\right)\cos\theta_3 + 2zL\sin\theta_3 + x^2 + y^2 + z^2 + b^2 + c^2 + L^2 - 2xb + 2yc - l^2 = 0 \qquad (11) $$

The three independent scalar equations are of the form:

$$ E_i\ \cos\theta_i + F_i\ \sin\theta_i + G_i = 0 \qquad i = 1,2,3 \qquad (12) $$

Where E_i, F_i and G_i depend on the coordinates $\{x, y, z\}$. Using the tangent half-angle substitution:

$$ t_{i_{1,2}} = \frac{-F_i \pm \sqrt{E_i^2 + F_i^2 - G_i^2}}{G_i - E_i} \qquad (13) $$

Then:

$$ \theta_i = 2\tan^{-1}(t_i) \qquad (14) $$

Two inverse kinematic model solutions are possible for each leg of the Delta Robot. The first one is for a knee kinked out whereas for the second one, the knee is kinked in. In total, eight different combinations are possible. We will use the case where the three knees are kinked out.

The differential kinematics model can be obtained simply by differentiating equations (6) with respect to the time. Written in matrix-vector form:

$$ [\boldsymbol{A}]\{\dot{\boldsymbol{X}}\} = [\boldsymbol{B}]\{\dot{\boldsymbol{\theta}}\} $$

$$ \begin{bmatrix} x & y + a + LC_1 & z + LS_1 \\ 2(x+b) - \sqrt{3}LC_2 & 2(y+c) - LC_2 & 2(z + LS_2) \\ 2(x-b) + \sqrt{3}LC_3 & 2(y+c) - LC_3 & 2(z + LS_3) \end{bmatrix} \begin{Bmatrix} \dot{x} \\ \dot{y} \\ \dot{z} \end{Bmatrix} = \begin{bmatrix} b_{11} & 0 & 0 \\ 0 & b_{22} & 0 \\ 0 & 0 & b_{33} \end{bmatrix} \begin{Bmatrix} \dot{\theta}_1 \\ \dot{\theta}_2 \\ \dot{\theta}_3 \end{Bmatrix} \qquad (15) $$

Where:

$$ b_{11} = L[(y+a)S_1 - zC_1] $$

$$ b_{22} = -L\left[\left(\sqrt{3}(x+b) + y + c\right)S_2 + 2zC_2\right] $$

$$ b_{33} = L\left[\left(\sqrt{3}(x-b) - y - c\right)S_3 - 2zC_3\right] $$

$$ S_i = \sin\theta_i \quad C_i = \cos\theta_i $$

Substituting x, y and z in equation (14) gives the equations of the joint coordinates as function of time. Similarly, the substitution of $\dot{x}$, $\dot{y}$ and $\dot{z}$ in equation (15) yields a system of differential equations. This system can be solved numerically.

For an optimal control, a motion study has to be carried out showing multiple results concerning the torque of the actuators. The robot will work with a maximum payload of 2 Kg. The dynamics model needs the solution of 54 equations with 54 unknowns. If the needed torque of at least an actuator exceeds its nominal torque, a correction is needed because the desired motion will be lost. In this case, the maximum velocities and accelerations $\dot{u}_{max}$, $\ddot{u}_{max}$, $\dot{z}_{max}$and $\ddot{z}_{max}$ should be moderated.

VI. PROTOTYPE

In order to validate the algorithm, a small prototype is made using 3D printing technology. It is controlled using an Arduino-uno controller, and the code is written in Labview.

Figure 10: prototype

The conveyor is animated with a velocity $v_c = 1\ m/s$. The conveyor width is 12 cm. It is not possible to use the infrared detector with the prototype. For this reason, a series of inductive sensors and a series of capacitive sensors are used (Figure 11).

Figure 11: inductive detectors in the prototype

Instead of glass and plastic, metallic and plastic elements are used. The plastic parts are detected by the capacitive sensor only and the metallic by both sensors. Thus, metallic elements can be separated from the plastic ones on the conveyor. The position of the sensor gives the *y*-coordinate. The previous algorithm can be used in the same way. And the prototype could sort up to 3 parts per second.

VII. CONCLUSIONS AND FURTHER WORKS:

In this paper we presented the integration of a parallel manipulator in a waste-sorting system. Metallic objects are removed using electromagnets and eddy current. Plastic and glass are detected using an infrared sensor. Then the *y* coordinate is determined as well as the *x* coordinate of the object as function of time. We calculated the trajectory and the equation of motion for the pick-and-place operation. We used a fifth-order polynomial interpolation with a continuity of acceleration and velocity. In order to get the fastest motion, an optimization process was carried out. We developed an algorithm to find the position where each object must be picked and in which order, for the purpose of getting the maximum number of cycles per minute. In order to ensure that all objects are removed, non-equality constraints are included in the operational research. To take these constraints into consideration, the algorithm uses the penalty method: the objective function is penalized when a constraint is violated. Since the controller acts on the joint coordinates, we elaborated the inverse kinematics and differential models. Those models give the equation of the joint's motion as function of time.

In this paper, the trajectory used is a polynomial interpolation. The task can be performed much faster if b-splines are used with conditioned velocity and acceleration at intermediate points. In this case, interesting effects will be found for the motion strategies. Moreover, our prototype is very light. Therefore, no automatic control was needed. However, on the real device the inertia of the robot is not negligible. The objective is to sort more than 200 tons of waste per day. Thus, we need very high velocities leading to high non-linear effects and disturbances. The control will be a complicated task, and a classical PID controller will not work. Those aspects are going to be our future step.

ACKNOWLEDGEMENT: This work was supported by the AUF (www.auf.org)

REFERENCES

[1] MERLET. J.P. ,2000,"Parallel robots". Dordrecht: Kluwer Academic

[2] Bonev, I., 2001, ''Delta Parallel Robot—The Story of Success,'' on line available: http://www.parallelmic.org

[3] Cervantez-Sanchez, J. J., and Rendon-Sanchez, J. G., 1999, ''A Simplified Approach for Obtaining the Workspace of a Class of 2-DOF Planar Parallel Robot,'' Mech. Mach. Theory, **34.7**., pp. 1057–1073.

[4] Clavel, R., 1990, ''Device for the Movement and Positioning of an Element in Space,'' U.S. Patent 4976582, Dec. 11.

[5] Rey, L., and Clavel, R., 1999, ''The Delta Parallel Robot,'' *Parallel Kinematic Machine*, Boer, C. R., Molinari-Tosatti, L., Smith, K. S., eds., Springer, New York.

[6] Clavel, R., 1988, ''Delta, A Fast Robot with Parallel Geometry,'' *The 18th Int. Symposium on Industrial Robots (ISIR)*, pp. 91–100, Sydney, Australia.

[7] Codourey, A., 1996, "Dynamic Modeling and Mass Matrix Evaluation of the Delta Parallel Robot for Axes Decoupling Control," Proc. of IEEE/RSJ Int. Conf. on Intelligent Robots and Systems, pp. 1211–1218.

[8] Maurine, P., and Dombre, E., 1996, "A Calibration Procedure for the Parallel Robot Delta 4," Proc. of IEEE Int. Conf. on Robotics and Automation (ICRA'96), pp. 975–980, Minneapolis, MN.

[9] Miller, K., 1992, "The Proposal of a New Model of Direct Drive Robot Delta-4 Dynamics," Proc. of Int. Conf. on Advanced Robotics, pp. 411–416, Tokyo, Japan.

[10] Miller, K., 1995, "Experimental Verification of Modeling of Delta Robot Dynamics by Direct Application of Hamilton's Principle," Proc. of IEEE Int. Conf. on Robotics and Automation (ICRA'95), pp. 532–537, Nagoya, Japan.

[11] Miller, K., 1995, "On Accuracy and Computational Efficiency of Delta Direct Drive Robot Dynamics Mode," Proc. of Int. Sym. on Microsystems, Intelligent Materials and Robots, pp. 568–571, Sendai, Japan, 1995

[12] Miller, K., 1995, "Model-Based Control of Delta Direct Drive Parallel Robot; Trajectory Tracking Experiments," Proc. of the 26th International Symposium of Industrial Robots, pp. 491–496, Singapore.

[13] Miller, K., 1995, "Modeling of Dynamics and Model-Based Control of Delta Direct-Drive Parallel Robot," J. of Robotics and Mechatronics, 17.4., pp. 344–352.

[14] Miller, K., and Clavel, R., 1992, "The Lagrange-Based Model of Delta-4 Robot Dynamics," Robot System, 8.4., pp. 49–54.

[15] Stamper, R. C., Tsai, L. W., and Walsh, G. C., 1997, ‘‘Optimization of a 3-DOF Translational Platform for Well-Conditioned Workspace,’’ Proc. Of IEEE Int. Conf. on Robotics and Automation (ICRA’97), pp. 3250–3255, Albuquerque.
[16] Tsai, L. W., Walsh, G. C., and Stamper, R. C., 1996, ‘‘Kinematics of a Novel 3-DOF Translational Platform,’’ Proc. of IEEE Int. Conf. on Robotics and Automation (ICRA’96), pp. 3446–3451, Minneapolis, MN.
[17] Tsai, L. W., 1999, ‘‘The Enumeration of a Class of 3-DOF Parallel Manipulators,’’ Proc. of The 10th World Congress on the Theory of Machine and Mechanisms, pp. 1121–1126, Oulu, Finland.
[18] Tsai, L. W., and Joshi, S., 2002, ‘‘Kinematics and Optimization of a 3UPU Parallel Manipulator,’’ ASME J. Mech. Des., 122, No. 4, pp. 439–446.
[19] Bobrow, J. E., S. Dubowsky and J. S. Gibson, 1985, Time-Optimal Control of Robotic Manipulators Along Specified Paths, International Journal of Robotics Research 4(3), pp. 3-17.
[20] Braibant, V. and M. Geradin, 1987, Optimum Path Planning of Robot Arms, Robotica 5, pp. 323-331.
[21] Dubowsky, S. and Zvi. Shiller, 1984, Optimal Dynamic Trajectories for Robotic Manipulators, in Proceedings of the Fifih CISMIFToMM Symposium on Theory and Practice of Robots and Manipulators, pp. 133-143.
[22] Kim, B. K., and K. G. Shin, Mar. 1985, Minimum-Time Path Planning for Robot Arms and their Dynamics, IEEE Transactions on Sytems Man and Cybernetics SMC-15(2), pp. 213-223.
[23] Lin C. S., P. R. Chang and J. Y. S. Luh, 1983, Formulation and Optimization of Cubic Polynomial Joint Trajectories for Industrial Robots, IEEE Transactions on Automatic Control AC-28(12), pp. 1066-1074.
[24] Lin, C. S., and P. R. Chang, 1985, Approximate Optimum Paths of Robot Manipulators Under Realistic Physical Constraints, in Proceedings of the IEEE International Conference on Robotics and Automation, New York, pp. 737-742.
[25] Luh, J. Y. S. and C. S. Lin,1981, Optimal Path Planning for Mechanical Manipulators, ASME Journal of Dynamic Systems, Measurement and Control, vol 102, no. 6, pp. 142-1.51.
[26] Shiller, Z. and S. Dubowsky, 1985, On the Optimal Control of Robotic Manipulators with Actuator and End Effector Constraints, in Proceedings of the IEEE Conference on Robotics and Automation, New Yorkpp. 614-620.
[27] Pateloup V, Duc, E., P. Ray, B-spline approximation of circle arc and straight line for pocket machining, Computer Aided Design, V42, No. 9, pp 817 827
[28] Briot S., Khalil W., 2015, Dynamics of Parallel Robots. From Rigid Bodies to Flexible Elements. Springer, ISBN 978-3-319-19788-3
[29] Joines J. A., Houck C. R., 1994, on the use of non-stationary penalty functions to solve non-linear constrained optimization problems with GA’s, IEEE world congress on computational intelligence, Orlando, FL, USA, 27-29

APENDIX:

Phase *AB*:

$$\begin{aligned} x_A &= x_{pt_1} & x_B &= x_{cont} \\ \dot{x}_A &= v_c & \dot{x}_{B^-} &= \dot{x}_{B^+} \\ \ddot{x}_A &= 0 & \ddot{x}_{B^-} &= \ddot{x}_{B^+} \\ \dddot{x}_{A^-} &= \dddot{x}_{A^+} & \dddot{x}_{B^-} &= \dddot{x}_{B^+} \end{aligned} \tag{A1}$$

$$x_{AB} = a_{x_0} + a_{x_1}t + a_{x_2}t^2 + a_{x_3}t^3 + a_{x_4}t^4 + a_{x_5}t^5$$

$$\begin{aligned} y_A &= y_{pt_1} & y_B &= y_{cont} \\ \dot{y}_A &= 0 & \dot{y}_{B^-} &= \dot{y}_{B^+} \\ \ddot{y}_A &= 0 & \ddot{y}_{B^-} &= \ddot{y}_{B^+} \\ \dddot{y}_{A^-} &= \dddot{y}_{A^+} & \dddot{y}_{B^-} &= \dddot{y}_{B^+} \end{aligned} \tag{A2}$$

$$y_{AB} = a_{y_0} + a_{y_1}t + a_{y_2}t^2 + a_{y_3}t^3 + a_{y_4}t^4 + a_{y_5}t^5$$

$$\begin{aligned} z_A &= 0 & z_B &\geq 0 \\ \dot{z}_A &= 0 & \dot{z}_{B^-} &= \dot{z}_{B^+} \\ \ddot{z}_A &= 0 & \ddot{z}_{B^-} &= \ddot{z}_{B^+} \\ \dddot{z}_{A^-} &= \dddot{z}_{A^+} & \dddot{z}_{B^-} &= \dddot{z}_{B^+} \end{aligned} \tag{A3}$$

$$z_{AB} = a_{z_0} + a_{z_1}t + a_{z_2}t^2 + a_{z_3}t^3 + a_{z_4}t^4 + a_{z_5}t^5$$

Phase *BC*:

$$\begin{aligned} x_C &= x_{pt_2} & x_B &= x_{cont} \\ \dot{x}_C &= v_c & \dot{x}_{B^-} &= \dot{x}_{B^+} \\ \ddot{x}_C &= 0 & \ddot{x}_{B^-} &= \ddot{x}_{B^+} \\ \dddot{x}_{C^-} &= \dddot{x}_{C^+} & \dddot{x}_{B^-} &= \dddot{x}_{B^+} \end{aligned} \tag{A4}$$

$$x_{BC} = b_{x_0} + b_{x_1}t + b_{x_2}t^2 + b_{x_3}t^3 + b_{x_4}t^4 + b_{x_5}t^5$$

$$\begin{aligned} y_C &= y_{pt_2} & y_B &= y_{cont} \\ \dot{y}_C &= 0 & \dot{y}_{B^-} &= \dot{y}_{B^+} \\ \ddot{y}_C &= 0 & \ddot{y}_{B^-} &= \ddot{y}_{B^+} \\ \dddot{y}_{C^-} &= \dddot{y}_{C^+} & \dddot{y}_{B^-} &= \dddot{y}_{B^+} \end{aligned} \tag{A5}$$

$$y_{BC} = b_{y_0} + b_{y_1}t + b_{y_2}t^2 + b_{y_3}t^3 + b_{y_4}t^4 + b_{y_5}t^5$$

$$\begin{aligned} z_C &= 0 & z_B &\geq 0 \\ \dot{z}_C &= 0 & \dot{z}_{B^-} &= \dot{z}_{B^+} \\ \ddot{z}_C &= 0 & \ddot{z}_{B^-} &= \ddot{z}_{B^+} \\ \dddot{z}_{C^-} &= \dddot{z}_{C^+} & \dddot{z}_{B^-} &= \dddot{z}_{B^+} \end{aligned} \tag{A6}$$

$$z_{BC} = b_{z_0} + b_{z_1}t + b_{z_2}t^2 + b_{z_3}t^3 + b_{z_4}t^4 + b_{z_5}t^5$$

Phase *CD*:

$$\begin{aligned} x_C &= x_{pt_2} & x_D &= x_{cont} \\ \dot{x}_C &= v_c & \dot{x}_{D^-} &= \dot{x}_{D^+} \\ \ddot{x}_C &= 0 & \ddot{x}_{D^-} &= \ddot{x}_{D^+} \\ \dddot{x}_{C^-} &= \dddot{x}_{C^+} & \dddot{x}_{D^-} &= \dddot{x}_{D^+} \end{aligned} \tag{A7}$$

$$x_{CD} = c_{x_0} + c_{x_1}t + c_{x_2}t^2 + c_{x_3}t^3 + c_{x_4}t^4 + c_{x_5}t^5$$

$$\begin{aligned} y_C &= y_{pt_2} & y_D &= y_{cont} \\ \dot{y}_C &= 0 & \dot{y}_{D^-} &= \dot{y}_{D^+} \\ \ddot{y}_C &= 0 & \ddot{y}_{D^-} &= \ddot{y}_{D^+} \\ \dddot{y}_{C^-} &= \dddot{y}_{C^+} & \dddot{y}_{D^-} &= \dddot{y}_{D^+} \end{aligned} \tag{A8}$$

$$y_{CD} = c_{y_0} + c_{y_1}t + c_{y_2}t^2 + c_{y_3}t^3 + c_{y_4}t^4 + c_{y_5}t^5$$

$$\begin{aligned} z_C &= 0 & z_D &\geq 0 \\ \dot{z}_C &= 0 & \dot{z}_{D^-} &= \dot{z}_{D^+} \\ \ddot{z}_C &= 0 & \ddot{z}_{D^-} &= \ddot{z}_{D^+} \\ \dddot{z}_{C^-} &= \dddot{z}_{C^+} & \dddot{z}_{D^-} &= \dddot{z}_{D^+} \end{aligned} \tag{A9}$$

$$z_{CD} = c_{z_0} + c_{z_1}t + c_{z_2}t^2 + c_{z_3}t^3 + c_{z_4}t^4 + c_{z_5}t^5$$

Phase *DE*:

$$\begin{aligned} x_E &= x_{pt_3} & x_D &= x_{cont} \\ \dot{x}_E &= v_c & \dot{x}_{D^-} &= \dot{x}_{D^+} \\ \ddot{x}_E &= 0 & \ddot{x}_{D^-} &= \ddot{x}_{D^+} \\ \dddot{x}_{E^-} &= \dddot{x}_{E^+} & \dddot{x}_{D^-} &= \dddot{x}_{D^+} \end{aligned} \tag{A10}$$

$$x_{DE} = d_{x_0} + d_{x_1}t + d_{x_2}t^2 + d_{x_3}t^3 + d_{x_4}t^4 + d_{x_5}t^5$$

$$\begin{aligned} y_E &= y_{pt_3} & y_D &= y_{cont} \\ \dot{y}_E &= 0 & \dot{y}_{D^-} &= \dot{y}_{D^+} \\ \ddot{y}_E &= 0 & \ddot{y}_{D^-} &= \ddot{y}_{D^+} \\ \dddot{y}_{E^-} &= \dddot{y}_{E^+} & \dddot{y}_{D^-} &= \dddot{y}_{D^+} \end{aligned} \tag{A11}$$

$$y_{DE} = d_{y_0} + d_{y_1}t + d_{y_2}t^2 + d_{y_3}t^3 + d_{y_4}t^4 + d_{y_5}t^5$$

$$z_E = 0 \quad z_D \geq 0$$
$$\dot{z}_E = 0 \quad \dot{z}_{D^-} = \dot{z}_{D^+} \tag{A12}$$
$$\ddot{z}_E = 0 \quad \ddot{z}_{D^-} = \ddot{z}_{D^+}$$
$$\dddot{z}_{E^-} = \dddot{z}_{E^+} \quad \dddot{z}_{D^-} = \dddot{z}_{D^+}$$
$$z_{DE} = d_{z_0} + d_{z_1}t + d_{z_2}t^2 + d_{z_3}t^3 + d_{z_4}t^4 + d_{z_5}t^5$$

Phase *EF*:

$$x_E = x_{pt_3} \quad x_F = x_{cont}$$
$$\dot{x}_E = v_c \quad \dot{x}_{F^-} = \dot{x}_{F^+} \tag{A13}$$
$$\ddot{x}_E = 0 \quad \ddot{x}_{F^-} = \ddot{x}_{F^+}$$
$$\dddot{x}_{E^-} = \dddot{x}_{E^+} \quad \dddot{x}_{F^-} = \dddot{x}_{F^+}$$
$$x_{DE} = e_{x_0} + e_{x_1}t + e_{x_2}t^2 + e_{x_3}t^3 + e_{x_4}t^4 + e_{x_5}t^5$$
$$y_E = y_{pt_3} \quad y_F = y_{cont}$$
$$\dot{y}_E = 0 \quad \dot{y}_{F^-} = \dot{y}_{F^+} \tag{A14}$$
$$\ddot{y}_E = 0 \quad \ddot{y}_{F^-} = \ddot{y}_{F^+}$$
$$\dddot{y}_{E^-} = \dddot{y}_{E^+} \quad \dddot{y}_{F^-} = \dddot{y}_{F^+}$$
$$y_{DE} = e_{y_0} + e_{y_1}t + e_{y_2}t^2 + e_{y_3}t^3 + e_{y_4}t^4 + e_{y_5}t^5$$
$$z_E = 0 \quad z_F \geq 0$$
$$\dot{z}_E = 0 \quad \dot{z}_{F^-} = \dot{z}_{F^+} \tag{A15}$$
$$\ddot{z}_E = 0 \quad \ddot{z}_{F^-} = \ddot{z}_{F^+}$$
$$\dddot{z}_{E^-} = \dddot{z}_{E^+} \quad \dddot{z}_{F^-} = \dddot{z}_{F^+}$$
$$z_{EF} = e_{z_0} + e_{z_1}t + e_{z_2}t^2 + e_{z_3}t^3 + e_{z_4}t^4 + e_{z_5}t^5$$

Known values:

In phases *AB, CD and EF*

$$x_A = x_{pt_1} \Longrightarrow a_{x_0} = x_{pt_1} \tag{A16}$$
$$\dot{x}_A = v_c \Longrightarrow a_{x_1} = v_c \tag{A17}$$
$$\ddot{x}_A = 0 \Longrightarrow a_{x_2} = 0 \tag{A18}$$
$$x_C = x_{pt_2} \Longrightarrow c_{x_0} = x_{pt_2} \tag{A19}$$
$$\dot{x}_C = v_c \Longrightarrow c_{x_1} = v_c \tag{A20}$$
$$\ddot{x}_C = 0 \Longrightarrow c_{x_2} = 0 \tag{A21}$$
$$x_E = x_{pt_2} \Longrightarrow e_{x_0} = x_{pt_2} \tag{A22}$$
$$\dot{x}_E = v_c \Longrightarrow e_{x_1} = v_c \tag{A23}$$
$$\ddot{x}_E = 0 \Longrightarrow e_{x_2} = 0 \tag{A24}$$
$$y_A = y_{pt_1} \Longrightarrow a_{y_0} = y_{pt_1} \tag{A25}$$
$$\dot{y}_A = 0 \Longrightarrow a_{y_1} = 0 \tag{A26}$$
$$\ddot{y}_A = 0 \Longrightarrow a_{y_2} = 0 \tag{A27}$$
$$y_C = y_{pt_2} \Longrightarrow c_{y_0} = y_{pt_2} \tag{A28}$$
$$\dot{y}_C = 0 \Longrightarrow c_{y_1} = 0 \tag{A29}$$
$$\ddot{y}_C = 0 \Longrightarrow c_{y_2} = 0 \tag{A30}$$
$$y_E = y_{pt_2} \Longrightarrow e_{y_0} = y_{pt_2} \tag{A31}$$
$$\dot{y}_E = 0 \Longrightarrow e_{y_1} = 0 \tag{A32}$$
$$\ddot{y}_E = 0 \Longrightarrow e_{y_2} = 0 \tag{A33}$$
$$z_A = 0 \Longrightarrow a_{z_0} = 0 \tag{A34}$$
$$\dot{z}_A = 0 \Longrightarrow a_{z_1} = 0 \tag{A35}$$
$$\ddot{z}_A = 0 \Longrightarrow a_{z_2} = 0 \tag{A36}$$
$$z_C = 0 \Longrightarrow c_{z_0} = 0 \tag{A37}$$
$$\dot{z}_C = 0 \Longrightarrow c_{z_1} = 0 \tag{A38}$$
$$\ddot{z}_C = 0 \Longrightarrow c_{z_2} = 0 \tag{A39}$$
$$z_E = 0 \Longrightarrow e_{z_0} = 0 \tag{A40}$$
$$\dot{z}_E = 0 \Longrightarrow e_{z_1} = 0 \tag{A41}$$
$$\ddot{z}_E = 0 \Longrightarrow e_{z_2} = 0 \tag{A42}$$

In phases *BC* and *DE*

$$x_B = x_{cont} \Longrightarrow b_{x_0} = x_{cont} \tag{A43}$$
$$y_B = y_{cont} \Longrightarrow b_{y_0} = y_{cont} \tag{A44}$$
$$x_D = x_{cont} \Longrightarrow d_{x_0} = x_{cont} \tag{A45}$$
$$y_D = y_{cont} \Longrightarrow d_{y_0} = y_{cont} \tag{A46}$$

A. *Motion along x*

Phase *AB*

$$x_B = x_{cont} \Longrightarrow a_{x_3}T_1^3 + a_{x_4}T_1^4 + a_{x_5}T_1^5 + x_{pt_1} + v_cT_1 = x_{cont} \tag{A47}$$
$$\dot{x}_{B^-} = \dot{x}_{B^+} \Longrightarrow v_c + 3a_{x_3}T_1^2 + 4a_{x_4}T_1^3 + 5a_{x_5}T_1^4 = b_{x_1} \tag{A48}$$
$$\ddot{x}_{B^-} = \ddot{x}_{B^+} \Longrightarrow 6a_{x_3}T_1 + 12a_{x_4}T_1^2 + 20a_{x_5}T_1^3 = 2b_{x_2} \tag{A49}$$
$$\dddot{x}_{A^-} = \dddot{x}_{A^+} \Rightarrow 6a_{x_3} = \dddot{x}_{A^-} \tag{A50}$$
$$\dddot{x}_{B^-} = \dddot{x}_{B^+} \Longrightarrow 6a_{x_3} + 24a_{x_4}T_1 + 60a_{x_5}T_1^2 = 6b_{x_3} \tag{A51}$$

Phase *BC*

$$x_C = x_{pt_2}$$
$$\Longrightarrow x_{cont} + b_{x_1}T_{i123_1} + b_{x_2}T_{i123_1}^2 + b_{x_3}T_{i123_1}^3 + b_{x_4}T_{i123_1}^4 + b_{x_5}T_{i123_1}^5 = x_{pt_2} \tag{A52}$$
$$\dot{x}_C = v_c$$
$$\Longrightarrow b_{x_1} + 2b_{x_2}T_{i123_1} + 3b_{x_3}T_{i123_1}^2 + 4b_{x_4}T_{i123_1}^3 + 5b_{x_5}T_{i123_1}^4 = v_c \tag{A53}$$
$$\ddot{x}_C = 0$$
$$\Longrightarrow 2b_{x_2} + 6b_{x_3}T_{i123_1} + 12b_{x_4}T_{i123_1}^2 + 20b_{x_5}T_{i123_1}^3 = 0 \tag{A54}$$
$$\dddot{x}_{C^-} = \dddot{x}_{C^+} \Longrightarrow 6b_{x_3} + 24b_{x_4}T_{i123_1} + 60b_{x_5}T_{i123_1}^2 = 6c_{x_3} \tag{A55}$$

Phases *CD* and *DE*

$$x_D = x_{cont} \Longrightarrow x_{pt_2} + v_cT_2 + c_{x_3}T_2^3 + c_{x_4}T_2^4 + c_{x_5}T_2^5 = x_{cont} \tag{A56}$$

$$\dot{x}_{D^-} = \dot{x}_{D^+} \Longrightarrow v_c + 3c_{x_3}T_2^2 + 4c_{x_4}T_2^3 + 5c_{x_5}T_2^4 = d_{x_1} \quad \text{(A57)}$$

$$\ddot{x}_{D^-} = \ddot{x}_{D^+} \Longrightarrow 6c_{x_3}T_2 + 12c_{x_4}T_2^2 + 20c_{x_5}T_2^3 = 2d_{x_2} \quad \text{(A58)}$$

$$\dddot{x}_{D^-} = \dddot{x}_{D^+} \Longrightarrow 6c_{x_3} + 24c_{x_4}T_2 + 60c_{x_5}T_2^2 = 6d_{x_3} \quad \text{(A59)}$$

$$x_E = x_{pt_3} \Longrightarrow x_{cont} + d_{x_1}T_{i123_2} + d_{x_2}T_{i123_2}^2 + d_{x_3}T_{i123_2}^3 + d_{x_4}T_{i123_2}^4 + d_{x_5}T_{i123_2}^5 = x_{pt_3} \quad \text{(A60)}$$

$$\dot{x}_E = v_c \Longrightarrow$$

$$d_{x_1} + 2d_{x_2}T_{i123_2} + 3d_{x_3}T_{i123_2}^2 + 4d_{x_4}T_{i123_2}^3 + 5d_{x_5}T_{i123_2}^4 = v_c \quad \text{(A61)}$$

$$\ddot{x}_E = 0 \Longrightarrow 2d_{x_2} + 6d_{x_3}T_{i123_2} + 12d_{x_4}T_{i123_2}^2 + 20d_{x_5}T_{i123_2}^3 = 0 \quad \text{(A62)}$$

$$\dddot{x}_{E^-} = \dddot{x}_{E^+} \Longrightarrow 6d_{x_3} + 24d_{x_4}T_{i123_2} + 60d_{x_5}T_{i123_1}^2 = 6e_{x_3} \quad \text{(A63)}$$

Phase *EF*

$$x_F = x_{cont} = e_{x_3}T_3^3 + e_{x_4}T_3^4 + e_{x_5}T_3^5 \quad \text{(A64)}$$

$$\ddot{x}_{F^-} = \ddot{x}_{F^+} \Longrightarrow 6e_{x_3}T_3 + 12e_{x_4}T_3^2 + 20e_{x_5}T_3^3 = \ddot{z}_{F^+} \quad \text{(A65)}$$

B. *Motion along y*

Phase *AB*

$$y_B = y_{cp} \Longrightarrow a_{y_3}T_1^3 + a_{y_4}T_1^4 + a_{y_5}T_1^5 + y_{pt_1} = y_{cp} \quad \text{(A66)}$$

$$\dot{y}_{B^-} = \dot{y}_{B^+} \Longrightarrow 3a_{y_3}T_1^2 + 4a_{y_4}T_1^3 + 5a_{y_5}T_1^4 = b_{y_1} \quad \text{(A67)}$$

$$\ddot{y}_{B^-} = \ddot{y}_{B^+} \Longrightarrow 6a_{y_3}T_1 + 12a_{y_4}T_1^2 + 20a_{y_5}T_1^3 = 2b_{y_2} \quad \text{(A68)}$$

$$\dddot{y}_{A^-} = \dddot{y}_{A^+} \Rightarrow 6a_{y_3} = \dddot{y}_{A^-} \quad \text{(A69)}$$

$$\dddot{y}_{B^-} = \dddot{y}_{B^+} \Longrightarrow 6a_{y_3} + 24a_{y_4}T_1 + 60a_{y_5}T_1^2 = 6b_{y_3} \quad \text{(A70)}$$

Phase *BC*

$$y_C = y_{pt_2}$$

$$\Longrightarrow y_{cp} + b_{y_1}T_{i123_1} + b_{y_2}T_{i123_1}^2 + b_{y_3}T_{i123_1}^3 + b_{y_4}T_{i123_1}^4 + b_{y_5}T_{i123_1}^5 = y_{pt_2} \quad \text{(A71)}$$

$$\dot{y}_C = 0$$

$$\Longrightarrow b_{y_1} + 2b_{y_2}T_{i123_1} + 3b_{y_3}T_{i123_1}^2 + 4b_{y_4}T_{i123_1}^3 + 5b_{y_5}T_{i123_1}^4 = 0 \quad \text{(A72)}$$

$$\ddot{y}_C = 0$$

$$\Longrightarrow 2b_{y_2} + 6b_{y_3}T_{i123_1} + 12b_{y_4}T_{i123_1}^2 + 20b_{y_5}T_{i123_1}^3 = 0 \quad \text{(A73)}$$

$$\dddot{y}_{C^-} = \dddot{y}_{C^+} \Longrightarrow 6b_{y_3} + 24b_{y_4}T_{i123_1} + 60b_{y_5}T_{i123_1}^2 = 6c_{y_3} \quad \text{(A74)}$$

Phases *CD* and *DE*

$$y_D = y_{cg} \Longrightarrow y_{pt_2} + c_{y_3}T_2^3 + c_{y_4}T_2^4 + c_{y_5}T_2^5 = y_{cg} \quad \text{(A75)}$$

$$\dot{y}_{D^-} = \dot{y}_{D^+} \Longrightarrow 3c_{y_3}T_2^2 + 4c_{y_4}T_2^3 + 5c_{y_5}T_2^4 = d_{y_1} \quad \text{(A76)}$$

$$\ddot{y}_{D^-} = \ddot{y}_{D^+} \Longrightarrow 6c_{y_3}T_2 + 12c_{y_4}T_2^2 + 20c_{y_5}T_2^3 = 2d_{y_2} \quad \text{(A77)}$$

$$\dddot{y}_{D^-} = \dddot{y}_{D^+} \Longrightarrow 6c_{y_3} + 24c_{y_4}T_2 + 60c_{y_5}T_2^2 = 6d_{y_3} \quad \text{(A78)}$$

$$y_E = y_{pt_3} \Longrightarrow y_{cg} + d_{y_1}T_{i123_2} + d_{y_2}T_{i123_2}^2 + d_{y_3}T_{i123_2}^3 + d_{y_4}T_{i123_2}^4 + d_{y_5}T_{i123_2}^5 = y_{pt_3} \quad \text{(A79)}$$

$$\dot{y}_E = 0 \Longrightarrow$$

$$d_{y_1} + 2d_{y_2}T_{i123_2} + 3d_{y_3}T_{i123_2}^2 + 4d_{y_4}T_{i123_2}^3 + 5d_{y_5}T_{i123_2}^4 = 0 \quad \text{(A80)}$$

$$\ddot{y}_E = 0 \Longrightarrow 2d_{y_2} + 6d_{y_3}T_{i123_2} + 12d_{y_4}T_{i123_2}^2 + 20d_{y_5}T_{i123_2}^3 = 0 \quad \text{(A81)}$$

$$\dddot{y}_{E^-} = \dddot{y}_{E^+} \Longrightarrow 6d_{y_3} + 24d_{y_4}T_{i123_2} + 60d_{y_5}T_{i123_1}^2 = 6e_{y_3} \quad \text{(A82)}$$

Phase *EF*

$$y_F = y_{cont} = e_{y_3}T_3^3 + e_{y_4}T_3^4 + e_{y_5}T_3^5 \quad \text{(A83)}$$

$$\dot{y}_F = 0 \Longrightarrow 3e_{y_3}T_3^2 + 4e_{y_4}T_3^3 + 5e_{x_5}T_3^4 = 0 \quad \text{(A84)}$$

C. *Motion along z*

Phase *AB*

$$z_B = z_{cont} \Longrightarrow a_{z_3}T_1^3 + a_{z_4}T_1^4 + a_{z_5}T_1^5 = z_{cont} \quad \text{(A85)}$$

$$\dot{z}_{B^-} = \dot{z}_{B^+} \Longrightarrow 3a_{z_3}T_1^2 + 4a_{z_4}T_1^3 + 5a_{z_5}T_1^4 = b_{z_1} \quad \text{(A86)}$$

$$\ddot{z}_{B^-} = \ddot{z}_{B^+} \Longrightarrow 6a_{z_3}T_1 + 12a_{z_4}T_1^2 + 20a_{z_5}T_1^3 = 2b_{z_2} \quad \text{(A87)}$$

$$\dddot{z}_{A^-} = \dddot{z}_{A^+} \Rightarrow 6a_{z_3} = \dddot{z}_{A^-} \quad \text{(A88)}$$

$$\dddot{z}_{B^-} = \dddot{z}_{B^+} \Longrightarrow 6a_{z_3} + 24a_{z_4}T_1 + 60a_{z_5}T_1^2 = 6b_{z_3} \quad \text{(A89)}$$

Phase *BC*

$$z_C = 0$$

$$\Longrightarrow z_{cont} + b_{z_1}T_{i123_1} + b_{z_2}T_{i123_1}^2 + b_{z_3}T_{i123_1}^3 + b_{z_4}T_{i123_1}^4 + b_{z_5}T_{i123_1}^5 = 0 \quad \text{(A90)}$$

$$\dot{x}_C = 0$$

$$\Longrightarrow b_{z_1} + 2b_{z_2}T_{i123_1} + 3b_{z_3}T_{i123_1}^2 + 4b_{z_4}T_{i123_1}^3 + 5b_{z_5}T_{i123_1}^4 = 0 \quad \text{(A91)}$$

$$\ddot{z}_C = 0$$

$$\Longrightarrow 2b_{z_2} + 6b_{z_3}T_{i123_1} + 12b_{z_4}T_{i123_1}^2 + 20b_{z_5}T_{i123_1}^3 = 0 \quad \text{(A92)}$$

$$\dddot{z}_{C^-} = \dddot{z}_{C^+} \Longrightarrow 6b_{z_3} + 24b_{z_4}T_{i123_1} + 60b_{z_5}T_{i123_1}^2 = 6c_{z_3} \quad \text{(A93)}$$

Phases *CD* and *DE*

$$z_D = z_{cont} \Longrightarrow c_{z_3}T_2^3 + c_{z_4}T_2^4 + c_{z_5}T_2^5 = z_{cont} \quad \text{(A94)}$$

$$\dot{z}_{D^-} = \dot{z}_{D^+} \Longrightarrow 3c_{z_3}T_2^2 + 4c_{z_4}T_2^3 + 5c_{z_5}T_2^4 = d_{z_1} \quad \text{(A95)}$$

$$\ddot{z}_{D^-} = \ddot{z}_{D^+} \Longrightarrow 6c_{z_3}T_2 \ + 12c_{z_4}T_2^2 + 20c_{z_5}T_2^3 = 2d_{z_2} \quad \text{(A96)}$$

$$\dddot{z}_{D^-} = \dddot{z}_{D^+} \Longrightarrow 6c_{z_3} + 24c_{z_4}T_2 \ + 60c_{z_5}T_2^2 = 6d_{z_3} \quad \text{(A97)}$$

$$z_E = 0 \Longrightarrow z_{cont} + d_{z_1}T_{i123_2} + d_{z_2}T_{i123_2}^2 + d_{z_3}T_{i123_2}^3 + d_{z_4}T_{i123_2}^4 + d_{z_5}T_{i123_2}^5 = 0 \quad \text{(A98)}$$

$$\dot{z}_E = 0 \Longrightarrow$$

$$d_{z_1} + 2d_{z_2}T_{i123_2} + 3d_{z_3}T_{i123_2}^2 + 4d_{z_4}T_{i123_2}^3 + 5d_{z_5}T_{i123_2}^4 = 0 \quad \text{(A99)}$$

$$\ddot{z}_E = 0 \Longrightarrow 2d_{z_2} + 6d_{z_3}T_{i123_2} + 12d_{z_4}T_{i123_2}^2 + 20d_{z_5}T_{i123_2}^3 = 0 \quad \text{(A100)}$$

$$\dddot{z}_{E^-} = \dddot{z}_{E^+} \Longrightarrow 6d_{z_3} + 24d_{z_4}T_{i123_2} + 60d_{z_5}T_{i123_1}^2 = 6e_{z_3} \quad \text{(A101)}$$

Phase *EF*

$$z_F = z_{cont} = e_{z_3}T_3^3 + e_{z_4}T_3^4 + e_{z_5}T_3^5 \quad \text{(A102)}$$

$$\ddot{z}_{F^-} = \ddot{z}_{F^+} \Longrightarrow 6e_{z_3}T_3 \ + 12e_{z_4}T_3^2 + 20e_{z_5}T_3^3 = \ddot{z}_{F^+} \quad \text{(A103)}$$

ОПТИМИЗИРОВАННЫЙ МЕТОД СИСТЕМЫ СОРТИРОВКИ ОТХОДОВ С ИСПОЛЬЗОВАНИЕМ ПАРАЛЛЕЛЬНОГО МЕХАНИЗМА

С. Кассис, Р. Ризк
Ливанский университет, Бейрут, ЛИВАН

АННОТАЦИЯ

Сортировка отходов является новой проблемой во всем мире. Выполнение задачи требует высокой частоты при легкой полезной нагрузке. Идеальным решением для этой задачи является использование параллельного механизма.

Для быстрой работы оптимизация траектории является обязательной. Это может значительно повысить эффективность. В этой статье мы рассмотрены ряд операций с двумя разными целями.

Цель состоит в том, чтобы свести к минимуму глобальное время процесса сортировки отходов. Робот должен забрать из конвейера стеклянные и пластиковые предметы и разместить их в двух разных контейнерах. Поскольку имеется ряд операций, нет необходимости в остановке механизма на время в каком-либо месте. В результате траектория больше не будет плоской.

Траектория проектируется в рабочем пространстве; управление же производится в пространстве кинематических пар. Таким образом, расчет обратной кинематической и дифференциальной модели является обязательным. Наконец, представлено экспериментальное подтверждение на небольшом прототипе.

Proceedings of the 1st International Conference MES-2018 / ИРМ-2018
MECHANICAL ENGINEERING SOLUTIONS
Design, Simulation, Testing and Manufacturing
September 17-19, 2018, Yerevan, ARMENIA

MES2018-37

APPLICATION METHODOLOGY OF ELECTRONIC CAMS

Miroslav VÁCLAVÍK[1] and Petr JIRÁSKO[2]

[1]VÚTS, a.s., Liberec, CZ, e-mail: miroslav.vaclavik@vuts.cz

[2] VÚTS, a.s., Liberec, CZ, e-mail: petr.jirasko@vuts.cz

ABSTRACT

Electronic cam systems are modern means of flexible industrial automation and are used to realize the motion functions of working links of manufacturing and handling mechanisms. We are talking about an electronic cam system because the application is a combination of servomotor control (controller, servo inverter, regulation, and displacement law), inputs, outputs, communication and the control system software itself, including combinations of servo drives and conventional mechanisms.

INTRODUCTION

Conventional cam mechanisms are a standard part of many processing and handling machines. Their massive expansion is associated with the use of CNC machine tools. More numerous applications of electronic cams in machines in the processing industry appear much later in connection with the development of computing technology, electronics and electrical engineering in the form of controlled servo drives. Also demands for a flexible change of motion functions have become topical. The applications of conventional and electronic cams are essentially the same, i.e. the drive of mechanism working links based on the technological demands placed on *displacement laws*. Both groups of cam systems (conventional and electronic) excel in their specific features. Requirements for the working movements of the mechanisms are quite different, so in such cases an analysis of the application problem is necessary, which includes, as much as possible, the potential variants and mutual combinations. In essence, we are looking for the answer to the question: *"When is it convenient to use a programmable electronic cam and when a conventional cam"?* In analyzing, it is important not to favor either of these two systems but to seek optimal solutions based on the best features of both systems. Applications of conventional cams are well known, so we will focus on electronic cam systems.

In the paper, the basic terms and common initial properties, which are obtained by solving discrete computational models with their verification on dynamic stands, will be declared. The next text deals with the methodology of the applications of electronic cams themselves, which describes their principal properties that in parallel with the conventional cam mechanisms lead to the principle of mechatronic differential.

The system of the Japanese company Yaskawa [4] is used to investigate the general characteristics of the dynamics of electronic cams.

NOMENCLATURE

Abbreviations regarding the PLC program:

PLC Programmable Logic Controller
HSS High-Speed Scan
MP2000/3000 Yaskawa Machine Controller
MPE720 System Integrated Engineering Tool
PERR Positional Error
MFCE1 PLC user function template

ELECTRONIC CAM

The *electronic cam* is a *servo drive* (*synchronous servomotor* powered by a frequency inverter-*servo inverter* and controlled by a *controller*), which performs an actuating *motion function* on the output

shaft of the servomotor rotor, utilizing the dynamic properties of the displacement laws or their derivatives (1st and 2nd). Thus, the motion function assigns the angular variable of the servomotor shaft to the time, the length variable in the case of a linear servomotor. The controller can be programmed in the *PLC* area and in the continuous motion area through the development environment. The electronic cam of VÚTS is programmed in the *PLC* area. In every *PLC* program *scan*, the *position, velocity* and *torque size* of the servomotor are defined by output registers. Most manufacturers of electronic cams use a cascade control structure of servo inverters, consisting of a position controller (usually proportional), a speed controller (usually proportional integral) and a torque controller (or a current controller, usually proportional integral). From the point of view of the mechanical engineering applications of mechanism working link drives, the term *electronic cam* means such a use of a servomotor (as a powerful force link) which is *alternative* to drives that are possible combinations of cam linkage mechanisms driven by conventional asynchronous motors.

In the basic features, the processing machine is a system of mechanisms that implements the given technology, for example, with compound cam mechanisms. Generally speaking, between the *conventional cam* and the *working link* with the desired motion it is a kinematic chain of planar or spatial mechanisms that transforms the desired working motion into the main link of the basic cam mechanism (the task of kinematic *synthesis*), for example, the *radial cam rocker.* Depending on the geometry of the basic cam mechanism, then, by calculations of the kinematic synthesis, we can determine the coordinates of the active area (surface) of the cam. *It is possible to assign* the rotation motion of a conventional radial cam rocker to the shaft of the electronically controlled *servomotor* or to assign the transformed displacement law of the rocker, including the 1st and 2nd derivatives, to the servomotor shaft.

DISPLACEMENT LAW, MOTION FUNCTION AND POSITIONAL ACCURACY OF THE MOTION FUNCTION

The function assigning a position quantity of a particular link of a compound cam mechanism to *time* will be called the *motion function* of that link. The motion function of the electronic cam (theoretical, real) is the movement of the servomotor shaft (*Slave*) in dependence on time, and this motion function kinematically excites a transmission mechanism dynamic system of the kinematic chain at the end of which is a working link. The corresponding derivatives of the motion function by time are quantities *velocity* and *acceleration*.

The function assigning to *position* of a particular link a position quantity of another link of the compound cam mechanism will be called *displacement law.* The displacement law of the electronic cam is the theoretical function of the servomotor shaft position (*Slave*) on the position of the virtual shaft (*Master*), or virtual rotation. The relevant derivatives of the displacement law with respect to the virtual shaft position are the *1st and 2nd derivatives* of the displacement law (0. derivative is often referred to as the stroke itself). The first and the second derivatives of the displacement law are often referred to as the first and second transmission functions; in the following text (see also *Figure 1* and *Figure 2*), the displacement law is indicated by the symbol $\boldsymbol{\Pi}$.

The relationship between the *displacement law* and the *motion function* of the same link, for example, the driven link of the basic cam mechanism, is shown in both schematic Figures (see *Figure 1* and *Figure 2*).

The displacement law (0-zero, 1st and 2nd derivatives) of the electronic cam transformed by the angular velocity and acceleration of the virtual shaft is a theoretical motion function. The difference between the desired *theoretical* and *actual* (*real*) motion function is the *position accuracy* of the *motion function* of the electronic cam (hereinafter referred to as *PERR*). One of the aims of electronic cam applications is to achieve the best possible match between the theoretical motion function and the real one on the servomotor shaft. *PERR* is principal and its size is a function of cascade control parameters in the servo inverter, external dynamic (inertial) and technological (production) loads.

DISCRETE COMPUTATIONAL MODELS AND STANDS, APPLICATIONS

The issue of electronic cam applications is closely related to the applications of conventional cam mechanisms. In essence, it is the same problem of ensuring the *mechanism working link drive* in the optimum way. The working link of the mechanism is usually the final (output) link of the kinematic chain of the compound cam mechanism with its defined *displacement law.* The displacement law of the working link is performed generally by a non-constant transmission function (basic cam mechanism, electronic cam servomotor or another mechanism) at the input of the kinematic chain that generates a motion function. This motion function is a kinematic excitation of a dynamic system with *stiff* or *compliant* links which the compound cam mechanism actually is. Thus, kinematic excitation is derived from a *mechanical*, *electronic* or *combined* cam mechanism.

Because we come from a *single view of driving the mechanism's working links* in *classical* or *electronic* ways, we will present a diagram of discrete models of both types of mechanisms with intangible compliances and damping, motion equations are in References [1]. *Figure 1* shows a discrete model of a conventional cam mechanism with compliances in the driven and driving parts. To construct the equations of motion in the studied model, *classical Lagrange equations of the second type* can be used for independent general coordinates, which are deflections of the links of the

cam mechanism due to the flexible constraints, or also the coordinates of the driving link. When deriving equations of motion, we will use the designing of the positions of the links in absolute coordinates (q_i) and we do not consider the influence of gravity.

The motion equations of the electronic cam mechanism are derived in References [1] and are deduced in the same way as in the case of the conventional cam mechanism according to the discrete model in *Figure 2* with the *principal compliance* of the *stator/rotor* electromagnetic constraint and the output compliance in the driven part of the mechanism. For reasons of analogy with the conventional mechanism, there are also exhibited links with zero moments of inertia, which have their mechanical equivalent in the form of a conventional mechanism with two output compliances.

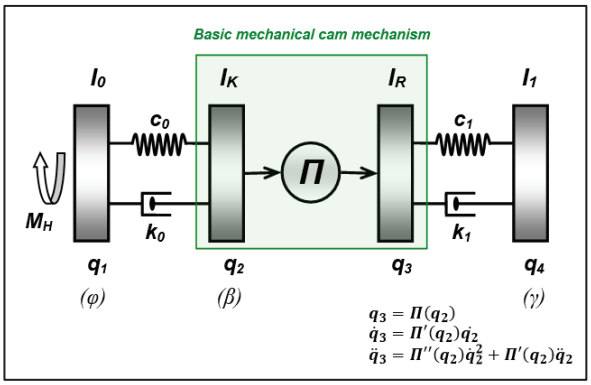

Figure 1. Discrete model of a conventional cam mechanism

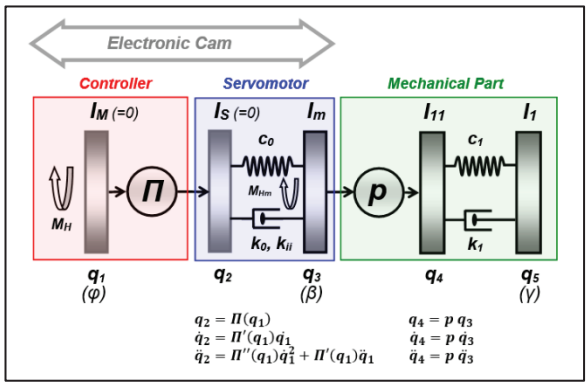

Figure 2. Discrete model of an electronic cam

At this point we will give a short note to the difference from the numerical solution of the conventional cam mechanism model. We will not describe the principles of servo drive regulation, but we just note that most servo drives have a cascade control structure with torque, velocity and position feedback. Regulators are, as a rule, proportional (P) and proportional integral (PI). In the numerical solution we are dealing with such an interference in the equations of motion so that the characteristic quantity, which *PERR* - the position deviation of the servo drive (the difference between the actual position of the servomotor shaft and the theoretical position) is, corresponds as much as possible to the reality of the P/PI modes. *PERR* is then a criterion for the accuracy of a given model [2]. The results of the SW simulations were verified on the dynamic stands according to *Figure 3* and *Figure 4*. Because of the limited scope of this paper, the comparison results are not shown.

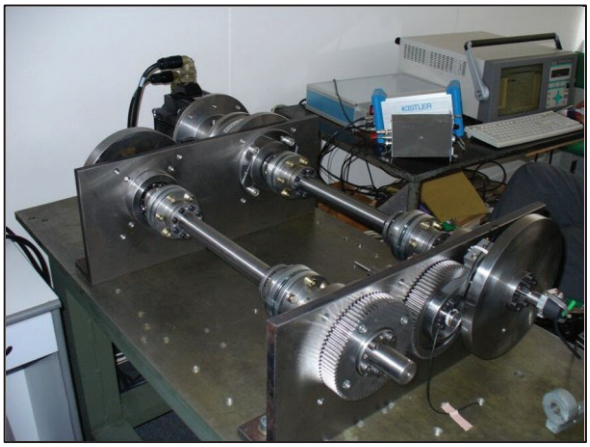

Figure 3. Stand of a conventional cam mechanism

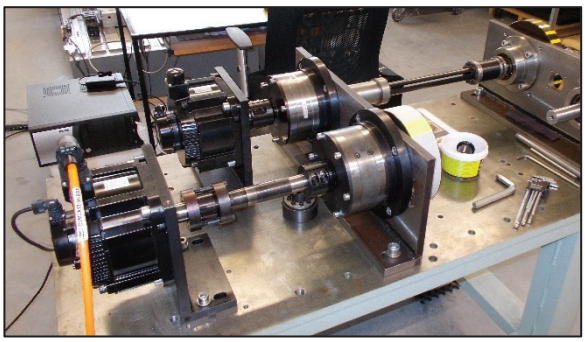

Figure 4. Stand of a Yaskawa's electronic cam

We will briefly mention the main implications of a *compliant (flexible) driven output*. The precision of the end position of the working link (γ according to *Figure 1* and *Figure 2)* in the *rest interval* of the motion function is judged by the extreme value of accelerations of the *residual* vibrations [3]. The criterion of positional accuracy is then the so-called *residual response spectrum* for the kinematic excitation of the compliant system by the displacement law [1] [4]. The residual spectrum, *specific* for a given displacement law, will be used to determine the parameters (*speed, stroke angle* or *moment of inertia*) in which oscillation is minimized [1].

The discrete models of both cam systems and their mathematical description with their respective compliances have the same basis in the analytical methods of the technical mechanics. Intangible flexible constraints, including damping, are the source of vibrations that respond to kinematic excitation by *motion function* (position, speed, acceleration). The motion function is derived from the *displacement law* (stroke, 1st and 2nd derivatives). The description of the

stator/rotor compliant electromagnetic constraint by the quantities of *stiffness and damping* is in no way related with their values to the values of the control parameters of the cascade structure of torque, speed and position constraint in the servo inverter. They describe only the physical essence that states that it is a flexible constraint with a high degree of damping (in the numerical solution it is necessary to distinguish the P/PI control). Specific values are experimentally verified based on dynamic stand tests. This *"mechanical engineering"* view gives us an idea of the basic behavior of conventional and electronic mechanisms. The design intent is always to use the minimum number of links of the kinematic chain of a mechanism with rigid links. In the case of a conventional cam mechanism, it is the rigid drive of a cam with the working link, preferably directly on the rocker or follower of the basic three-link cam mechanism. For example, this idea corresponds to a step gearbox according to the source [5].

In the case of the application of an electronic mechanism with a rigid mechanical output part, it always remains *principal* the compliance of the electromagnetic *stator/rotor* constraint in the servomotor. This constraint, or its stiffness, is a function of control parameters in the servo inverter. In the following text we declare the mechanical part as rigid and we will deal with the possibilities of adjusting the control parameters of the servo inverter and with manipulating the data of the displacement laws with regard to the minimization of the positional error of the *PERR motion function*, which we consider as the function of stiffness of the *stator/rotor* flexible constraint, the dynamic load of inertia masses (working link, including the rotor of the servomotor) and a possible external technological load.

APPLICATION METHODOLOGY OF ELECTRONIC CAMS

For both cam systems (conventional, electronic), it is virtually the same, and that is the *drive of the working link* of a processing machine mechanism.

By *conventional cams*, we mean compound cam mechanisms with arbitrary basic cam mechanisms, as described, for example, in References [1]. These mechanisms are well known with their pros and cons. Positive properties include, for example, high dynamics, relatively low price and structural variability, the disadvantages are their single-purposiveness, the influence of clearances, compliances in the input and output kinematic chain, the wear (cams are often needed as spare parts).

Electronic cams are mechanisms that consist of *control* (hardware is an operating controller with SW development environment) and *drive* (servo inverter, servomotor). We are often talking about the electronic cam system since the electronic cam application unifies recently independent fields (mechanics, software, electronics, control and regulation, etc.) in it and is a classic case of a rapidly growing field of *mechatronics*. The advantages of electronic cams are their easy change of displacement laws and usability in manufacturing systems as elements of flexible automation, low maintenance requirements, and reliability. The disadvantages are, for example, their lower dynamics, higher acquisition costs, high qualification requirements for preparation and implementation of applications.

KINETOSTATIC DIMENSIONING OF ELECTRONIC CAM

The kinetostatic calculation is essential in particular for the electronic cam, and we will briefly call it "*servomotor dimensioning*". It is a selection of a servomotor according to the manufacturer's catalog, which will optimally meet the requirements for the respective drive of the mechanism working link with the defined *displacement law.* The servomotor must meet the requirements for *maximum torque*, *effective torque* (current load) and *maximum instantaneous speed*, for example, according to the data sheet of *Figure 5*.

Servomotor Model: SGMGV-□□□		03D	05D	09D	13D	20D
Rated Output*	kW	0.3	0.45	0.85	1.3	1.8
Rated Torque*	N·m	1.96	2.86	5.39	8.34	11.5
Instantaneous Peak Torque*	N·m	5.88	8.92	13.8	23.3	28.7
Rated Current*	A_{rms}	1.4	1.9	3.5	5.4	8.4
Instantaneous Max. Current*	A_{rms}	4	5.5	8.5	14	20
Rated Speed*	min^{-1}					
Max. Speed*	min^{-1}					3000
Torque Constant	$N·m/A_{rms}$	1.55	1.71	1.72	1.78	1.50
Rotor Moment of Inertia	$\times 10^{-4}$ kg·m^2	2.48 (2.73)	3.33 (3.58)	13.9 (16)	19.9 (22)	26 (28.1)

Figure 5. A part of the Yaskawa SGMGV servomotor catalog sheet

What is the torque and what is the link with the conventional cam mechanism is described in the following text. *Figure 6* illustrates schematically (in the introduced symbols *Figure 1* and *Figure 2*) a general *conventional* mechanism with *non-constant transmission* with one degree of freedom. Under this scheme, it is possible to imagine one of the basic cam mechanisms (for example, radial, axial, globoid cam with a rocker) or any planar mechanism (for example, four-bar linkage, and eccentric mechanism). The *input* motion is described by the *motion function* $f(t)$.

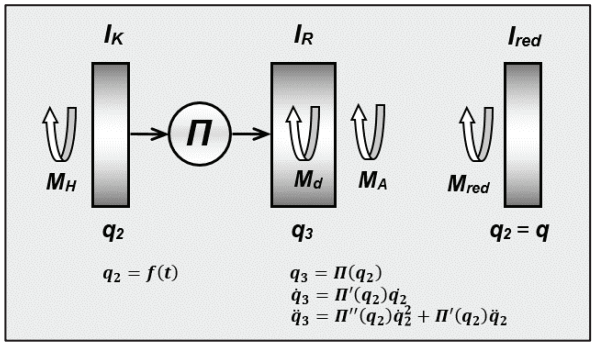

Figure 6. Diagram of a common conventional mechanism with non-constant transmission and reduction to the input link

In this case, the motion equation is deduced by the reduction method, where the reduced moment of inertia I_{red} results from the equality of *kinetic energies* before and after the reduction, a similarly reduced moment M_{red} results from the equality of *elementary pieces of work* or *performances* of working forces before and after the reduction.

After modifications, we will get

$$I_K\ddot{q}_2 + I_R\,\Pi'(q_2)[\Pi'(q_2)\ddot{q}_2 + \Pi''(q_2)\dot{q}_2^2] - M_A\,\Pi'(q_2) = M_H \quad (1)$$

and by substituting for $\ddot{q}_3 = \Pi'(q_2)\ddot{q}_2 + \Pi''(q_2)\dot{q}_2^2$, it is

$$I_K\ddot{q}_2 + (I_R\ddot{q}_3 - M_A)\Pi'(q_2) = M_H.$$

If $\dot{q}_2 = \omega = konst$ and $M_d = I_R\ddot{q}_3$ is the accelerating driving torque at the output (the same sense with acceleration), then the accelerating driving torque at the input is

$$M_H = (I_R\ddot{q}_3 - M_A)\Pi'(q_2) = (M_d - M_A)\Pi'(q_2) \quad (2)$$

and for $M_A = 0$ with the mere action of inertia forces, it is

$$M_H = I_R\ddot{q}_3\Pi'(q_2) = I_R\omega^2\Pi'(q_2)\Pi''(q_2) = M_d\Pi'(q_2) \quad (3)$$

The operative character of the drive torque M_H is determined by the product of the *first* and *second* derivatives $\Pi'\Pi''$ of the displacement law. In the literature describing displacement laws [6] [7], this function of the product is often presented and tabulated for its predictive capacity with respect to the required driving torque of a given displacement law.

Relationships (2) and (3) describe the basic difference between the *conventional* cam or any mechanism with one degree of freedom and an *electronic* cam when the servomotor is the source of the motion of the output (q_3, I_R). With the same *motion function* of the working link, the required *driving accelerating moment* M_H of the conventional cam at the input (q_2, I_K) is given by the relation (2), (3) for $\dot{q}_2 = konst$, or $\dot{q}_2 = konst$ and $M_A = 0$. The required *drive accelerating torque on the electronic cam servomotor shaft* (on the output working link (q_3, I_R), which does not participate in the response to the dynamic inertia moment of servomotor rotor) is of the size $\bar{M}_{Hel} = M_d = I_R\ddot{q}_3$. For $\dot{q}_2 = konst$, or $\dot{q}_2 = konst$ and $M_A = 0$ (which is the majority of technical applications), it applies

$$M_H = (\bar{M}_{Hel} - M_A)\Pi'(q_2), \text{ or } M_H = \bar{M}_{Hel}\Pi'(q_2). \quad (4)$$

The practical impact is obvious. With the same motion function of the working link in the application of a conventional and electronic cam, and with the appropriate geometric design of the conventional cam mechanism, the *driving torque* of a conventional cam achieves *smaller values* at the same instantaneous output of both cam systems. To the *drive accelerating torque on the electronic cam servomotor shaft* that is required by a particular application, there must be added a *drive accelerating torque* that responds to the dynamic inertia moment of the rotor of the servomotor. The sum of these moments is the required **drive accelerating moment of the servomotor M_{Hel} of the electronic cam** whose maximum and effective value is the manufacturer's catalog parameter. These relationships (2), (3) and (4) describe such a comparison when an electronic cam replaces a conventional mechanism with its direct drive of the working link (q_3, I_R).

The servomotor rotor significantly loads the drive. It is necessary to distinguish between the term *drive accelerating torque on the electronic cam servomotor shaft (further usable)* and *the drive accelerating torque of the electronic cam servomotor* (catalog value). It is obvious that when implementing the displacement law, a situation may arise, for example, by increasing the speed of the virtual shaft (*Master*), when the servomotor is loaded by itself. To reduce or to eliminate the influence of dynamics of the servomotor rotor, the *mechatronic differential* described in the following text is used.

IMPLEMENTATION OF DISPLACEMENT LAWS IN THE YASKAWA CONTROL SYSTEM

By generalizing, we conclude that the *realization of an electronic cam* in the development environment of *any* drive control system is the processing of the *displacement law* data with its derivatives (stroke, 1st and 2nd derivatives) into the servomotor *output shaft motion function* (position, speed and acceleration). The system further processes *speed* and *acceleration* values into *speed and torque Feed Forward*s with respect to inertia masses and other external (technological) force load.

The electronic cam is programmed in the *PLC (Ladder Diagram - HSS area)*. In *each PLC high-scan*, there is defined the ***position*** (at the most basic level it is the information that tells by how many *increments-pulses* in the High-Scan time interval, the *encoder* of the servomotor or the servomotor shaft will be rotated), ***speed*** and ***size*** of the ***torque*** of the servomotor by the *output registers (OLxxxx)*. Data sets of kinetostatic quantities are transferred to the controller's memory areas, where they are further independently transformed by defined units as required. These are, in particular, the *scaling*, the mutual phase shift of the values of the *1st and 2nd derivatives of displacement laws* with regard to the stroke, various independent superpositions with arbitrary data in order to minimize

the *positional error (PERR)* of the motion function of the electronic cam.

The basic building block of the control system programmed in the *PLC* (*MPE720-Yaskawa* development environment) is the *user function*. The user function is illustrated with its *inputs, outputs* and *bidirectional address communication* in *Figure 7* in the form of the general function *MFCE1* in the *PLC Ladder* Diagram. The productivity of programming work and the collaboration of several programmers in one project of the control system required unification, or a *user function template* that remains always the same or will be modified according to the agreed rules. This facilitates the orientation and creation of documentation of developed programs and user functions. The template structure of the *MFCE1* general user function according to *Figure 7* is in the References [8].

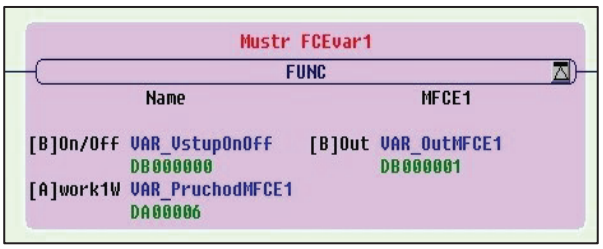

Figure 7. User function (inputs, outputs and communication, MFCE1 in PLC)

SERVO DRIVE CONTROL

Control of servo drives is carried out through parameters that are given available by the manufacturer. We use the *Yaskawa* electronic cam system (*Sigma V* servo drives, *MP2000/3000* series controllers). The aim is to set such values where the *stator/rotor* electromagnetic constraint is as stiff as possible (from the point of view of the technical mechanics). These are the following parameters:

Pn100 … Speed Loop Gain [Hz]
Pn101 … Speed Loop Integral Time Constant [ms]
Pn102 … Position Loop Gain [s^{-1}]
Pn401 … Torque Reference Filter Time Constant [ms]

There is no room for a deeper analysis of the drive *control* methodology in various electronic cam design applications. We only point out that the correct setting of the control parameters is *essential* with regard to the technology implemented with the requirements for high positioning accuracy of the working link of a mechanism. To estimate the values of the control parameters or the positioning accuracy of the working link at the design stage of the machine is *very problematic* without prior experience with a similar device.

There are several approaches to identifying parameters. The Yaskawa system offers several modes of *autotuning*, which did not prove itself, however, at our place. Automatic parameter setting did not reach the required values. On a stand with direct rotary drive and load, we have reset the manual setting of parameters according to the following procedure (steps 1 to 3 recommended by the manufacturer) when the default values of the parameters are *level* 4 (Pn100 / Pn101 / Pn102 / Pn401 = 40[Hz] / 20[ms] / 40[s^{-1}] / 1[ms]):

1. Reduction by 10-20% Pn401, check Pn401 <= 1000/(2π*Pn100*4)
2. Increase by 10-20% Pn100 and decrease by 10-20% Pn101, check Pn101 >= 4000/(2π*Pn100)
3. Increase Pn102 below *Stable Gain*, i.e. Pn102 <= 2π*Pn100/4

Steps 1 through 3 can be repeated to the vibration level. In our case, however, we are monitoring a positional error and therefore we will terminate the identification when the positional error stops significantly decreasing between the individual steps or reaches the required size. *Figure 8* shows a PERR error position record when realizing the displacement law according to *VDI 2143* [7] whose *2nd derivative* is red drawn. The green function is *PERR* in the control *level 4*, the purple *PERR* function is in the manual setting of the control parameters. The speeds are set so that the maximum dynamic inertia moment (load and rotor) reaches the *Rated Torque* according to the servomotor data sheet. The control system processes the *position* data and the data of the *1st and 2nd derivatives* of displacement law into *Feed Forward* of speed and moment. The *PERR* size is a consequence of only the *principal* compliance of the *stator/rotor* electromagnetic constraint.

For a more accurate illustration, the *PERR* positional error is expressed in an arc measure on the radius of 180/π (about 57 mm) in *Figure 8* and *Figure 9*.

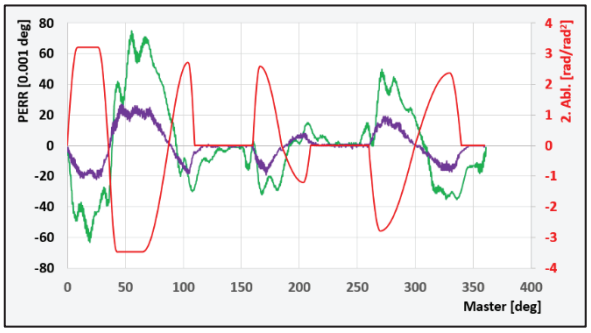

Figure 8. PERR positional error and the 2nd derivative of the tested displacement law according to VDI2143

PERR POSITIONAL ERROR

As it was said, the *positional error* (*PERR*) of the *motion function* is dependent on the control parameters and the dynamics of inertial and external load forces. In the case of the stand test according to *Figure 8*, it is only dynamic inertial forces of the load and rotor of the servomotor. The *displacement law* data and *mass parameters* (load, rotor) are processed into the position of the servomotor shaft and the feed forward

constraints in each *PLC scan 1ms*. According to *Figure 8* (purple data), it is clear that the character of *PERR* is mirrored with respect to the 2nd derivative of the displacement law. Another *PERR* minimization can be achieved by using the data of the *2nd derivative*, which are available in the controller memory, and by merging them with the position data [9] after the necessary transformation. An effective option is also the use of the mutual *phase shift of data of the 1st and 2nd derivatives of the displacement law*, including the scale of their values. In *Figure 9*, it is *PERR* at a phase shift of the *1st derivative* by 0.17 deg with the same assignment and *PERR* has decreased approximately 4 times.

The reason why we put emphasis on the size of *PERR* and its minimization in applications of electronic cams are the requirements of precise manufacturing technologies (for example, single-purpose machine tools) and the correct function of the *mechatronic differential* in non-periodic (step) displacement laws applications, where the desired rest is a superposition of movements of a conventional and an electronic mechanism.

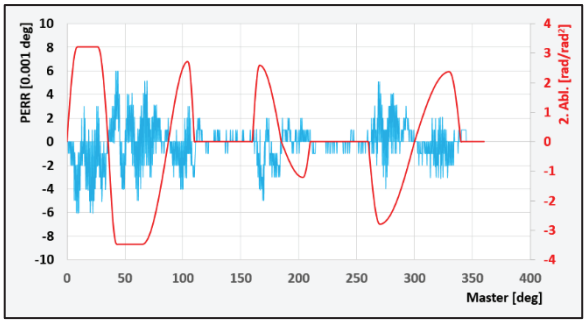

Figure 9. Minimized PERR and the 2nd derivative of displacement law according to VDI 2143

MECHATRONIC DIFFERENTIAL

The mechatronic differential is sufficiently described in the References [10]. With the direct serial use of conventional rotary servomotors with gearboxes or reducers, the demands on the motion dynamics of the servomotor rotor are high. The servomotor is heavily loaded by its own momentum of inertia of the rotor, which significantly reduces the applicability area of electronic cams. This mentioned deficiency is largely eliminated by the *way* of driving the working links of the mechanisms by means of a *mechatronic differential driving system* [11]. *Figure 10* and *Figure 11* show CAD models in double embodiment. On the functional model according to *Figure 10*, the principle was verified, according to *Figure 11*, an industrial prototype was made.

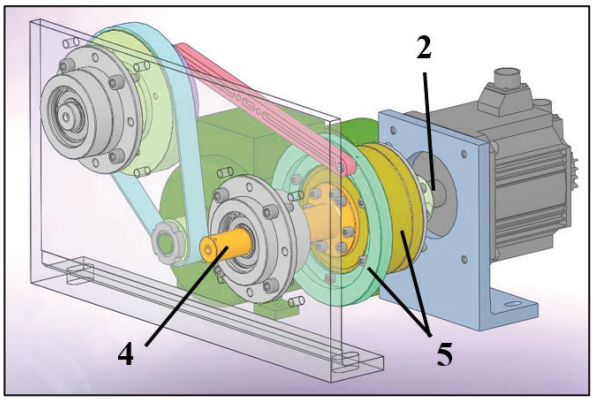

Figure 10. Mechatronic differential – force movement derived from the four-bar mechanism

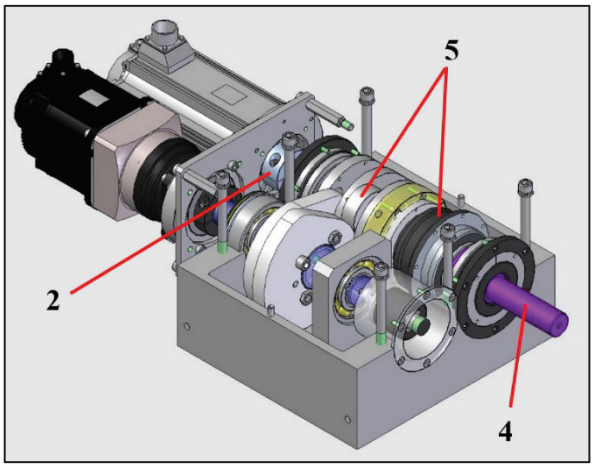

Figure 11. Mechatronic differential – force movement derived from the radial double cam

We will briefly describe the principle. The central gearbox is used as a differential. One input is the force movement **5**, which is derived from the conventional (classic) mechanism (link mechanism, cam mechanism). The second input is movement **2**, which is derived from an electronic cam. The superposition is the resultant desired movement **4**.

The *mechatronic differential* of *Figure 11* is *the first experimental prototype* of its kind. It is currently not designed for any particular application. It is used to verify the computational models with reality, to verify the different control modes, the creation of the functions of the own control system and to verify the *PERR* minimization methods. On the basis of the acquired knowledge, it is possible to optimize all important parameters (servomotor power, gear ratios, displacement laws and geometry of the double cam mechanism) taking into account the specific requirements of the production technologies.

We have focused on *step motion functions*, which are a productivity limiting factor in many applications. These include, for example, rotary carousel tables and stepping manipulation mechanisms. The requirement is the shortest turning time because in the resting part

there is a production process itself. Conventional step cam mechanisms with radial cams are limited by their geometry and the usability of electronic cams is limited by the dynamics of the servomotor rotor. The mechatronic differential shows a strong *synergy* in the mutual interaction of the *conventional* and *electronic* mechanisms in the motion functions, where realization by individual mechanisms is not possible. In step mechanisms, it *principally* separates the dynamics of the servomotor rotor from the step or stroke (displacement) of the working movement which is idle time from the manufacturing point of view. Thus, the mechatronic differential increases the productivity of production processes based on stepped (non-periodic) motion functions.

A remarkable feature of the mechatronic differential is the possibility of combining the size and sense of the basic transmission of the differential $\pm i$ and the stroke of the double cam rocker relative to the desired work step or stroke (lift). As a consequence, there is another possibility of reducing the driving moment of the *electronic cam* **2** drive since the reduced moment of inertia of the servomotor rotor (reduced by the second power of transmission i) is forcefully "engaged" in the dynamic equilibrium of the link **5**.

APPLICATION – RADIAL CAM GRINDER

The BRV-300 CNC radial cam grinder according to *Figure 12* is based on modular units of renowned manufacturers. The control system has been fully developed in VÚTS based on a long-term research of applications of electronic cams, which are integrated in the system and allow efficient control of NC production axes according to different grinding conditions. The control system allows carrying out dimensional analyses of the contour of a cam without removing the workpiece from the machine. The rotary interpolation axis is realized by a direct rotary drive, the sliding interpolation axis is then carried out by a linear unit and a drive by a standard rotary servomotor. Grinding the cam contour is a movement with negligible dynamic inertia forces, so the main issue is the own CNC control system with requirements that are dictated by the cam grinding technology. In development, there is the second generation of the machine, which has both interpolation axes realized by direct drives.

Figure 12. BRV-300 CNC radial cam grinder

APPLICATION – FOLDING RULER WOODEN SLAT MILLING MACHINE

The uniqueness of the machine is in a central carousel rotary table with an inertia moment of 80 [kgm2] with 21 controlled axes, which perform machining on the basis of the data files of the displacement laws (position, 1st and 2nd derivatives). The carousel table is also conceptually designed with an electronic cam and a constant transmission in the form of axial spiral gear that is kinematically defined as an axial cam with a rocker and a roller. On the rotating table, it is demonstrated the main feature of electronic cams with the main application problem, which is the *achievement of the required positional accuracy*. The positional accuracy of the machined slats was required in the order of hundreds of a millimeter (axis tolerance of the machined configuration). This modern, electronically controlled machine replaced the concept of a classic machine with cam linkages with a central drive realized by an asynchronous motor. This is an exemplary use of a mechatronic approach to machine solving which requires a rapid change of motion functions or changing the machined configuration in the folding meter slat.

The following Figures represent:

Figure 13: One of the possible variants of the machined assemblies. The axis tolerance of the machined assembly is 0.05 [mm]. Machining takes place through various tools in the planar movement of X and Z interpolation axes.

Figure 14: The CAD model and reality of a complete machine with optical barriers on the touch screen.

Figure 15: Top and bottom machining point with X and Z interpolation NC axes. The slat is machined in one position on both sides. Depth is still constant and

is controlled based on slat thickness laser measurement.

Figure 16: Diagram of a carousel rotary table with a constant gear ratio i = 40 between the servomotor shaft and the working rotation. The axial worm is designed as an axial double cam with a rocker and a roller.

Figure 17: Positional error of the servomotor in all 16 positions. Machine cycle is 60 [min-1]. Step time, or rotation and rest time is 0.5 [sec]. The values of the control parameters of the servo inverter could not be set to a "higher" stiffness of the stator/rotor electromagnetic constraint due to the resonance of some parts of the mechanism. The real time for machining is then shortened to about 0.35 [sec].

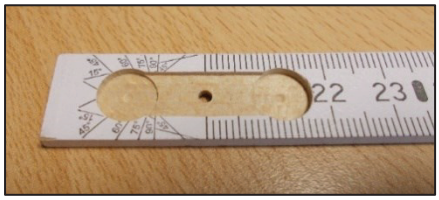

Figure 13. Folding ruler slat

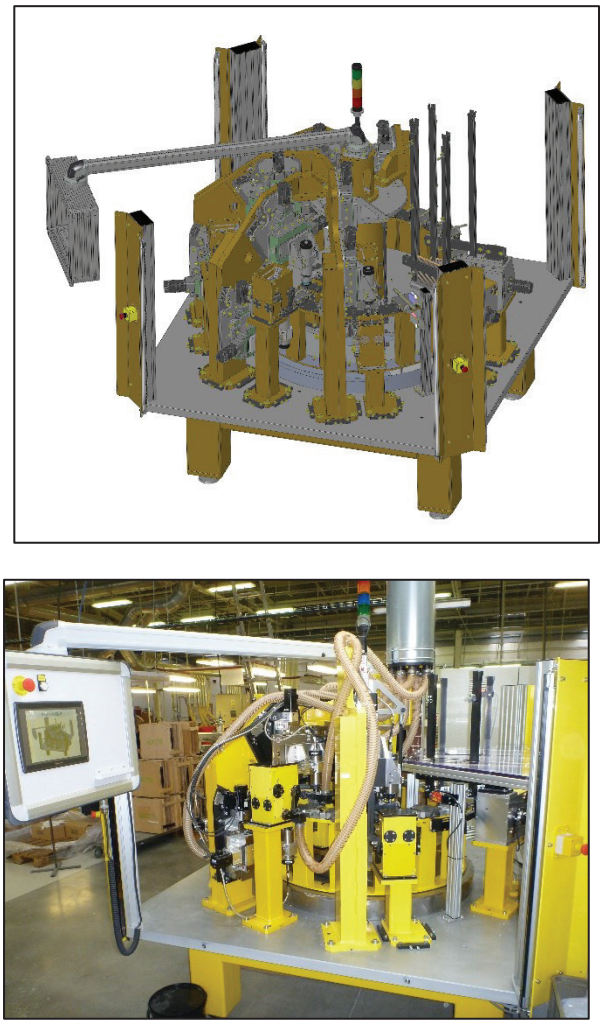

Figure 14. CAD machine model and reality

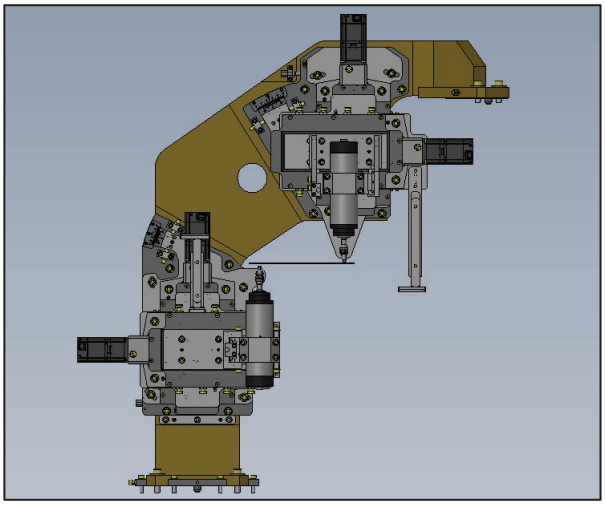

Figure 15. Two machining positions in X, Z axes for one slat

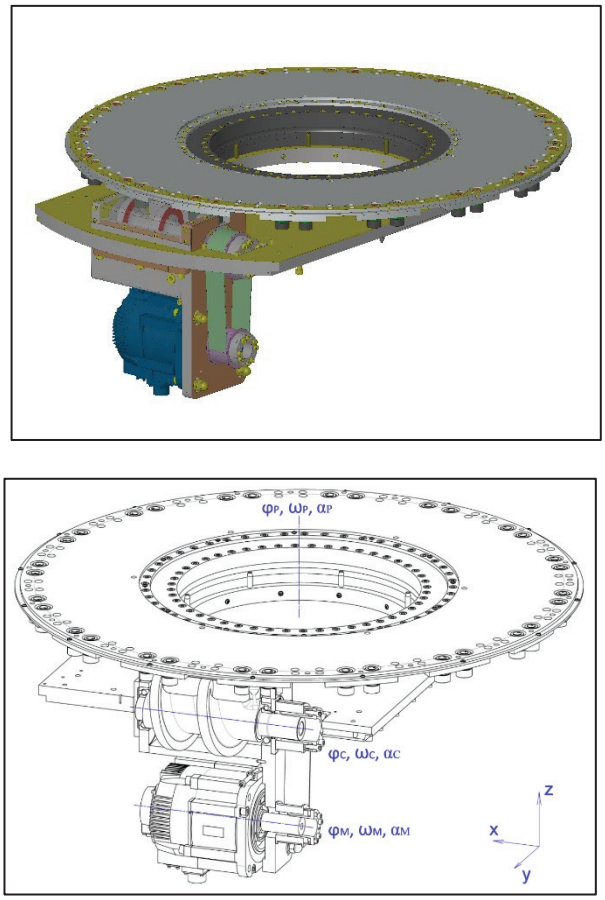

Figure 16. Carousel turntable with 16 positions

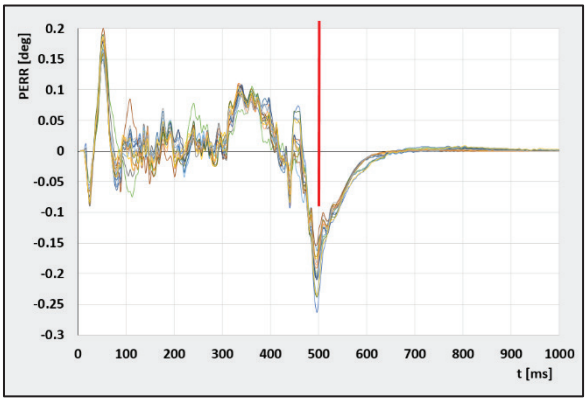

Figure 17. PERR positional errors of the servomotor in all 16 positions

CONCLUSION

Over the period we have been dealing with the issue of electronic cams, a number of applications have been implemented. This is mainly the realization of the working movements of the mechanisms of single-purpose machines with different requirements for PERR positional error. There have always been applications inclusive complete machine control systems. These include, for example, special woodworking machines and interpolation NC axes drives of the grinder for radial cams. As a major problem with the applications of electronic cams in similarly demanding machines, we see in the problematic estimation of the control parameters of the servo inverter and the size of the passive resistances that affect the PERR positional error. In applications where there are high demands on the precision of the position of the working links with a high dynamics of inertia forces, it is often a very risky step. Applying electronic cams in these cases requires gradual development steps.

The authors of the paper have developed the mentioned electronic cam application methodology at their workplace, leading even to the possible use of a unique mechatronic differential according to the European patent [11].

REFERENCES

1. Jirásko, P., Václavík, M., *Residual Spectra of Displacements of Conventional and Electronic Cams*, National conference Engineering Mechanics 2009, Svratka (CZ), May 11-14, 2009 (Svratka, Czech Republic)
2. Jirásko, P., Dostrašil, P., Václavík, M., *Approximation of periodic displacement law with Fourier series in the applications of mechanisms with electronic cam*. 2015 MeTrApp IGM, Aachen
3. Václavík, M., Jirásko, P., *Residual vibrations in the drives of working links of electronic cam mechanisms*, ICoVP 2011, Praha (CZ)
4. Integrated Machine Controller MP3200 (LITERATURE NO. KAEP C880725 02A)
5. Koloc, Z., Václavík, M.: *Cam Mechanisms*, Elsevier 1993
6. Volmer J., und Autorenkollektiv, *Getriebetechnik-Kurvengetriebe*, VEB Verlag Technik Berlin 1989
7. VDI 2143 Bewegungsgesetze für Kurvengetriebe
8. Jirásko, P., Crhák, V., Bureš P., *The conception of the control system of radial cam grinder*, IFToMM Liberec 2012, Czech Republic
9. Jirásko, P., Bušek, M., *Position Accuracy of Motion Functions of Electronic Cams*. IFToMM Liberec 2008, Czech Republic
10. Václavík, M., Jirásko, P., *Electronic Cams in Serial and Parallel Combination with Conventional Mechanisms in the Drives of Mechanism Working Links.* The First IFToMM Asian Conference on Mechanism and Machine Science, October 21 - 25, 2010, Taipei, Taiwan
11. Jirásko, P., *Způsob a zařízení k pohonu členů strojních mechanismů*, CZ301095, EP2078882.
12. Juliš, K., Brepta, R. a kol.: *TP 66 2.díl - Dynamika*, SNTL 1987

МЕТОДОЛОГИЯ ПРИМЕНЕНИЯ ЭЛЕКТРОННЫХ КУЛАЧКОВ

Мирослав ВАЦЛАВИК и Петр ЖИРАСКО
ВУТС, Либерец, ЧЕШСКАЯ РЕСПУБЛИКА

АННОТАЦИЯ

Электронные кулачковые системы – это современные средства гибкой промышленной автоматизации и используются для реализации функций движения рабочих звеньев производственных и манипуляционных механизмов. В статье рассматривается электронная кулачковая система, потому что приложение представляет собой комбинацию сервомоторного управления (контроллер, сервопреобразователь, регулирование и функция перемещения), входы, выходы, связь и программное обеспечение системы управления, включая комбинации сервоприводов и обычных механизмов.